Circulation of Oyster Harbour

Nick D'Adamo

Contents

Contents (cont'd)

Figures

Contents (cont'd)

Contents (cont'd)

Tables

Plate

Acknowledgements

Dr Des Mills of the Marine Impacts Branch of the Environmental Protection Authority coordinated the current meter and drogue tracking exercises, and provided managerial support for the study. Dr Mills also assisted in the collection and interpretation of CTD and circulation data. Dr Chris Simpson, Mr Kim Grey and Mr Stephen Chase of the Marine Impacts Branch assisted in field work and data analysis. Dr David Luketina (Centre for Water Research, University of Western Australia) reviewed the manuscript. The Centre for Water Research provided assistance in the field (Mr Terry Smith, Mr Tony Jenkinson, Mr Bernard van der Klip, Mr Sotiri Battalis) as well as computer software and hardware for the reduction of CTD data. Professor Jorg Imberger of that Centre assisted in the scientific interpretation of the data. The Australian Surveying and Land Information Group performed all drogue measurements. The Flinders Institute of Atmospheric and Marine Science and Mr Don Wallace, through the Western Australian Department of Marine and Harbours, provided tidal data. The Albany office of the Bureau of Meteorology provided meteorological data.

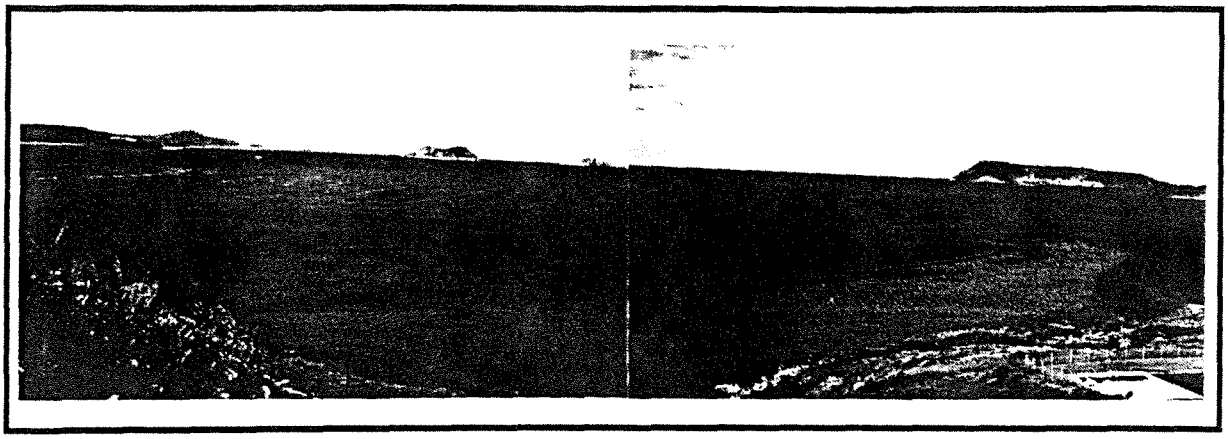

Plate 4.1 Buoyant jet from Oyster Harbour, 25 July 1988 at approximately 1500 hours. The view is looking approximately east out over King George Sound from King Point. Note the multiple slick lines.

Summary

This report presents field data and analytical calculations which highlight the nature of internal circulation and mixing in the shallow south-west Australian estuary of Oyster Harbour. The characteristics of exchange between the estuary and the adjacent oceanic embayment of King George Sound are also investigated.

This study forms a component of the Albany Harbours Environmental Study 1988-1989 (Simpson and Masini, 1990) conducted by the Environmental Protection Authority of Western Australia. That study was motivated by a need to both understand and recommend ways to ameliorate the effects of eutrophication and consequent extensive seagrass dieback in both Oyster Harbour and Princess Royal Harbour. The eutrophication was identified to have resulted from excessive loadings of nutrients via rivers, drains, industrial and domestic sources over the last 30-40 years (Simpson and Masini, 1990).

Flows driven by density differences as well as flows driven by winds and tides play important roles in basin-scale transport within the harbour and in exchange processes between the estuary and the adjacent oceanic embayment of King George Sound. The results of this investigation serve to illustrate the hydrodynamic traits of this estuary throughout the year under the following conditions:

- strong and weak river discharge periods;
- calm, moderate and strong wind conditions;
- neap and spring tide conditions; and
- strong atmospheric heating and cooling periods.

Data collected during typical winter and summer hydrological conditions are analysed and show that, in general, the harbour can be hydrodynamically described as salt-wedge in nature, with the strength of vertical and horizontal stratification in salinity, temperature and therefore density being dependent primarily on the rate of buoyancy flux introduced to the harbour via its major rivers, the King and Kalgan, and on the strength and duration of wind mixing. The tide is also important as it acts to drive a cyclic influx and efflux of water through the mouth as a salt-wedge.

Wind mixing is estimated to be capable of penetrating to the bottom of the deep central regions of the harbour when wind velocities climb significantly above 5-10 m s^{-1} for periods greater than about 10-15 hours in winter and 6 hours in summer. Wind mixing is least effective in winter due to the occurrence of strong vertical density gradients set up by the introduction of appreciable amounts of freshwater by rivers during winter discharge events. In contrast, during summer there is only a relatively weak introduction of buoyancy flux via small river discharges, groundwater inputs and solar heating, and hence the vertical stratification is much less intense than during winter.

The flushing characteristics of the harbour are determined as best as possible, given the complicated nature of the physical structure of the harbour. It is estimated that total replacement of the harbour volume by typical strength forcings (winds, tides and density currents) is of the order of 10 days. The surface waters are likely to have the lowest retention times in the harbour (1-2 days) throughout the year, particularly during winter as a result of a strong southward directed pressure gradient at the surface due to the buoyancy flux that enters the northern region of the harbour via the King and Kalgan rivers. Consequently, during winter, surface river discharge traverses the harbour as a buoyant layer less than about 1 m thick and emanates out into King George Sound as a buoyant jet.

During a typical summer period, the movement of the density structure near the bottom was tracked in the harbour over a number of consecutive tidal cycles. The measurements revealed the cyclic upstream and downstream movement of the salt-wedge during flood and ebb tides, respectively. Additionally, the data indicated that there was a residual (tidally averaged) inward propagation of the salt-wedge. A simple first order calculation of the residual volumetric influx

due to this process resulted in an estimate of the order of 4-10 days for the time it would take for the equivalent of one harbour volume to enter the harbour.

The stratification in Oyster Harbour is postulated to be important in governing the availability of nutrients contained in river discharges to benthic macroalgae. On the basis of the hydrodynamic calculations in this report, it is concluded that vertical mixing is unlikely to be sufficiently strong, on average, to facilitate a complete availability of nutrients to benthic macroalgae during the winter flood discharge periods when nitrogen and phosphorus loadings to Oyster Harbour are greatest. The greatest vertical transport of nutrients probably occurs during periods of weaker river discharge, when the stratification is relatively less intense and vertical mixing agents, such as the wind, can cause downward mass transport at higher rates than during the periods of high river discharge.

1. Introduction

In 1988 the Western Australian Government requested the Environmental Protection Authority of Western Australia (EPA) to conduct a two-year investigation into the ecological degradation of the Albany harbours, namely Oyster Harbour and Princess Royal Harbour, located on the south coast of Western Australia. That study was termed the Albany Harbours Environmental Study 1988-1989 and a synthesis of the results of the various components of the study was produced by Simpson and Masini (1990). As part of that study, the EPA identified a need to understand the hydrodynamic characteristics of the internal mixing, and transport of water and nutrients (that are brought down in river discharge), within Oyster Harbour and between Oyster Harbour and the adjacent oceanic waters of King George Sound. This report presents the results of a study on the hydrodynamics of Oyster Harbour. The hydrodynamics of Princess Royal Harbour is also being investigated as part of the Albany Harbours Environmental Study 1988-1989 by Mills and D'Adamo (in prep.).

Oyster Harbour is an estuary and lies approximately 10km to the northeast of the town of Albany. It has a surface area of approximately 16 sq km and communicates with King George Sound via a relatively narrow channel at Emu Point. Figure 1.1 shows the location of Oyster Harbour, King George Sound and the nearby embayment of Princess Royal Harbour which lies immediately southeast of Albany.

Extensive clearing of land for agriculture over much of Oyster Harbour's catchment has occurred during the last 30 years. Most of this land is used for broad acre farming and sheep grazing and is regularly fertilized with nitrogenous and phosphatic compounds. A small but significant percentage of these nutrients leach into runoff and are discharged into Oyster Harbour via the catchment's two major rivers, the King and Kalgan (Figure 1.1).

It is estimated that Oyster Harbour has received average annual loads of about 30 tonnes of total phosphorus (P) and about 350 tonnes of total nitrogen (N) via river discharge since the early 1960s (Simpson and Masini, 1990). This has led to the prolific growth of epiphytic algae and the macroalga *Cladophora* sp. in Oyster Harbour (Hillman *et al.*, 1991a). Before this period the macroalga was not a major component of Oyster Harbour's benthic communities (McKenzie, 1964). However, the high rate of P and N loading has altered the ecological balance in the harbour to the extent that *Cladophora* sp. is now present in nuisance proportions. At last estimate there were of order 1200 tonnes dry weight of macroalgae in Oyster Harbour having a spatially averaged benthic areal distribution of approximately 77 g dry weight m^{-2} (Hillman *et al.*, 1991a). This harbour is classified as eutrophic according to the classification scheme for trophic status described by McComb and Lukatelich (1986) for Australian embayments.

The algae have smothered and shaded what were once extensive stands of seagrass communities (*Posidonia australis, Posidonia sinuosa and Amphibolis antarctica*) leading to their extensive dieback with over 80 percent of the original seagrass biomass in Oyster Harbour now lost due to light limitation.

The bulk of nutrients that enter Oyster Harbour arrive via buoyant river discharge. As is typical in estuaries, riverine freshwater enters the system at the surface as buoyant fronts, leading to the vertical and horizontal stratification of salinity. In the absence of sufficiently strong environmental forcings (such as wind, tide or atmospheric heating and cooling) mixing of these gravitational overflows, with resident harbour water, will be minimal and the stratification will persist. Internal currents, vertical mixing and exchange with the ocean will be governed by four main mechanisms; tidal pumping, wind mixing, streamflow, and currents driven by density differences. In regions where tidal flows are strong, such as in narrow channels, currents driven by the tides will dominate the hydrodynamic behaviour. In other regions of the estuary mixing and transport will be due to a complicated interplay between all four mechanisms.

This report presents the results of a study on the mixing and transport of mass within Oyster Harbour and on the nature of hydraulic exchange between Oyster Harbour and King George Sound. Because Oyster Harbour is estuarine in physical nature the investigation addresses hydrodynamic questions related to the influence of environmental forcings (wind, tide, streamflow, solar heating and atmospheric cooling) on the density structure of Oyster Harbour, which is typically stratified vertically and horizontally in both temperature and salinity.

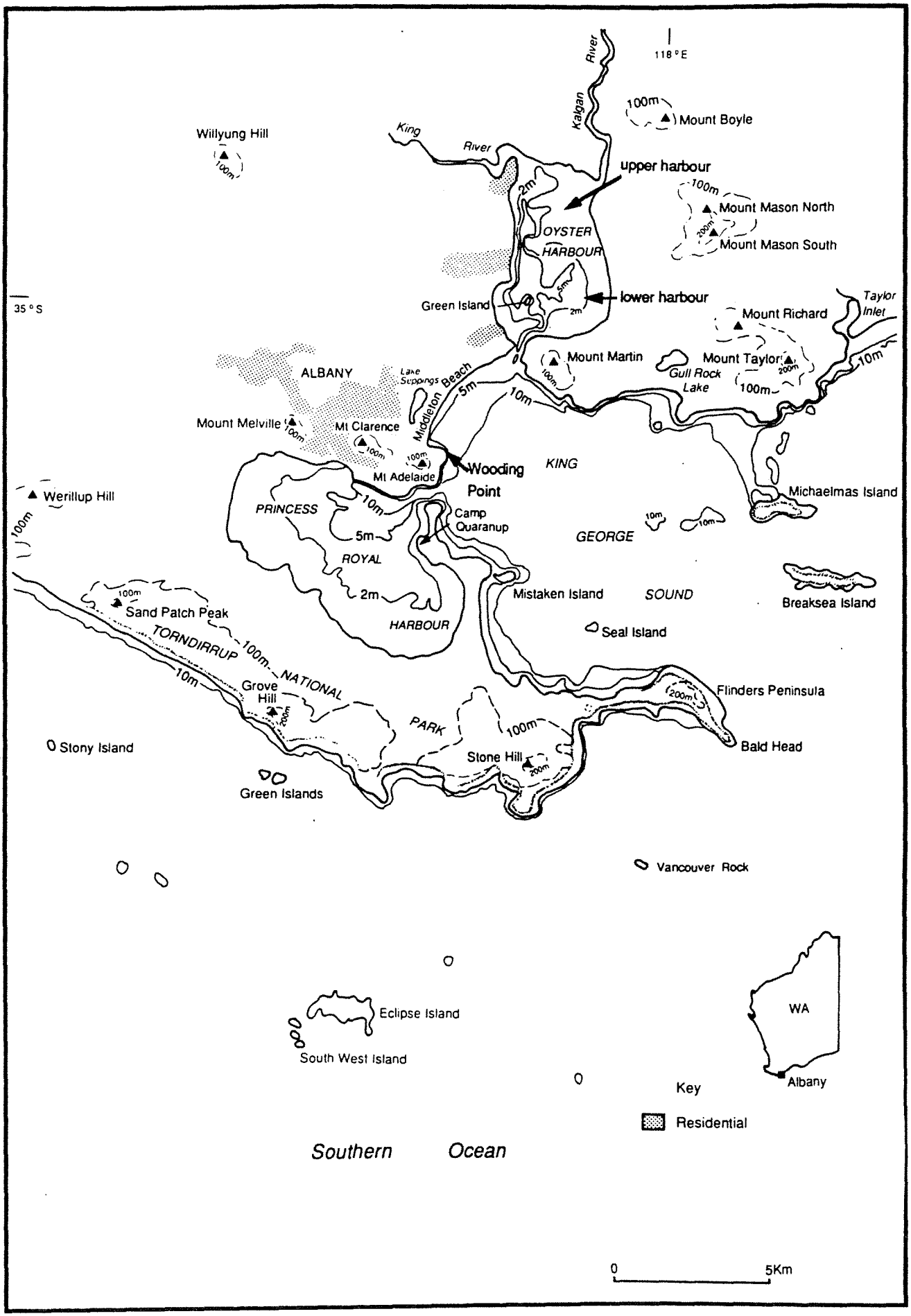

Figure 1.1 Albany's harbours and adjacent areas

Most of the riverine discharge into Oyster Harbour occurs in winter from about June to August. Important mixing agents such as winds and atmospheric heating and cooling can also display seasonal differences. Because of this seasonality, the circulation of Oyster Harbour in summer and winter is discussed separately in this report.

The study was undertaken by the Marine Impacts Branch of the EPA, with assistance from the Centre for Water Research (University of Western Australia), and the Australian Surveying and Land Information Group. Existing information of the water structure, local meteorology, river flows and current patterns were complemented by intensive field surveys conducted for this study.

The study had the following overall aims:

- to determine the seasonal characteristics of stratification in Oyster Harbour;
- to quantify the influence of winds, streamflow, tides, and atmospheric heating and cooling on the internal mixing and transport characteristics of Oyster Harbour; and
- to determine the exchange characteristics between Oyster Harbour and King George Sound.

A description of the hydrology, bathymetry, rainfall, water level variation, winds and topography of Oyster Harbour and its adjacent water bodies is given in Chapter 2.

The data set utilised for this study is described in Chapter 3.

Chapters 4 and 5 discuss the respective winter and summer hydrodynamics of Oyster Harbour.

Chapter 6 presents the conclusions of the study.

2. Site

2.1 Site location, topography and bathymetry

Oyster Harbour is situated approximately 10km northeast of the town of Albany, on the south coast of Western Australia (Figure 1.1). Its centre lies approximately at latitude 34° 58' S and longitude 117° 57' E. It is roughly rectangular in shape, has approximate dimensions of 3km by 5km and its longest axis is aligned north-south. It was formed by the drowning of the lower valley of the tributary King-Kalgan river system during the Pleistocene eustatism (McKenzie, 1964).

The topography surrounding Oyster Harbour is dominated by hills (up to 200m in height) to the east (Figure 1.1) and gently undulating land (up to 40m in height) to the north and west. Gull Rock Lake to the south-east lies within a valley between two peaks (Mount Martin and Mount Richard). The King and Kalgan Rivers discharge into the northwest and northeast corners, respectively, of Oyster Harbour.

Oyster Harbour communicates with King George Sound via a relatively narrow channel at Emu Point which has an approximate width of 150m and maximum depth of about 12m. King George Sound is a much larger coastal embayment and opens out into the Southern Ocean. It receives some protection to the full force of the seas and swells of the Southern Ocean by islands, headlands, spits, bars and tombolas around its outer periphery (see Figure 1.1).

The shoreline running to the southwest of Emu Point forms a gently curving concave coastline 4km long and is named Middleton Beach. Middleton Beach is bounded to the south by Wooding Point which is the northern tip of a rocky headland (Figure 1.1). This rocky headland is the northern lip of the mouth of Princess Royal Harbour, which is an embayment situated adjacent to and southeast of the town of Albany.

Within Oyster Harbour the bathymetrical variation effectively divides the estuary into two relatively deep basins, one in the upper harbour and one in the lower harbour, as shown in Figure 2.1.

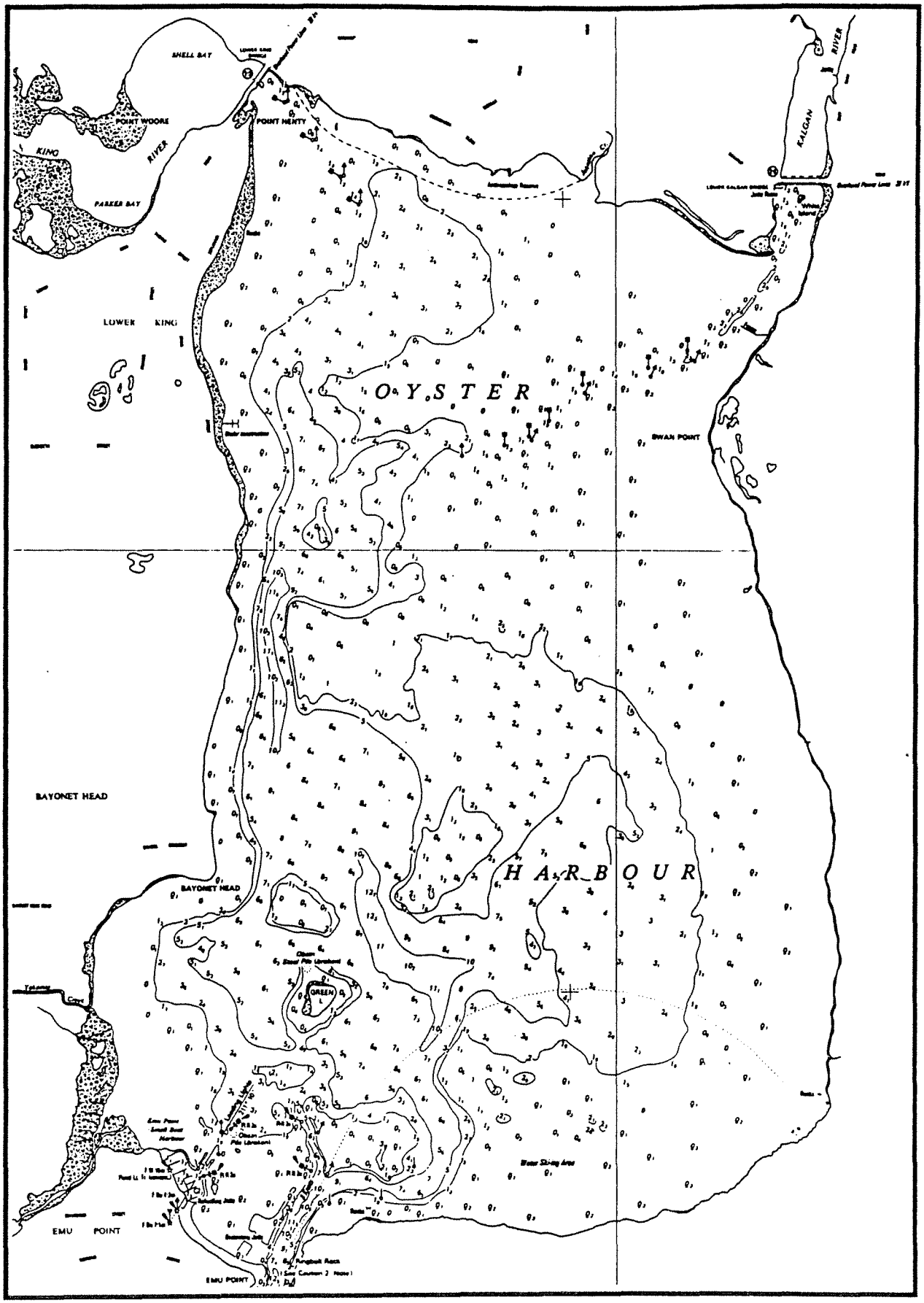

Figure 2.1 Bathymetry of Oyster Harbour

The basin in the upper harbour is the smallest and has a maximum depth of about 8m. A narrow channel, approximately 12m deep, forms the main hydraulic connection between the upper harbour and the larger basin of the lower harbour. The basin of the lower harbour has a maximum depth of approximately 12m and has Green Island situated in its southwest corner.

Another major feature of Oyster Harbour's bathymetry is the existence of extensive areas of peripheral shallows, with depths less than 1m occurring over approximately half of Oyster Harbour's total area (see Figure 2.1). The shallows are active depositional sites for sediments which arrive in river floods, particularly in the vicinity of the King and Kalgan River mouths. The entire eastern side of Oyster Harbour is relatively shallow and has an associated bathymetry that either dries or is less than 0.2m deep at low water. Along with similar regions in the southwest and northwest corners of the harbour these very shallow regions comprise about 40 percent of the harbour's total area.

McKenzie's (1964) description of the bathymetry of Oyster Harbour was based on surveys he conducted before the serious decline of the seagrass meadows. At the time, he defined the bathymetrical zones between the 1 and 6m depth contours as *Posidonia* slopes because of the abundance of *Posidonia* seagrasses in these zones. Hillman *et al* (1991a and b) have mapped the more recent spatial distribution of seagrass in Oyster Harbour and have shown that about 80 percent of Oyster Harbour's original seagrass biomass has been lost due to shading and smothering by macroalgae. As a consequence, much of the original area once covered by luxuriant seagrass meadows is now either barren or covered in macroalgae. The severe rate of decline in seagrass biomass for Oyster Harbour is highlighted in the data of total biomass for 1981, 1984 and 1988, presented in Figure 2.2 (data from Hillman *et al*, 1991b, diagram from Simpson and Masini, 1990).

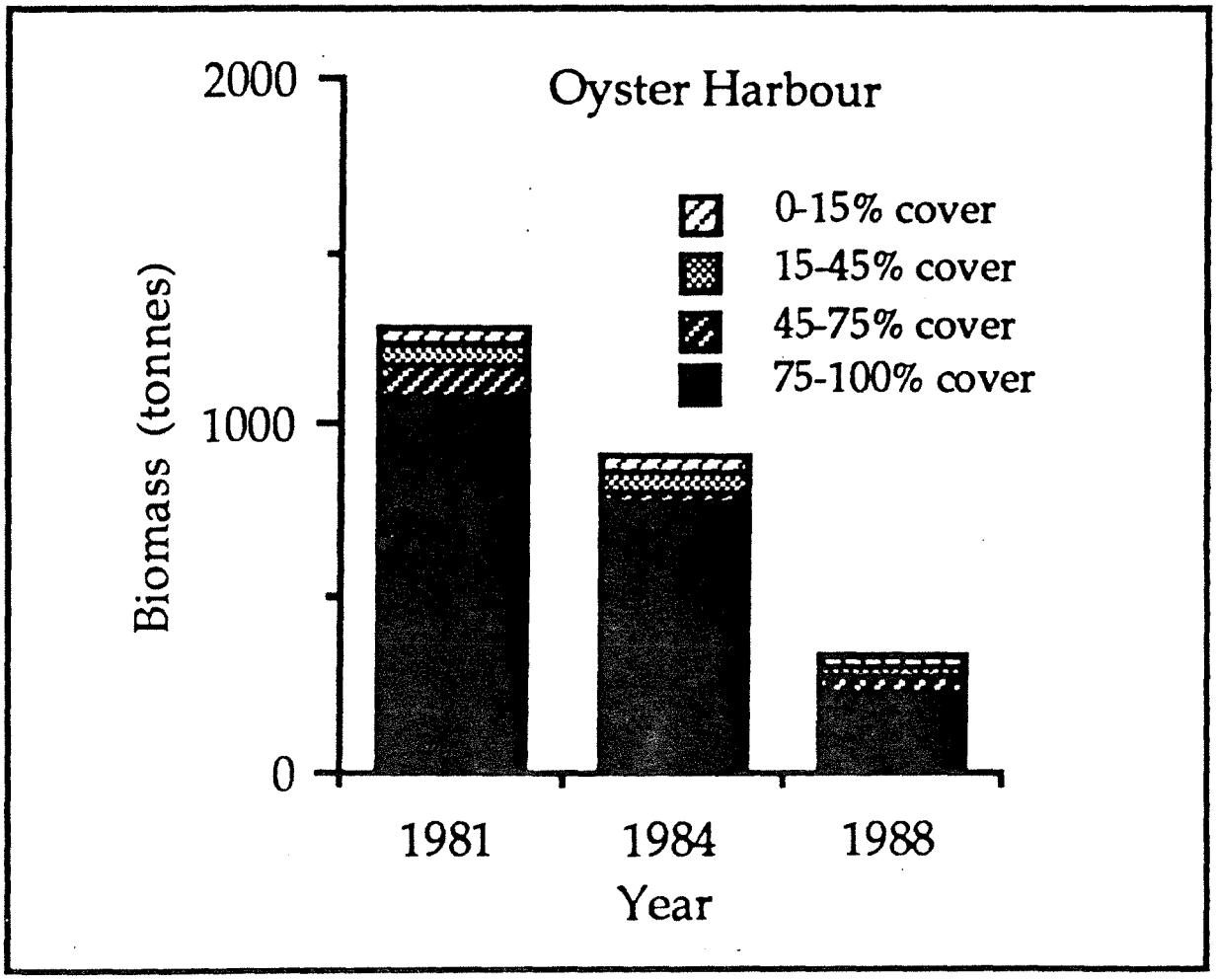

Figure 2.2 Decrease in seagrass biomass in Oyster Harbour from 1981 to 1988. (from Simpson and Masini, 1990)

2.2 Hydrology

Oyster Harbour receives seasonal freshwater discharges via the King and Kalgan Rivers, Yakamia Creek and other minor drains around the harbour's periphery. The Kalgan River is by far the largest contributor to total streamflow because of its very large catchment area when compared to the catchments of the King River and other drains and tributaries, as shown in Figure 2.3.

The bulk of freshwater flows and associated nutrient inputs occur in river flood flows caused by annual winter rainfall in the period from about June to August of each year (Simpson and Masini, 1990). However, the occasional passage of cyclonic depressions and low pressure fronts can result in significant amounts of rain on the catchments and lead to strong discharge events. Mr G Bott of the EPA has reduced Kalgan River discharge data for the period 1976 to 1988 (presented in Simpson and Masini, 1990) to produce the plot of daily discharge versus time shown in Figure 2.4. The extremely high discharge event evident in January 1982 was caused by the rainfall of cyclone Bruno's depression, which passed over the Kalgan River catchment.

Average total yearly discharge into Oyster Harbour is of the order of 50 million $m^3\ yr^{-1}$, but can vary from about 10 to 150 million $m^3\ yr^{-1}$ depending on rainfall (Simpson and Masini, 1990). Oyster Harbour has a volume of the order of 40 million m^3. So, in terms of equivalent harbour volumes the annual discharge of freshwater into Oyster Harbour can equate to up to 3 to 4 harbour volumes. This suggests the important influence that these rivers have on the seasonal hydrodynamics of Oyster Harbour in terms of their flux of buoyancy to the system.

2.3 Rainfall

The wettest six-monthly period of the year over the southwest of Western Australia, including Albany and its surrounding catchment areas, is from May to October (Bureau of Meteorology, 1984). The Bureau of Meteorology have analysed over 100 years (1877 to 1988) of rainfall data collected at Albany (station No. 009500, having coordinates 35° 01' S latitude and 117° 53' E longitude). The mean annual rainfall calculated from these data is 936mm and the mean monthly rainfall values are presented in Figure 2.5.

Rainfall events at Albany are typically of duration less than 1 week. Daily rainfall data collected by the Bureau of Meteorology at centennial oval, Albany, is shown in Figure 2.6 for 1988. These data highlight the occurrence of discrete rainfall peaks with durations of the order 3 to 5 days. These events generally accompany the passage of winter storms associated with anticyclonic low pressure systems that travel from west to east, extending in that direction right across the Australian continent. In winter the southern edges of these anticyclonic belts generally lie to the south of the State and therefore cause rainbearing winds from the southwest-northwest arc. During the summer months the anticyclonic belt moves southward and this gives rise to hot dry conditions as a result of a predominantly easterly air-stream.

2.4 Water level

The periodic water level variation in both Oyster Harbour and Princess Royal Harbour is primarily due to the oceanic tidal variation occurring in King George Sound. The Albany tide gauge is situated in Princess Royal Harbour at latitude 35° 02' S and longitude 117° 53' E. The tidal signal for Albany can be transferred to Oyster Harbour with little error in water level or phase (Don Wallace, Department of Marine and Harbours of Western Australia, pers. comm.).

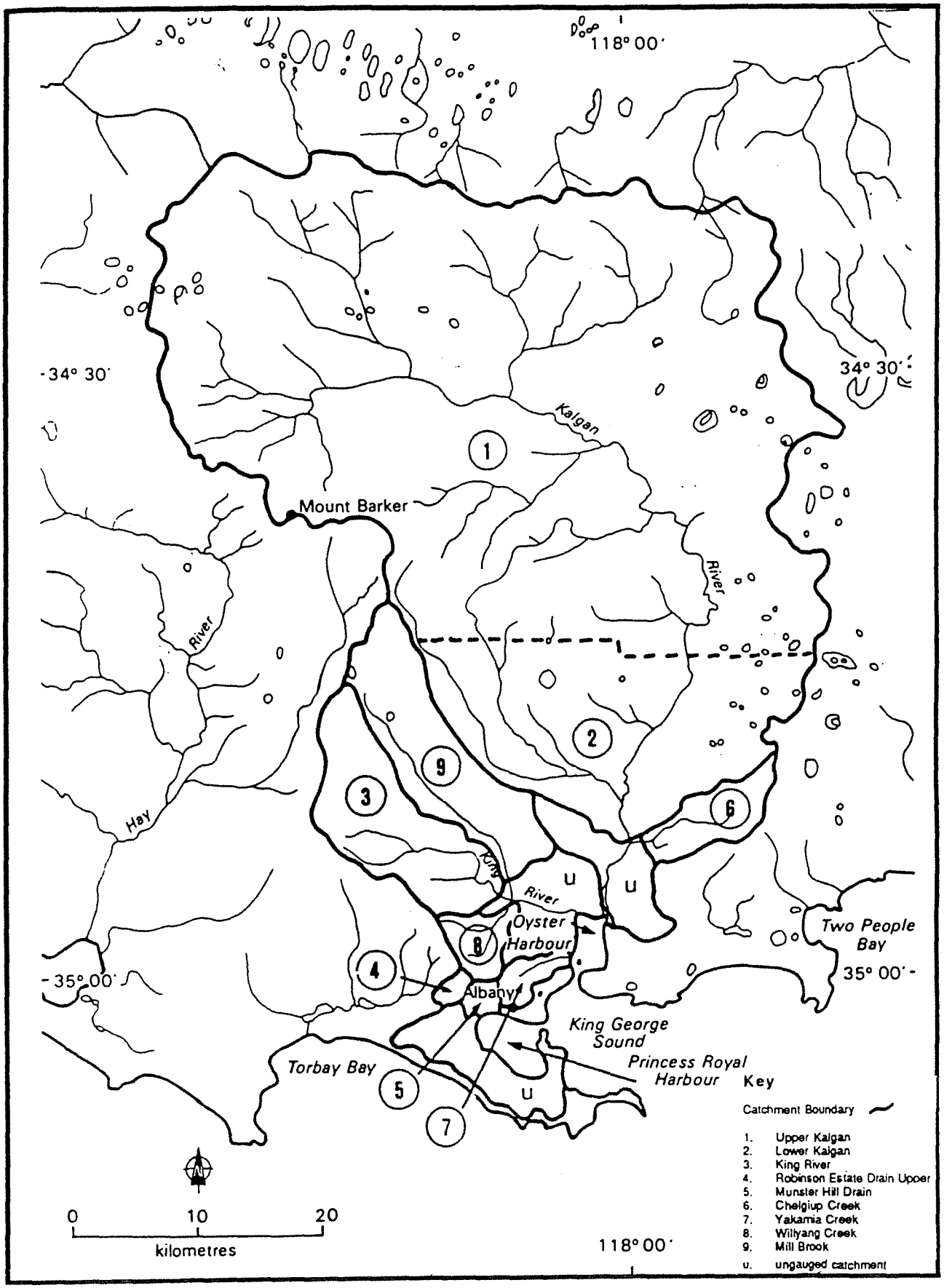

Figure 2.3 Drainage catchment boundaries for Oyster Harbour and Princess Royal Harbour (from Simpson and Masini, 1990).

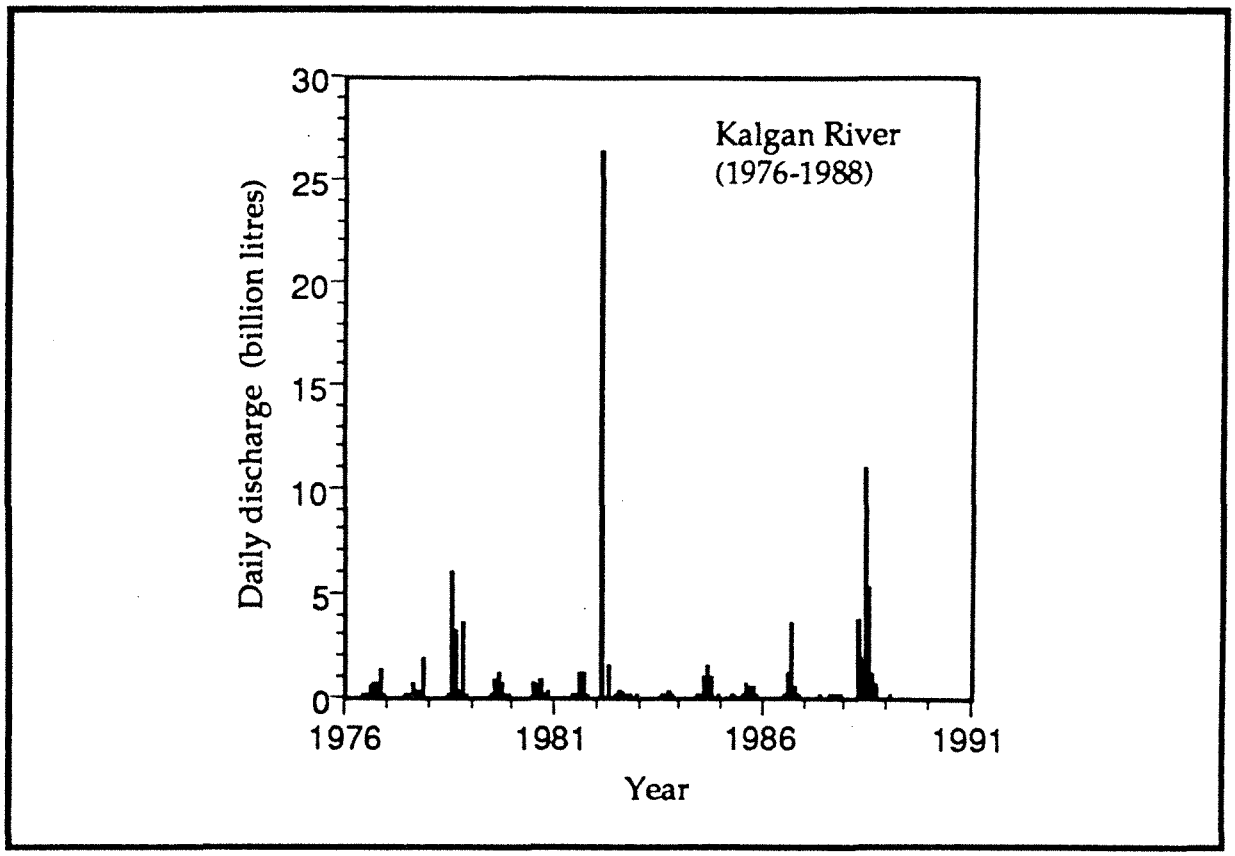

Figure 2.4 Discharge rates of the Kalgan River. Data period: 1976 - 1988 (from Simpson and Masini, 1990).

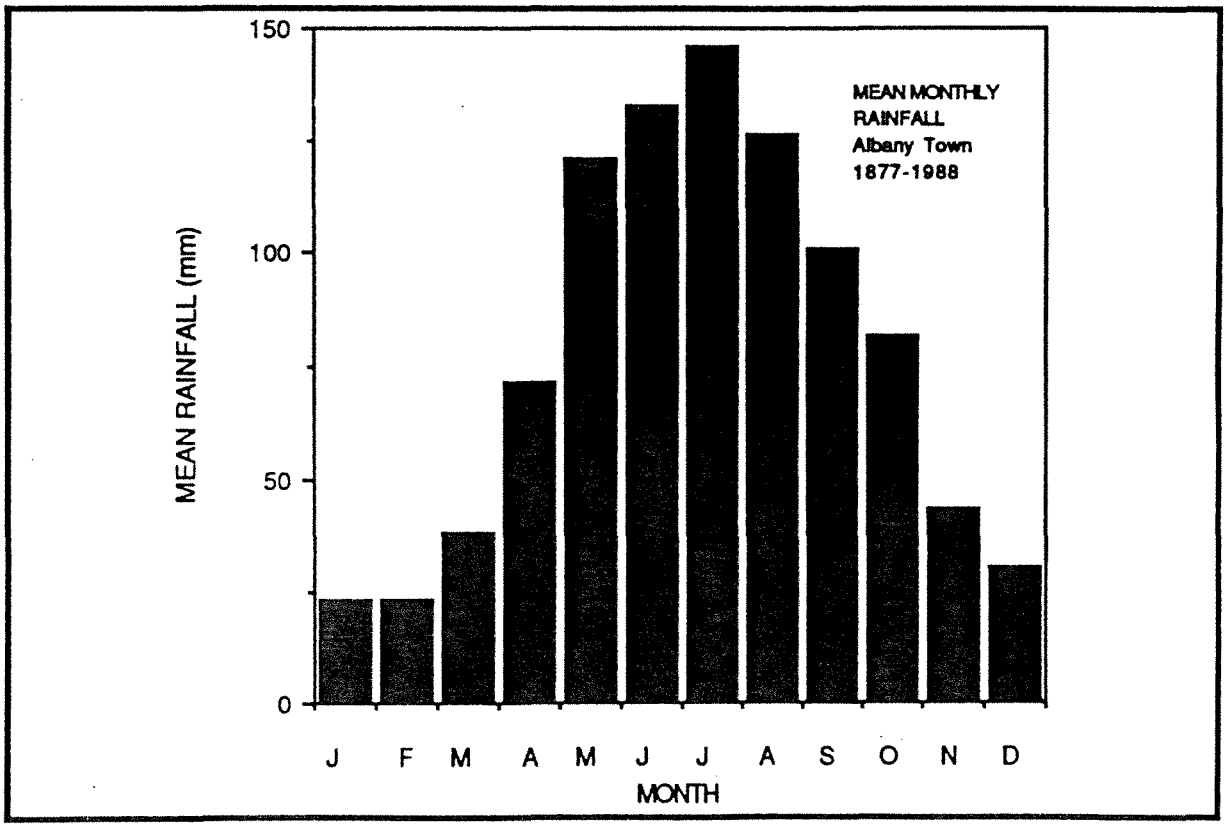

Figure 2.5 Mean monthly rainfall at Albany calculated from data from 1877 - 1988. (Data from Bureau of Meteorology.)

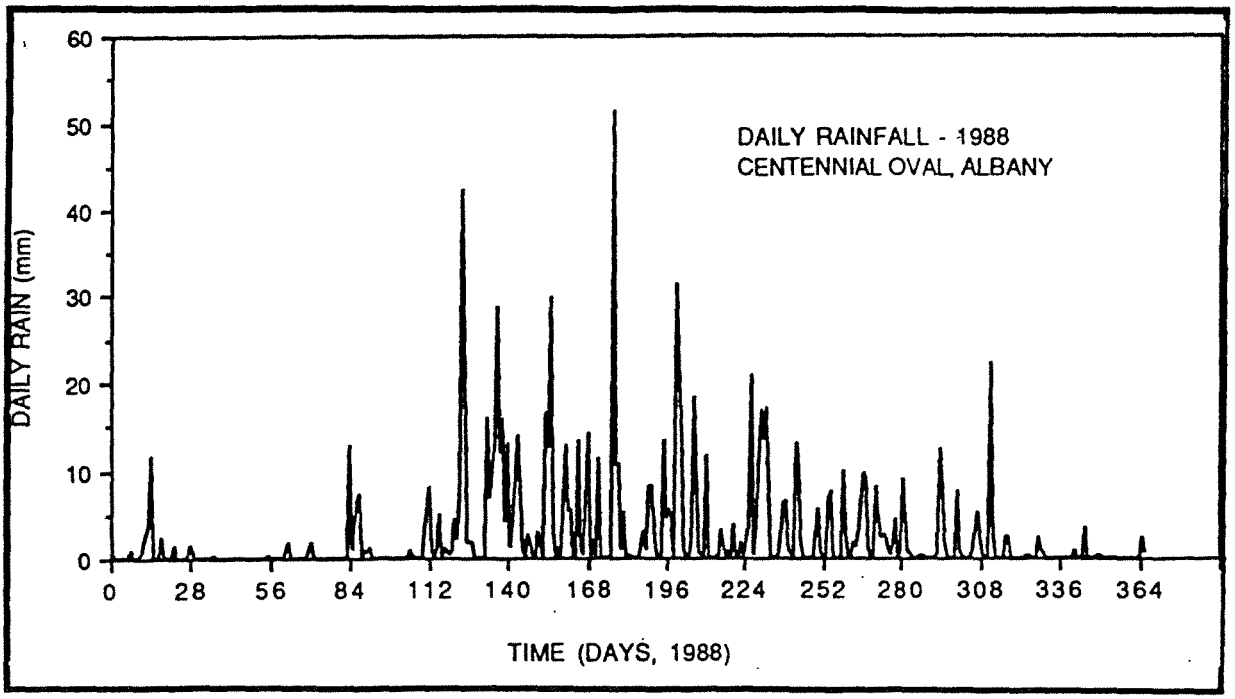

Figure 2.6 Daily rainfall at Centennial Oval, Albany, for 1988. Data from the Bureau of Meteorology.

The spectral characteristics of water level fluctuations at the Albany tide gauge were analysed for the period 31 Dec 1986 to 1 Jan 1988 by the Flinders Institute of Atmospheric and Marine Science, South Australia. The spectral energy plot resulting from that analysis is presented in Figure 2.7. These data highlight the dominating influence of the diurnal, and to a lesser extent, semi-diurnal components to the tidal signal for Albany.

The tides at Albany follow a typical neap to spring pattern with tidal amplitudes varying from about 0.15m to 0.6m. Hence, the water level in Oyster Harbour can change diurnally by as much as approximately 1.2m during spring tidal cycles or as little as approximately 0.3m during neap tidal cycles. A representative time series of water level recorded in February 1989 is shown in Figure 2.8 and these data highlight the features of the tide at Albany.

In addition to the astronomic tides discussed above, meteorological forcings can also cause significant fluctuations in the sea level of coastal waters. In particular, storm surges can occur along the coast during strong onshore winds. For example, Hodgkin and Di Lollo (1958) and Fandry *et al* (1984) found that very strong onshore winds associated with cyclonic depressions caused water level surges at Fremantle, Western Australia, of up to 1m. Significant depressions in coastal water levels could also be expected during very strong offshore winds.

2.5 Winds

Little work has been done in analysing the statistical properties of wind records for Oyster Harbour. The Bureau of Meteorology has an office in Albany which runs a meteorological station from which continuous chart recordings of wind speed and direction are made. These data are available from the Bureau as daily plots of wind speed and direction time series.

The Bureau also reduces the continuous wind data into 3 hourly readings of wind speed (to 0.5m s^{-1} accuracy) and direction (to 22.5 deg. accuracy). These analyses are performed, by officers of the Bureau, by reading from the charts the mean wind speed and direction that was recorded during the 10 minutes prior to the beginning of every third hour of each day, and in this way eight readings per day are recorded. Time series plots of wind speed from these 3 hourly data sets are presented in Figures 2.9 and 2.10 for the summer 1987/88 and winter 1988 periods, respectively. As shown, winds were variable at Albany and ranged from calms to violent storm conditions of nearly 20m s^{-1}.

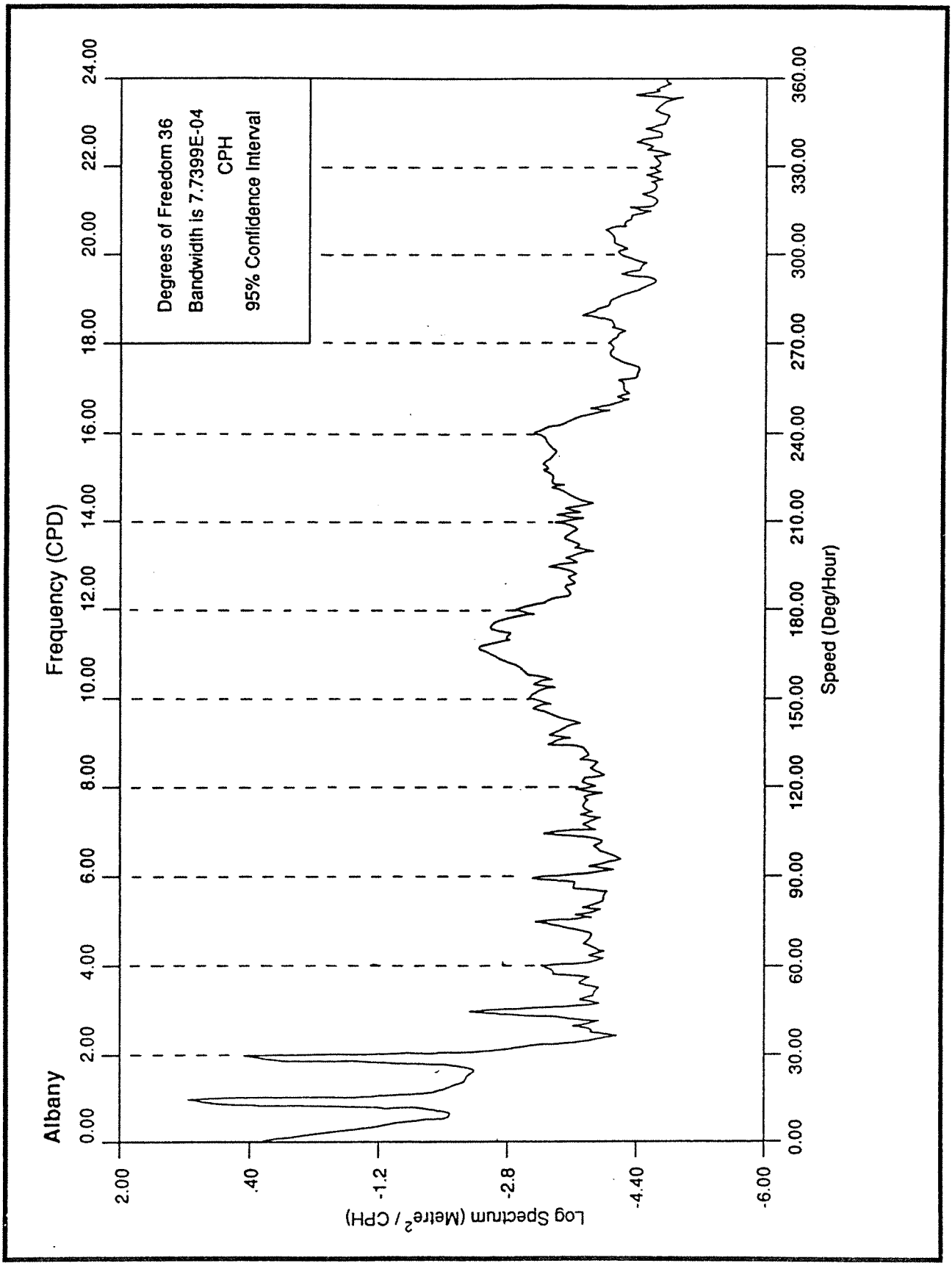

Figure 2.7 Spectral energy plot for tide date at Albany; Year - 1987. (Source: Flinders Institute of Atmospheric and Marine Science.)

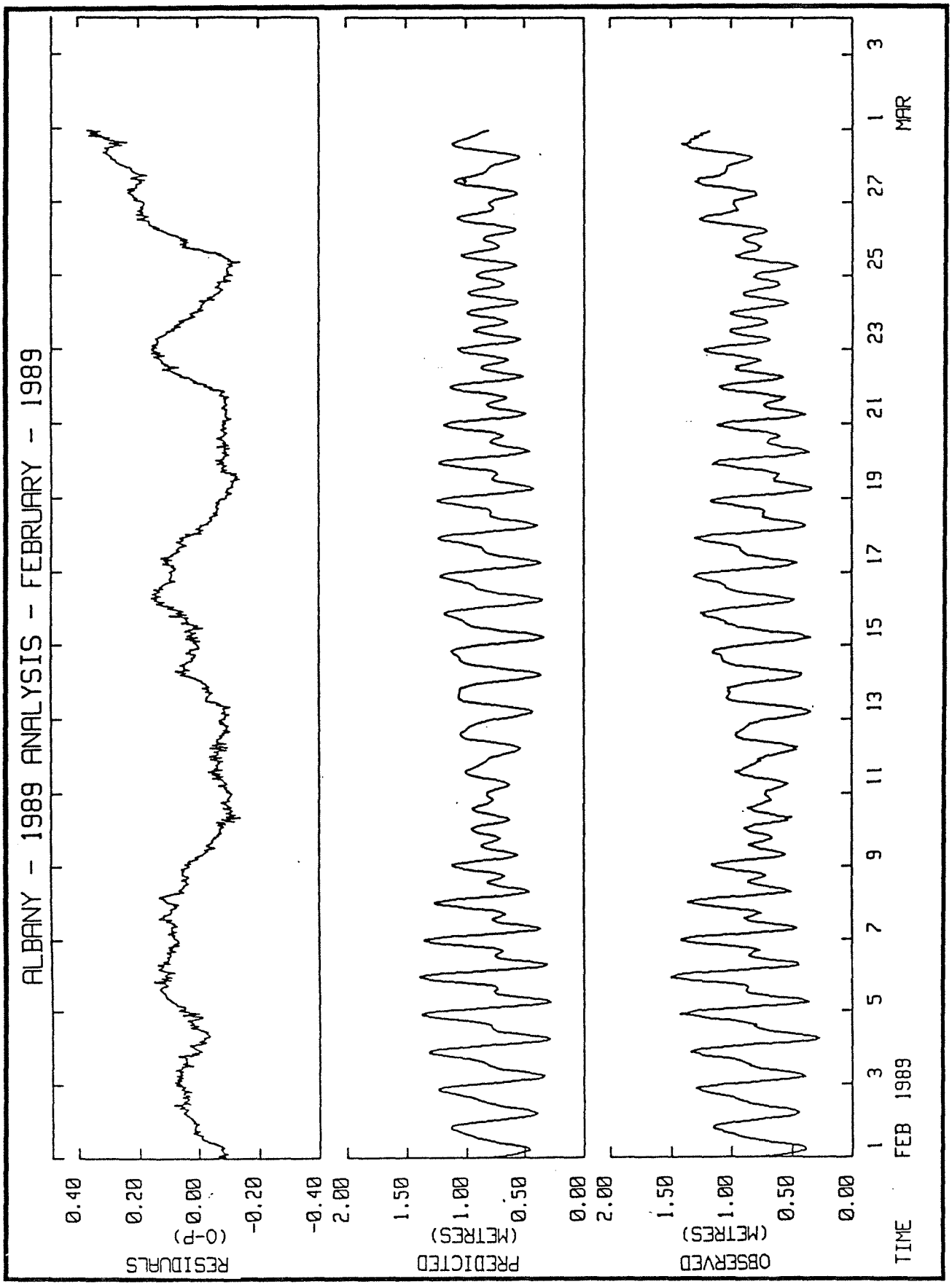

Figure 2.8 Water level at Albany for February 1989. (Source: Flinders Institute of Atmospheric and Marine Science.)

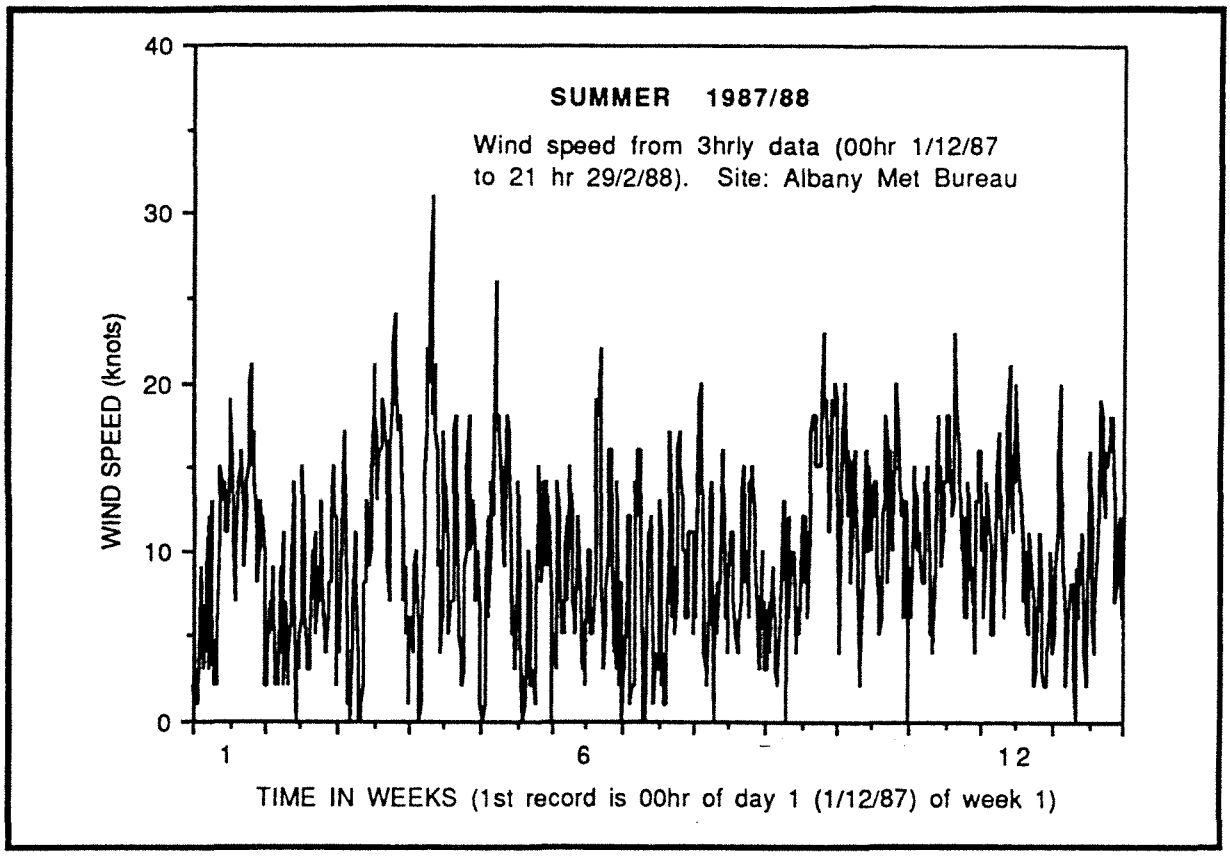

Figure 2.9 Time series of wind speed at Albany for the summer period: 1.12.87 to 29.2.88. Station: Albany Bureau of Meteorology.

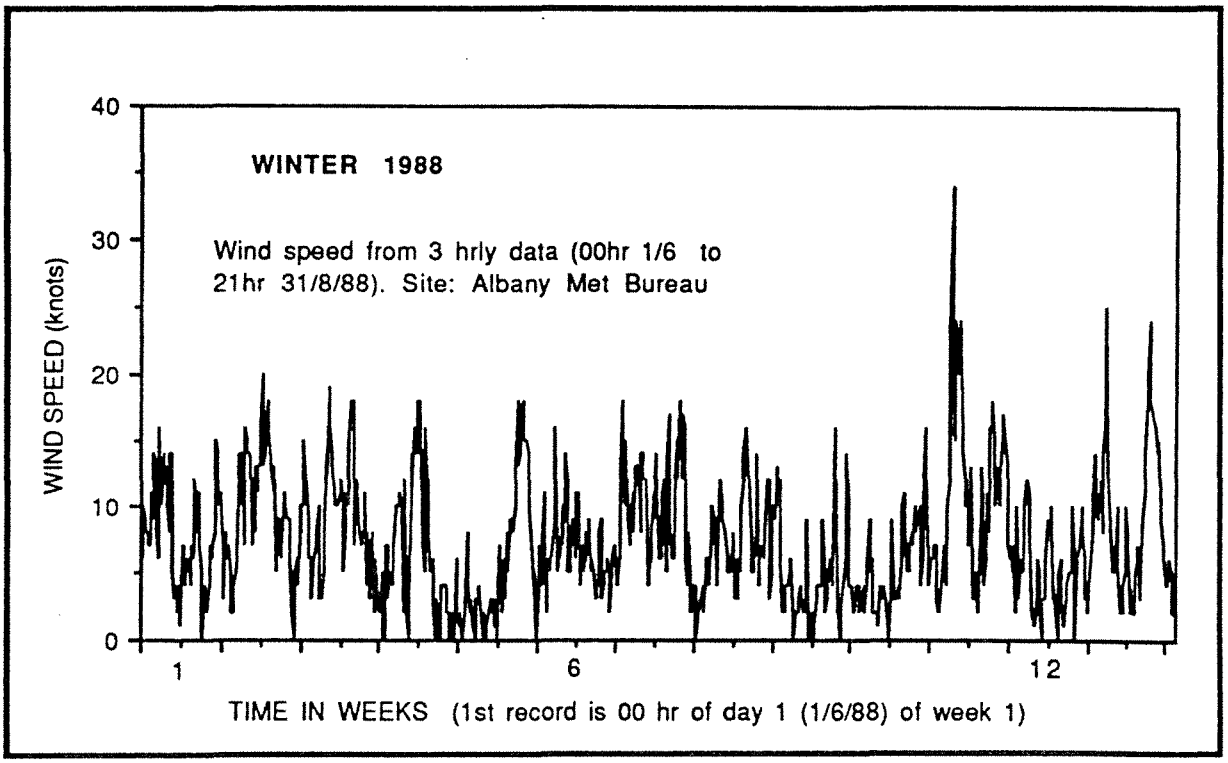

Figure 2.10 Time series of wind speed at Albany for the winter period: 1.6 to 31.8.88. Station: Albany Bureau of Meteorology.

Generally, in summer (December to February) the wind field is characterised by morning easterlies with speeds less than about 5m s^{-1} and stronger afternoon sea breezes with speeds up to 15m s^{-1}. However, the winds at Albany can vary from this classical land-sea breeze summer pattern in the summer months in response to the movement of pressure systems from west to east. Randomly occurring low pressure fronts can bring storm winds, typically from the northwest, and cyclonic depressions can sometimes pass over the Albany region and bring significant winds and amounts of rain during the summer months.

Approximately 32 % of the summer wind records in Figure 2.9 had speeds less than or equal to 3m s^{-1} and approximately 57 % of the records had speeds less than or equal to 5m s^{-1}. Of all the winter wind records in Figure 2.10, approximately 50 % had speeds less than or equal to 3m s^{-1} and approximately 75% of the records had speeds less than or equal to 5m s^{-1}.

Pattiaratchi (1991) has performed statistical analyses on hourly wind velocity data from the Sand Patch Peak wind station for the period 23 march 1990 to 22 January 1991. That wind station is run by the State Electricity Commission of Western Australia and the Sand Patch location is shown in Figure 1.1. Pattiaratchi's (1991) analysis shows that for the 300 day sample period winds were less than or equal to 5m s^{-1} for about 32 % of the records and less than or equal to 8m s^{-1} for about 54 % of the records.

The majority of summer winds at Albany arrive from within the southwest-east arc, as is indicated in Figure 2.11 which presents wind roses of wind speed and direction synthesized from observations taken twice daily (0900 and 1500) during January over a 19 year period at Albany airport. During the winter months (June to August) calmer morning winds occur typically from the northwest-north arc and swing to arrive predominantly from the southwest-northwest arc in the afternoon. This feature of the winter wind pattern is also indicated in Figure 2.11, presenting wind roses of wind speed and direction synthesized from observations taken twice daily (0900 and 1500) during July over a 19 year period at Albany airport.

3. Data

3.1 Seasonal stratification data

Seasonal stratification data of salinity and temperature were collected by the Centre for Water Research (Hillman *et al*, 1991a) at 2 to 4 week intervals between December 1987 and February 1989 at the five stations shown in Figure 3.1. Vertical profiles of salinity and temperature were made at approximately 0.5m vertical spacing in quick succession between stations using a Hamon Model 602 Auto-lab portable salinity-temperature bridge meter. The accuracy of these data are about 0.05 parts per thousand (ppt) and 0.1°C for salinity and temperature, respectively.

3.2 High resolution summer stratification data

Relatively high resolution data of the three-dimensional salinity and temperature structure of Oyster Harbour were collected from 13 to 17 February 1989. More than thirty stations (Figure 3.1) were sampled in quick succession over a fixed grid up to 5 times per day by profiling with a conductivity-temperature-depth (CTD) probe provided by the Centre for Water Research. Technical details of the CTD probe are given in Fozdar (1983).

The CTD probe collected data with a vertical resolution of 2-5cm at a sampling frequency of 50 hz. The temperature and salinity data from the CTD are returned at resolutions of 0.001°C and 0.001 ppt, respectively. The free falling probe descended at a rate of about 1m s^{-1} yielding up to 50 data points per vertical metre. The data were retrieved to an onboard mini-computer via a cable and were viewed on the graphics screen as vertical profiles. In this way the field work could be adjusted in the field as important dynamical processes and mechanisms became apparent during the data collection.

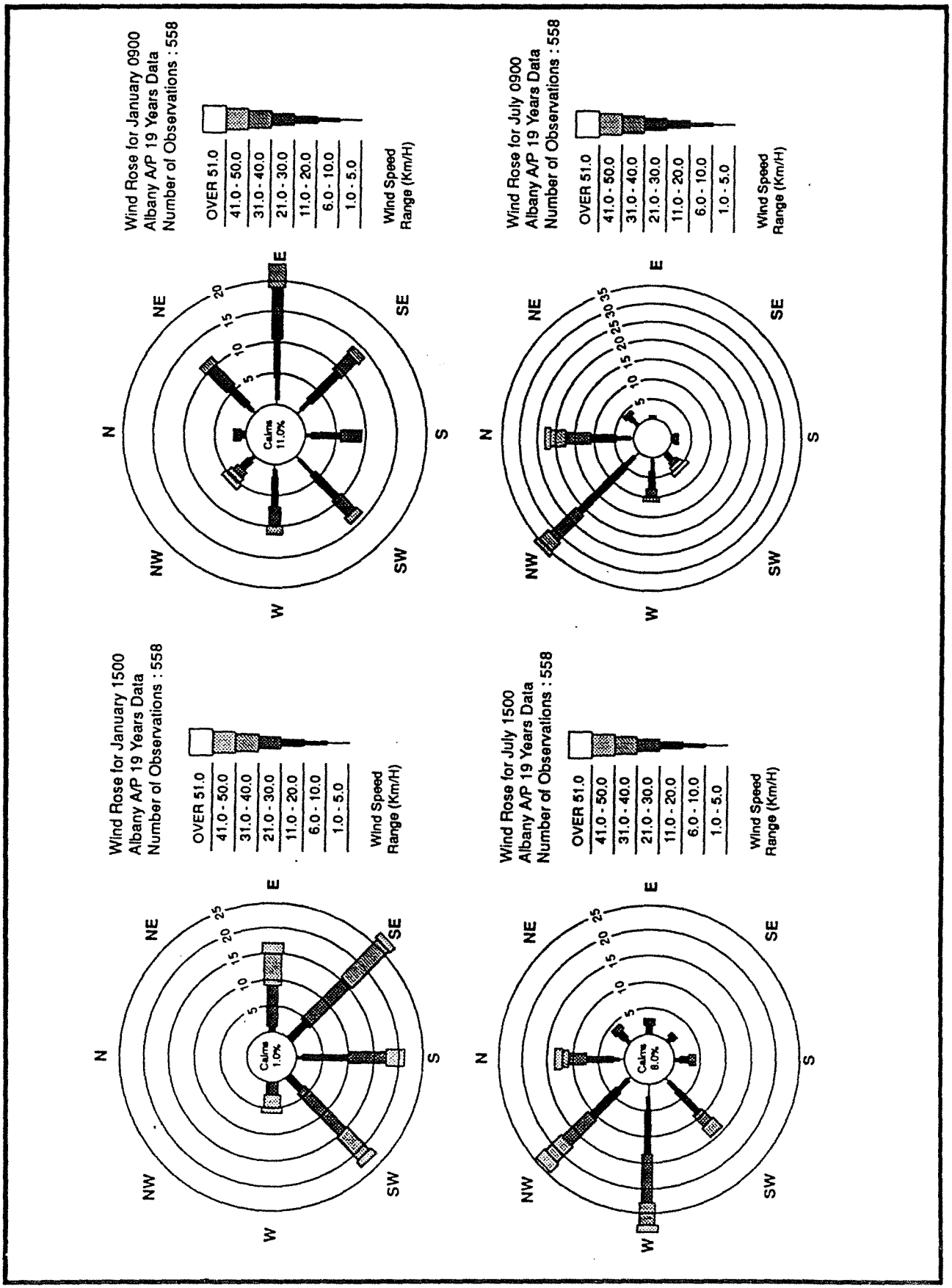

Figure 2.11 Wind roses from spot readings of wind speed at 0900 and 1500 for January and July over a 19 year period. Station: Albany airport.

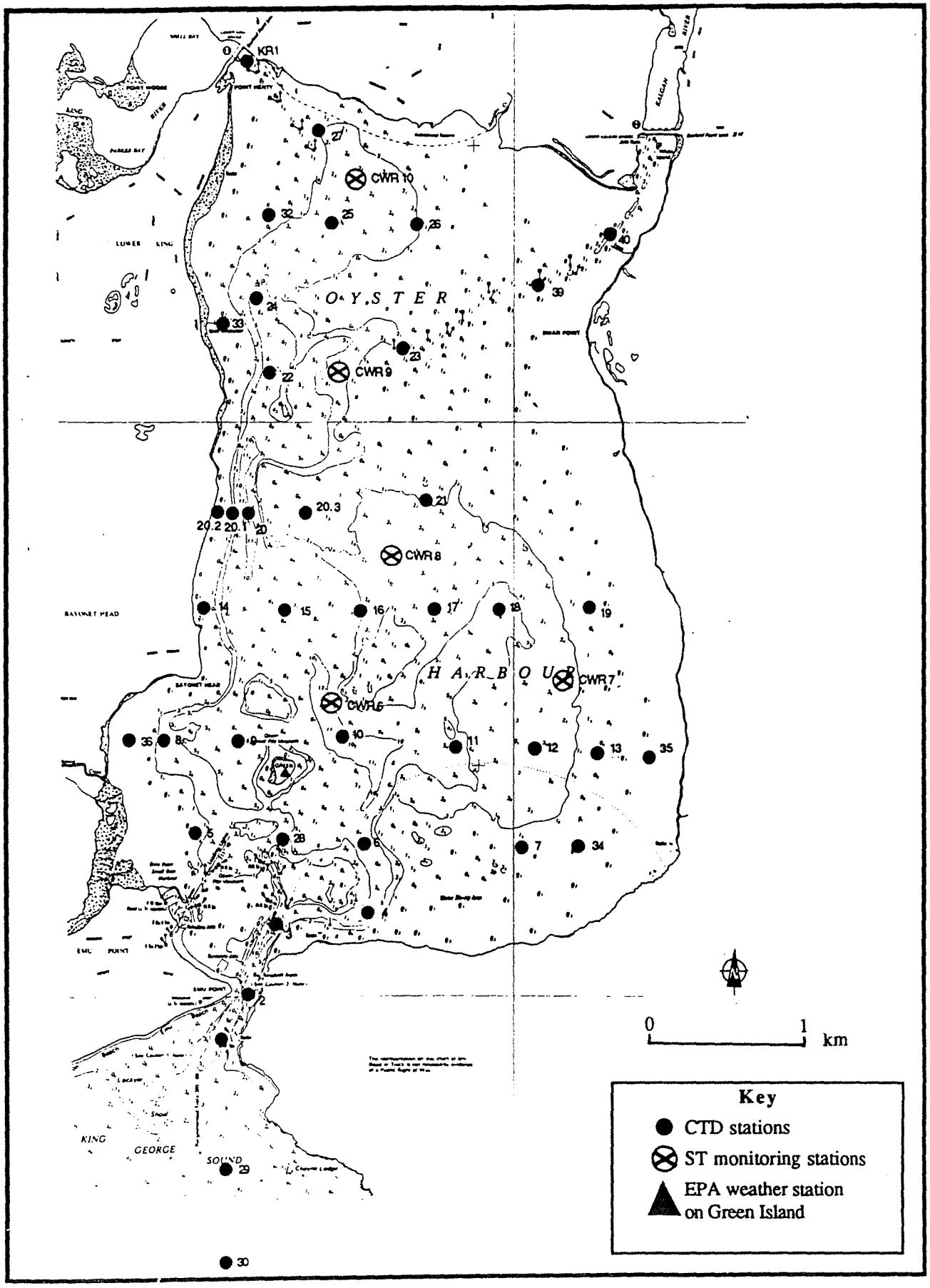

Figure 3.1 CTD, ST and Green Island weather station locations.

3.3 Meteorology and hydrology

Wind speed and direction data were obtained from the Albany office of the Bureau of Meteorology situated next to the Albany airport at coordinates of 34° 57' S and 117° 48' E. The office collected continuous chart recordings of wind speed and direction using a Dines pressure tube anemometer up to August 1988 and since then it uses a Synchrotac anemometer. The anemometer has an elevation of 10m above local ground level and 79m above mean sea level.

In addition to the above a UNIDATA weather station was installed on Green Island, Oyster Harbour (see Figure 3.1), by the EPA at a reduced level of 18.73m with respect to Australian Height Datum (AHD). This instrument measured wind speed and direction, solar short-wave radiation and air temperature from 13 to 17 February 1989 and these data were recorded as 10 minute averages.

The Albany office of the Bureau collects rainfall data from a gauge situated at Centennial Oval, in the town of Albany. This data is in the form of total daily rainfall. The Bureau have also analysed the statistical properties of over 100 years (1877 to 1988) of rainfall data collected at Albany (station No. 009500; coordinates, latitude 35° 01' S and longitude 117° 53' E).

Records of gauged streamflow exist for the Kalgan River for the period 1976-1988 and these data were collected by the Water Authority of Western Australia. The other rivers and creeks draining into Oyster Harbour have only been gauged during 1987 and 1988. Mr G. Bott of the EPA has analysed these data and the results of that analysis are presented in Simpson and Masini (1990).

3.4 Water level

The water level variation in Oyster Harbour due to astronomic tides and meteorological forcings can be assumed to follow very closely that measured by the Albany tide gauge (Don Wallace, Department of Marine and Harbours of Western Australia, pers. comm.). The Albany tide gauge is situated in Princess Royal Harbour, adjacent to the town, at coordinates latitude 35° 02' S and longitude 117° 53' E.

3.5 Currents

Two major field surveys of the currents in and around Oyster Harbour have been made to date.

The first survey was conducted by Dr D. Mills of the EPA in which four Neil Brown acoustic NBIS ACM-2 current meters were deployed in King George Sound, at the stations shown in Figure 3.2, from 5 November 1986 to 9 March 1987. These meters recorded integrated speed and direction over a predetermined sampling interval of 5 minutes as well as instantaneous temperature data every 5 minutes. Details of the current meter deployment are given in Table 3.1. Pattiaratchi *et al* (1991) has analysed some of the current meter data and the complete raw data set are archived at the premises of the Environmental Protection Authority (Ref: Dr Des Mills, EPA).

The second survey of currents was conducted by the EPA between 13 and 17 February 1989 and this involved drogue tracking. Free-drifting cross-vane drogues were deployed and tracked, using telemetry. The survey regions included the entire southern half of Oyster Harbour, the channel at Emu Point and the waters of King George Sound in front of the Oyster Harbour mouth. Both the internal circulation of Oyster Harbour and tidal flows out of and into Oyster Harbour were tracked.

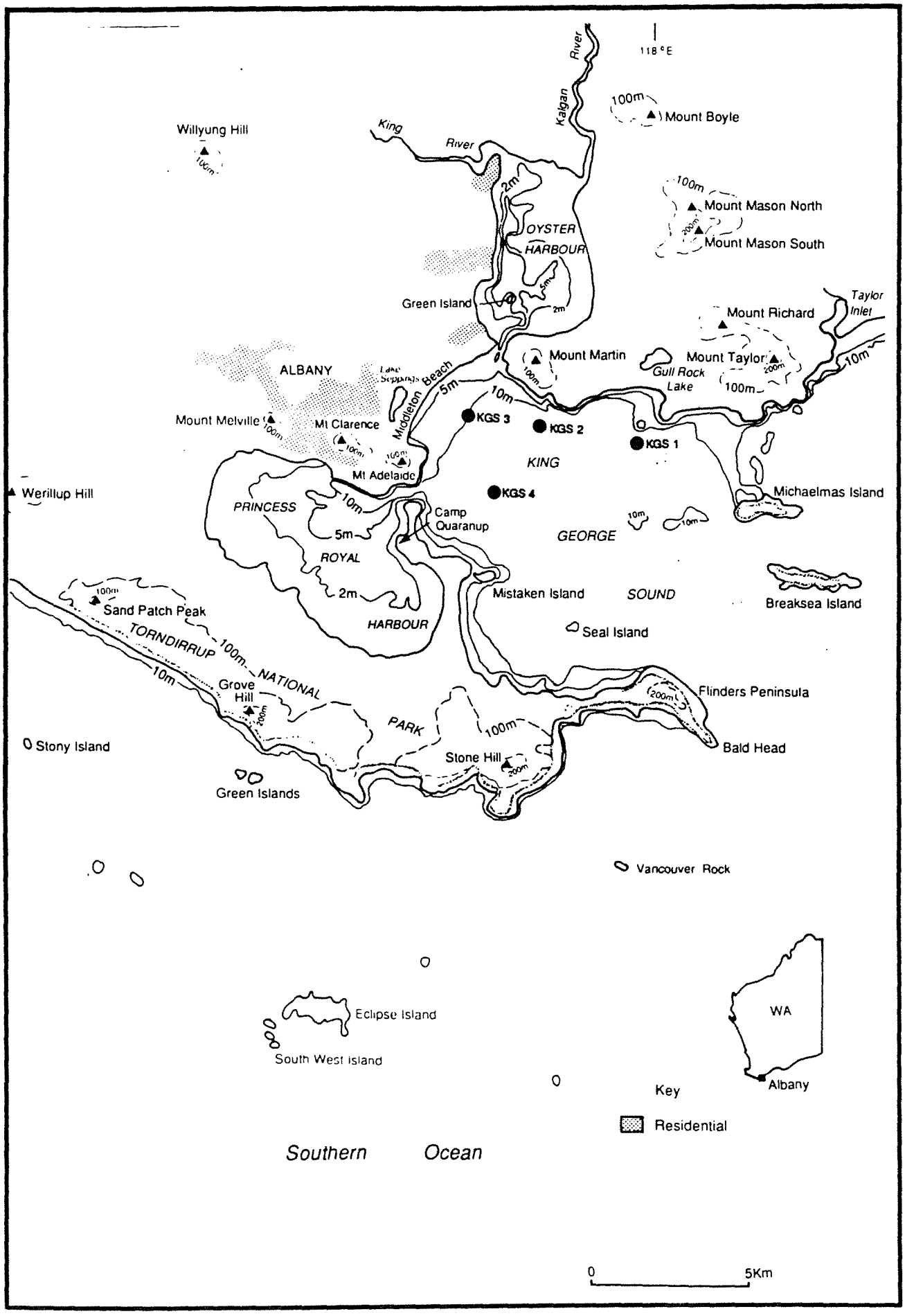

Figure 3.2 Location of current meter stations in King George Sound.

For the drogue-tracking exercise the Australian Land Information and Surveying Group (formerly known as the Australian Surveying Office) performed the position fixing, using the hydrographic survey vessel, *Mike Shephard.*

Table 3.1. Details of the deployment of current meters in King George Sound from 5 November, 1986 to 9 March, 1987 (Ref: Dr D Mills, EPA).

KING GEORGE SOUND CURRENT METER DEPLOYMENT DETAILS					
Current meter type: Sample interval (current): Sampling period:	Neil Brown acoustic NBIS ACM-2 5 minutes, integrated 5 Nov 1986 - 9 Mar 1987				
SITE CODE	CO-ORDS	WATER DEPTH (m)	HEIGHT ABOVE SEABED (m)	FIRST RECORD (5.11.86) [hr]	LAST RECORD (9.3.87) [hr]
GULL ROCK SOUTH (KGS1)	35°1'56"S 117°59'49"E	13.0	5.0	1635	1312
CHEYNE HEAD (KGS2)	35°1'31"S 117°57'37"E	19.0	9.0	1655	1334
MIDDLETON BAY (KGS3)	35°1'15"S 117°56'9"E	11.5	1.5	1615	1334
MISTAKEN ISLAND NORTH (KGS4)	35°2'46"S 117°56'40"E	11.0	5.0	1710	1303

3.6 Water quality, algal and seagrass studies

Hillman *et al* (1991 a and b) performed surveys of the water quality of Oyster Harbour, Princess Royal Harbour and King George Sound and have also surveyed the biomass and distribution of algae and seagrass in these three systems. The results of those studies are referred to in this report.

4. Winter dynamics

4.1 Streamflow

The rainfall season over Oyster Harbour's catchment generally lasts from about May to October (Figures 2.5 and 2.6). Rain occurs in events of short duration (typically less than about 5 days) which are then followed by pulses of freshwater discharge into the harbour via its rivers, creeks and drains, as is highlighted in the Albany rainfall and Kalgan River streamflow data in Figures 4.1a and b.

The initial winter pulses are the richest in nutrient concentration. This is because runoff from the first major rainfall event passes through soil that is left in a nutrient-rich state after the application of fertilizers during the preceding growing season. Figure 4.1c shows the total P pulse from the Kalgan River discharge of 4-6 May 1988 and this represents the highest concentration of total P recorded for 1988. As is shown in Figure 2.6 the first major rainfall events also occurred at this time in 1988.

These characteristics of the rainfall, runoff and associated nutrient transport in streamflows from the Oyster Harbour catchment were analysed by Mr G. Bott of the EPA and presented in Simpson and Masini (1990). As was pointed out in Simpson and Masini (1990) the discharge event of the Kalgan River from 4-6 May 1988 represented only 5 percent of the total annual discharge into Oyster Harbour from this river in 1988, whereas the associated input of total P from that event represented 42 percent of the total annual phosphorus load.

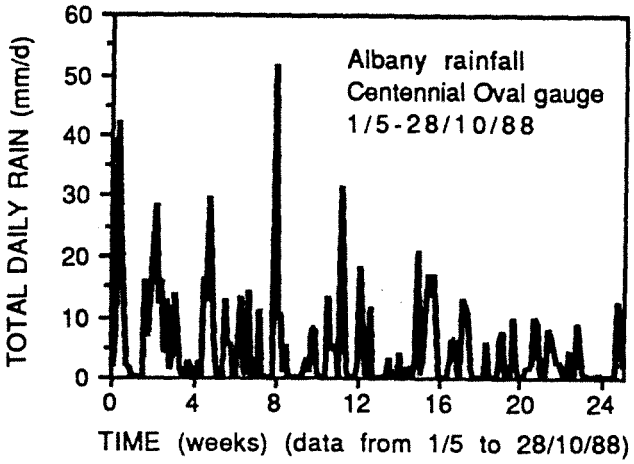

(A)

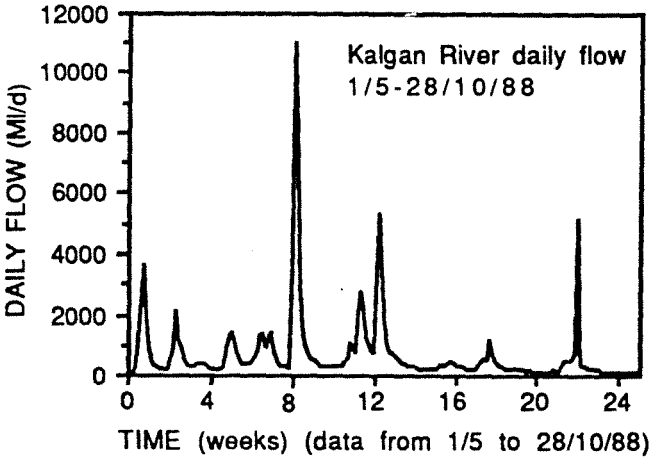

(B)

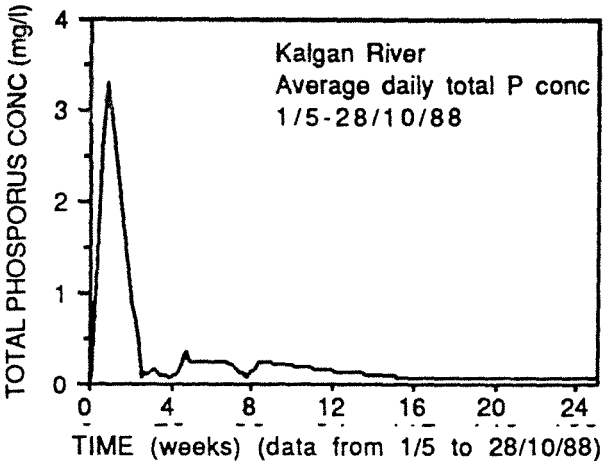

(C)

Figure 4.1 Albany daily rainfall, Kalgan River daily flow and Kalgan River average daily total P concentration for the period 1.5 to 28.10.88.

It is important to understand the vertical mixing and horizontal transport characteristics of buoyant river discharges, from an ecological point of view, because it necessary to quantify the biological availability of nutrients contained in them to the benthic plants (such as macroalgae and epiphytes). In addition, it is necessary to understand the flushing of nutrient-rich flows out to the adjoining waters of King George Sound.

Most of the leaching of nutrients, and their subsequent transport into Oyster Harbour in surface water runoff, occurs in response to the first major winter rains. Hence, vertical mixing during these periods will act as a primary control on nutrient availability and biotic uptake of a large proportion of Oyster Harbour's annual nutrient load.

In the following sections the build-up of stratification due to streamflow in winter, as well as the rate at which buoyant river discharge traverses the harbour, is discussed. The ability of environmental forcings to break down the stratification and the resulting vertical mixing is also analysed.

4.2 Stratification during floods

In this section we discuss stratification due to salinity gradients. Because the salinity gradients in winter are strong, they dominate the calculation of density and hence the density structure mirrors the salinity structure almost directly, with temperature having a lesser contribution to the density of the water.

Streamflow propagates over the denser marine water causing the harbour to be "capped" by a plume of outflowing brackish water less than 1m thick. This was recorded by salinity profile measurements during two separate field surveys, on 29 June and 20 July 1988 by the Centre for Water Research. Figures 4.2 and 4.3 show the respective longitudinal salinity structures of Oyster Harbour along a north-south transect for these two events. Peak flow rates for these two discharge events were about $130m^3\ s^{-1}$ and $30m^3\ s^{-1}$, respectively, representing a wide range of possible discharge rates into Oyster Harbour during winter (G Bott, pers. comm.). As shown, the vertical salinity difference in the upper metre of the water column is about 30 ppt. Below this depth the stratification was less intense with salinity gradually increasing to about 33 ppt at the bottom.

Winds were generally less than $3m\ s^{-1}$ during these two days and therefore would have had little influence on the vertical density structure of the harbour, as is indicated by the analysis on wind mixing in section 4.5, below.

4.3 Surface buoyant jets

During periods of high streamflow, or 'floods', the buoyant river discharge traverses the harbour and exits out into King George Sound as a buoyant frontal jet. A photograph of one such jet, taken on 25 July 1988 by Mr Kim Grey (EPA), is presented in Plate 4.1 (see page ii).

As is typical for such jets their surface dimensions are indicated by the presence of slick or foam lines at their leading edge (Luketina, 1987). These features form as a result of converging flow at the leading edge, which brings surface scum and foam together to concentrate at this region.

The jet shown in Plate 4.1 was observed at 1500 hrs on 25 July 1988. By that time the jet had propagated 5km out from the mouth of Oyster Harbour into King George Sound. The tide had been in ebb for approximately 7 hours and this yields a time-averaged flow speed for the jet of approximately $20cm\ s^{-1}$. This is consistent with Luketina's (1987) velocity measurements of a similar buoyant frontal structure from the Leschenault Inlet into Koombana Bay, Western Australia. Luketina (1987) observed that the jet into Koombana Bay propagated with a speed of approximately 25 to $30cm\ s^{-1}$ during most of its first 3 to 4 hours of travel when its buoyancy was the dominating driving force. After this time the front slowed considerably as viscous drag started to dominate the force balance governing the speed of the front.

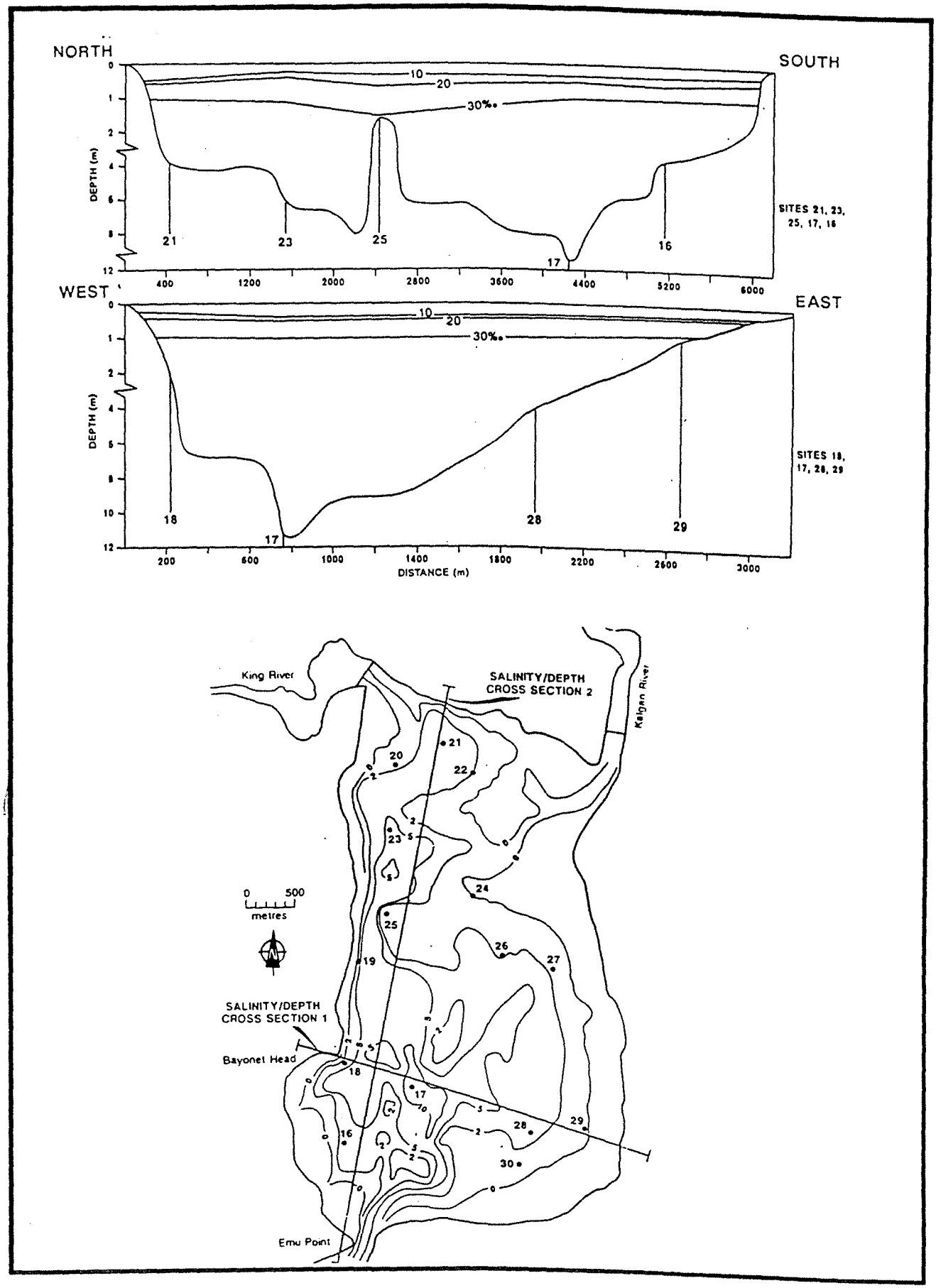

Figure 4.2 North-south and east-west contour plots of salinity structure in Oyster Harbour on 29 June, 1989 during a flood event. Transect paths are shown in the inset map. Kalgan River discharge was approximately 130m^3s^{-1}. Source: Hillman et al (1991a).

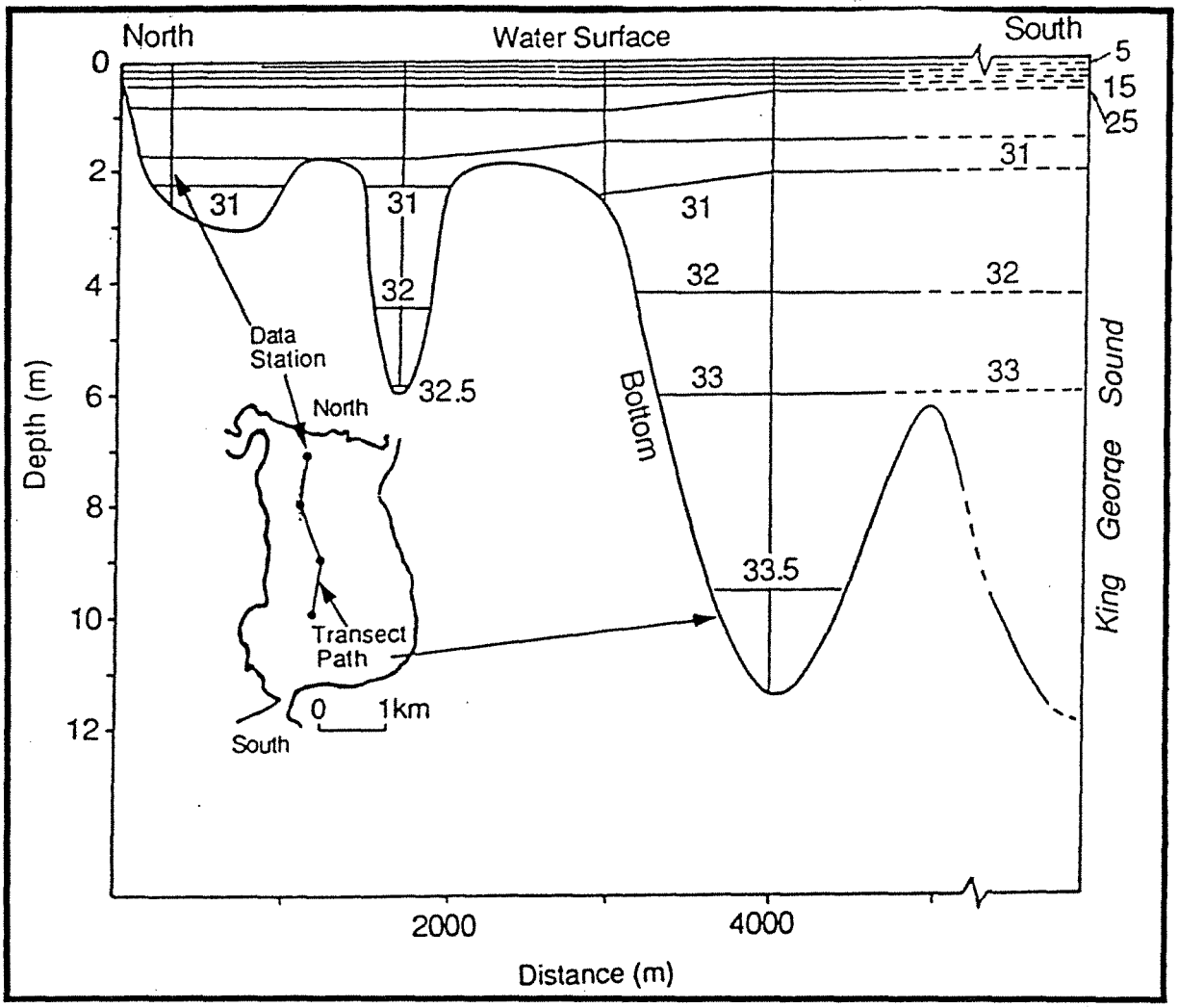

Figure 4.3 North-south contour plot of salinity structure in Oyster Harbour on 20 July, 1988 during a flood event. The transect path is shown in the inset map. Kalgan River discharge was approximately $30m^3s^{-1}$.

The multiple foam lines associated with the jet of 25 July 1989 (Plate 4.1) indicate the existence of sub-frontal jet structures within the main jet. These probably represent the leading edges of sub-fronts formed by discrete changes in the density or velocity of the source water at the mouth of the estuary (Luketina, 1987).

Often buoyant frontal jets are distinctly different in colour to that of the receiving water body. This is due to tannins, suspended sediment or organic detritus that can discolour fresh or brackish river water which forms the source of the frontal water.

An important implication of the occurrence of buoyant frontal jets in this system is that nutrients contained in the buoyant water could be unavailable to benthic plants due to the physical separation between the jet and bottom. As continuous monitoring of nutrient concentrations in streamflows has shown for 1988, the highest nutrient leaching rates from the respective catchments of the King and Kalgan Rivers occur during initial runoff periods. A significant proportion of annual P and N loading into Oyster Harbour occurs during these periods (Simpson and Masini, 1990).

An understanding of the rate at which buoyant streamflow traverses the harbour, as well as the ability of environmental forcings (winds, tides, streamflow, and atmospheric heating and cooling) to break down the stratification and lead to vertical mass transport during winter is critical to an understanding of the ecological behaviour of this estuary. These issues are addressed in the following sections.

4.4 Propagation of surface buoyant flood flows through Oyster Harbour

In this section, theoretical calculations are used to characterise the thicknesses and rates at which streamflows traverse Oyster Harbour for a wide range of discharge rates.

As previously stated, buoyant river discharge flows over the denser marine water of the harbour causing the harbour to be 'capped' by a gravitational overflow of less than 1m thickness (refer to Figures 4.2 and 4.3). The measurements of the stratification of Oyster Harbour taken during the flood events of 29 June and 20 July, 1988, did not capture the frontogenesis of these flows. The speeds at which those surface flows propagated through the harbour were not measured and so the analysis relies on a theoretical consideration.

If, for the winter flood events, we idealise the basin as a long and regular rectangular channel with a continuous source of buoyant discharge across the surface cross-section of the northern end, the following calculations can be made regarding the flow of this buoyant water through the harbour. A basic assumption made in the following analysis is that the point sources of fresh water from the King and Kalgan Rivers spread quickly across the harbour. In this way the idealisation of a laterally averaged surface flow can be made. In the following analysis it is also assumed that the surface flow traverses the harbour only under the influence of streamflow and density differential. All other environmental forcings are neglected in the first instance.

Didden and Maxworthy (1982) formally analysed the above scenario, theoretically and experimentally, using controlled laboratory experiments and developed a suite of asymptotic spreading relations. Those results (Didden and Maxworthy, 1982) are applicable for the case of a relatively thin surface gravity current with respect to the total depth of water. It will be shown in the following analysis of surface buoyant flows in Oyster Harbour that thicknesses of surface gravity currents from river discharge flows are likely to be of the order of 0.2m or less (in the absence of wind mixing) and this means that over most of the harbour's area and during average to spring tide conditions the depth of water in the harbour will be about three times or greater than that of the surface gravity current. During neap and ebb tide conditions surface flows will be significantly influenced by bottom friction over the peripheral shallows and the applicability of the spreading relations in describing the transport characteristics of throughflows of surface river discharges is appreciably restricted. Hence, the spreading relations of Didden and Maxworthy (1982) provide us with indicative tools for the prediction of the mean, tidally averaged, spreading characteristics of buoyant surface river discharges through Oyster Harbour. Appropriate proportionality constants can be drawn from the many experimental studies documented in the literature (eg Imberger *et al.*, 1976; Manins, 1976). The spreading relations for plane surface density currents, driven by a continuous source discharge at one end of a channel, define the propagation, R, and thickness, h, of such currents as a function of time. A number of spreading relations relevant to the present analysis are given in Table 4.1, and the basis for their derivation is described as follows.

For the plane surface density current, the driving gravity force works against both the inertia of the ambient fluid, which it displaces during its propagation, and the interfacial viscous retarding force. A "no-stress" condition at the upper surface is assumed and this implies that a viscous retarding force forms only at the shear layer between the current and ambient fluid.

Initially, the viscous drag on the gravity current is much smaller than the inertial force because of the small area over which the viscous stress can develop. In this "inertial" flow regime the inertial retarding force balances the driving gravity force.

After some critical transition time, t_c, the area of contact between the gravity current and the ambient fluid is large enough to result in the viscous drag becoming the dominant retarding force balancing the gravity force. This is termed the "viscous" flow regime.

Table 4.1. Spreading relations for plane surface density currents from a continuous discharge through a long regular rectangular channel (after, Didden and Maxworthy, 1982). These formulae are for the case of two homogeneous fluids of differing density. Where proportionality constants were not available only asymptotic formulae are presented.

REGIME	SPREADING RELATION	
Inertial	$R = 1.26(g'Q)^{1/3}t$	4.1
	$h = 0.8(Q^2/g')^{1/3}$	4.2
Viscous	$R \sim (g'Q^2/\nu^{1/2})^{1/4}t^{7/8}$	4.3
	$h \sim Q^{1/2}(\nu/g')^{1/8}t^{1/8}$	4.4
Time at which transition occurs from inertial to viscous regime	$t_c \sim (Q^4/g'^2\nu^3)^{1/3}$	4.5

R is the position of the current front as a function of time,
h is the thickness of the current front as a function of time,
$g' = (g\Delta\rho)/\rho$, the reduced acceleration due to gravity between the two fluids where $\Delta\rho$ is the density difference, g the acceleration due to gravity, and ρ the average density
Q is the nett discharge rate per unit width across the initial discharge zone,
ν is the kinematic viscosity of water (approximately equal to $1 \times 10^{-6} m^2 s^{-1}$), and
t is the time since the onset of discharge.

Using equations 4.1 to 4.5, the spreading behaviour of flood flows through OH is calculated for discharge rates of 10, 30, 100 and $200 m^3 s^{-1}$, which comprise a range typical for most rainfall events. The propagation, R, and thickness, h, of the surface density currents for these four flow cases are plotted as functions of time in Figures 4.4 and 4.5, respectively. These theoretical calculations indicate that, in the absence of wind and tide effects, typical flood discharge flows would traverse Oyster Harbour in times less than about one day and with thicknesses less than about 0.2m. Associated velocities for these flows would range from 5 to $30cm\ s^{-1}$.

Winds could retard or enhance the surface flow by superposing a surface drift of the order of 3 percent of the wind speed (Fischer *et al*, 1979 and Wu, 1969). Hence, a 5 to 20 knot wind speed range would lead to a 7 to $30cm\ s^{-1}$ range in surface wind drift. Hence, when winds are strong and opposed in direction to that of an outflow, they could completely restrict the exit of streamflows out into King George Sound for a short amount of time. On the other hand, when winds are strong and blowing downwind with respect to streamflows they could almost double the outflow speed.

Similarly, tidal currents could retard or enhance the surface flow during flood or ebb tides, respectively. This mechanism has not been verified in the field for winter flows. However, drogue measurements collected during February 1989 and discussed in Chapter 5, following, indicate that maximum tidal currents in Oyster Harbour, away from the outlet channel, are of the order $0.1m\ s^{-1}$. Hence, tidal forcing could temporarily arrest the outflow of buoyant surface water during the rising tide phase, but during the ebb phase this surface water would again propagate towards the mouth and into King George Sound under the combined barotropic tidal forcing and baroclinic forcing due to pressure gradients set up between the buoyant surface outflow and denser marine water of King George Sound.

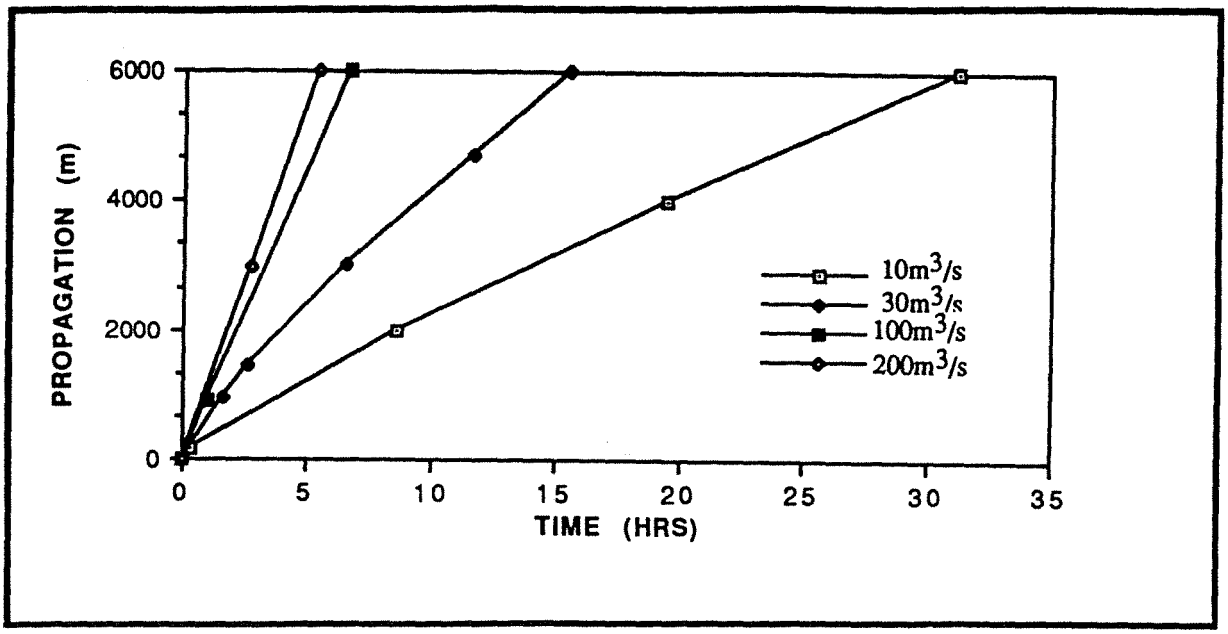

Figure 4.4 Theoretically predicted propagation of buoyant flood discharge flows through Oyster Harbour as a function of time for different river flow rates.

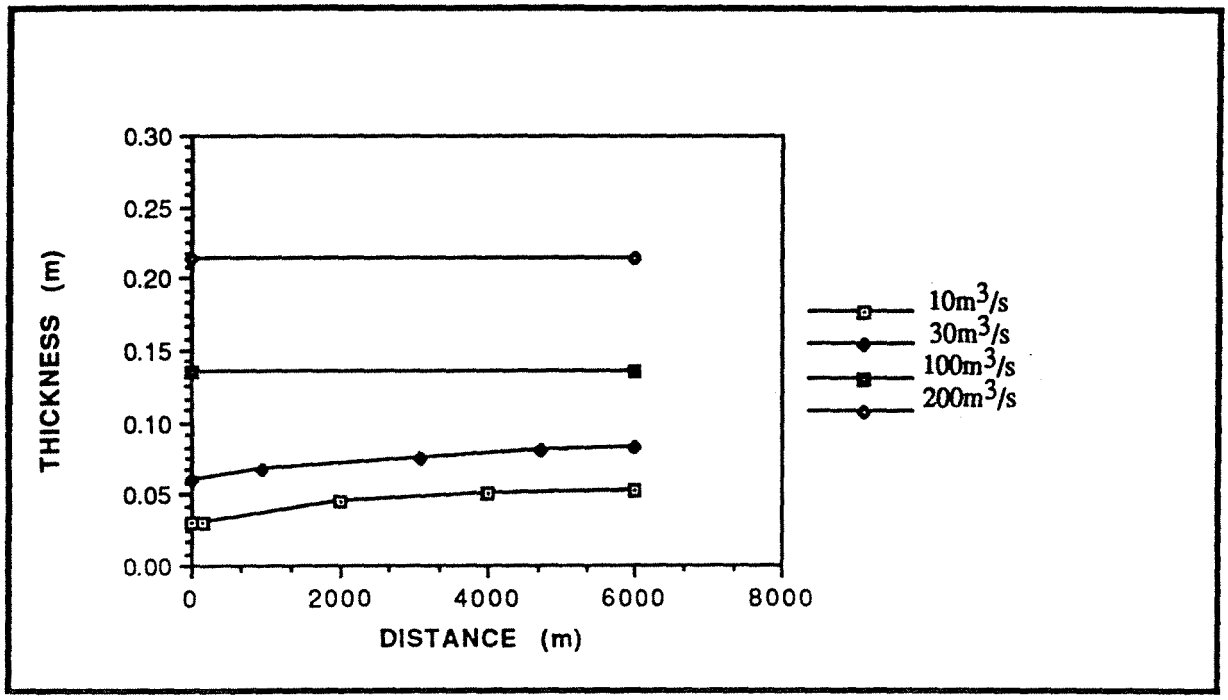

Figure 4.5 Theoretically predicted thickness of buoyant flood discharge flows through Oyster Harbour as a function of distance from the source (northern end of the harbour) for different net river flow rates.

In summary, it would appear that streamflows could traverse Oyster Harbour during periods of river discharge in times less than about two days. This estimation allows for the possible periodic retarding influence of upstream directed wind and tidal currents.

En-route to King George Sound the buoyant surface discharge flows could undergo mixing with the ambient marine water in the harbour due to a number of potential mixing agents. These mixing agents are interfacial shear, tidal mixing, differential heating and cooling, evaporation,

penetrative convection and wind mixing. The potential mixing of surface flows in Oyster Harbour is discussed in the following sections.

4.5 Mixing of surface buoyant flood flows in Oyster Harbour

4.5.1 Interfacial shear

Locally parallel flow between two fluids of differing density will induce interfacial mixing. This occurs as internal waves (called Kelvin-Helmholtz billows) break and collapse along the interface in a turbulent manner (Thorpe, 1987). The degree of mixing depends on the density difference and velocity shear between the two layers. The non-dimensional gradient Richardson number, Ri, can be used as a predictive indicator of the potential for interfacial shear to create Kelvin-Helmholtz billows which cause mixing in the interfacial region. The gradient Richardson number (for z positive downwards) is given by

$$Ri = [(g/\rho_o).(d\rho/dz)]/[(du/dz)^2], \qquad 4.6$$

where $d\rho/dz$ is the vertical density gradient across the interface, du/dz is the velocity gradient across the interface, ρ_o is the average density between the two layers and g the acceleration due to gravity.

In the absence of accurate density and velocity profile data a Richardson number based on bulk parameters can be used to indicate the stability of the vertical stratification during a shear event. This is given by

$$Ri \sim g'h/(\Delta u)^2, \qquad 4.7$$

where Δu is the velocity difference between the two flowing layers, h is the thickness of the interfacial gradient region, and g' is the reduced gravitational acceleration due to the density difference. The parameter g' is defined as $\Delta\rho g/\rho_o$, where $\Delta\rho$ is the density difference across the interface. A Richardson number of less than 1/4 indicates the likelihood of interfacial mixing. Turner (1973) has derived a relation giving the order of magnitude of the thickness of the mixed region resulting from an interfacial shear event, and this is given by

$$\delta \sim (\Delta u)^2/g'. \qquad 4.8$$

The theoretical proportionality constant for this relation varies from 0.075 to 0.3 and depends on the initial vertical structure in velocity and density across the interface. Sherman *et al* (1978) reviewed experimental and theoretical studies of interfacial mixing and adopted a constant of 0.3.

If we assume a relatively strong surface outflow for Oyster Harbour having a velocity of say 0.5m s^{-1} then the associated bulk Ri would be less than 1/4. This suggests that interfacial mixing would occur, and the vertical extent of this is calculated to be approximately 0.3m. Further mixing and consequent thickening of the interface by Kelvin-Helmholtz billowing will be negligible after the initial mixing event unless either the interface is sharpened by stirring of the upper layer or the velocity shear between the upper and lower layers is increased (Sherman *et al*, 1978). This analysis suggests that even for the most intense flood events in Oyster Harbour the interfacial shear mixing is likely to be small, with the outflowing surface buoyant layer maintaining a thickness, in the absence of wind or tidal mixing, of about 0.5m or less. This theoretical result is consistent with the measurements of the thicknesses of the surface buoyant outflows measured on 29 June and 20 July 1988, as shown in Figures 4.1 and 4.2, respectively.

4.5.2 Tidal mixing

As well as enhancing shear between the surface buoyant outflow and underlying marine water during flood tides, tidal flows also have the potential to cause boundary turbulence along the bottom of the harbour.

Ivey and Patterson (1984) used a vertical one-dimensional integral mixed-layer model to predict the bottom mixed layer depth generated from turbulent kinetic energy in a stratified flow along a lake bottom. Based on that analysis the following expression for bottom mixed layer depth, as a function of time, can be derived:

$$h_b(t) = u_{*b} (6C_{k*}/N_o^2)^{1/3} t^{1/3}, \qquad 4.9$$

where $h_b(t)$ = the height to which mixing has extended with respect to the bottom at time t, $u_{*b} = C_d^{1/2}U_b$ = the friction velocity at the bottom (this is a function of the bottom roughness coefficient , C_d, and flow velocity near the bottom, U_b), C_{k*}= a constant, taken by Ivey and Patterson (1984) to be the value of 1.9 as suggested by Hebbert *et al* (1979), and $N_o^2 = (g/\rho_o).(d\rho/dz)_o$, the initial buoyancy frequency squared, where $(d\rho/dz)_o$ is the initial vertical density gradient for a linear vertical stratification.

For the case of fully developed tidal flow in the entrance channel the following values are chosen to calculate the magnitude of mixing that could occur:

$U_b = 0.5 m s^{-1}$. This value is drawn from drogue measurements of currents tracked through the channel during February 1989 (see Chapter 5, following). This result can also be arrived at analytically by performing a simple mass balance through the channel for typical spring tides. If we assume that the harbour and channel have areas of 18×10^6 and 1×10^3, respectively, and that the tide rises at a rate of about $3 \times 10^{-5} m s^{-1}$ during typical spring floods (as estimated from the tidal data in Chapter 3), then an inflow velocity of the order of $0.5 m s^{-1}$ is calculated.

The coefficient C_d is taken to be equal to 0.001 and a $(d\rho/dz)_o$ of $0.3 kg m^{-3}$ per m is adopted This value of $(d\rho/dz)_o$ is derived using a linear variation in salinity of approximately 5 ppt over a depth of 10m.

Substituting the above values into Equ. 4.9 yields the following mixing law:

$$h_b(t) = 0.248\ t^{1/3}.$$

The time during which a cross-section of water flowing through the channel is subjected to the above mixing rate is given by the velocity of flow and length of channel. Taking a channel distance of 1000m and using a velocity of $0.5 m s^{-1}$ yields a time of 2000 seconds. At the end of this time the stratified fluid has traversed the channel and has been mixed by boundary turbulence vertically up from the bottom a distance of the order of 3m. We have used a $(d\rho/dz)_o$ that lies between values that are likely for summer and winter. In winter during strong streamflow periods the vertical salinity variation is likely to be of the order of 30 ppt, and hence vertical mixing will be weaker. In summer, when streamflow is low, vertical salinity differences will be due to a very thin layer of freshwater, with a thickness of order 10cm or less, derived from river baseflows. If we assume a very weak value for $(d\rho/dz)_o$ of $0.02 kg m^{-3}$ per m than a bottom mixed layer of approximately 8m is predicted.

These calculations indicate that bottom mixing in the channel could penetrate almost to the surface during weakly stratified periods. However, in general during winter the stratification is likely to be strong enough to restrict bottom mixing so that it does not reach the surface. Since tidal currents are at their strongest in the channel this conclusion can be extended to apply for the whole area of Oyster Harbour.

4.5.3 Differential heating and cooling

When two adjacent regions of equal density water are differentially heated, the warmer of the two will become the less dense and a horizontal gravity current of warmer (lighter) water will flow over an oppositely flowing undercurrent of colder (denser) water. Currents driven by density differences are referred to as baroclinic. Currents driven by other mechanisms, such as wind and water level variation, are referred to as barotropic. The importance of baroclinic circulation driven by differential heating and cooling has been reviewed by Imberger and Patterson (1990).

Differential heating can result when the following conditions are present; when there is a significant difference in bottom depth (the shallows heating during the day and cooling during the night at a greater rate than deeper waters); when there is a significant difference in turbidity between adjacent regions of water (the more turbid water absorbing the greatest amount of heat); when there is variable shading (the shaded regions remaining cooler); when there is a variable wind stress (evaporative and conductive cooling of the water surface increases with increasing wind stress); and, when there is spatially variable flux of either warmer or colder water from direct inputs such as tidal fronts or streamflows.

Horizontal differences in temperature produced by differential heating in south-west Australian lakes can be typically of the order 1 to 5 °C (Imberger and Patterson, 1990). The velocity scale of currents driven by the density differences set up by such temperature gradients can be estimated by the following relation (as reviewed by Simpson, 1982),

$$u \sim (g'h)^{1/2}, \qquad 4.10$$

where h is the vertical thickness of the density current.

Proportionality constants for Equ. 4.10 will be of order 0.5 for most situations (Simpson, 1982).

For a range of temperature differences of 1 to 5 °C corresponding density differences of order 0.2 to 1kg m^{-3} are calculated. According to equation 4.10 this would drive density currents with speeds of the order of 2 to 5cm s^{-1}, or in other terms 70 to 180m hr^{-1}. Such speeds for gravity currents driven by horizontal density gradients have been measured in south-west Australian water bodies (D'Adamo, 1985; Parker and Imberger, 1986). Typically, thicknesses of gravity currents driven by density differences near the surface are of the order of less than 1m.

From the above analysis, it is apparent that in the absence of strong tidal flows, winds or streamflows the residual forcing of surface waters by differential heating will assume an important role in the overall transport of mass in Oyster Harbour. This could therefore occur during calm periods in regions well away from the entrance channel when streamflow is low during summer and in between discharge events during winter.

4.5.4 Evaporation and penetrative convection.

Solar radiation will heat the water and cause some level of evaporation depending on the intensity of the radiation. In addition, night-time cooling will occur in surface waters as air temperatures drop below that of the water surface. Both these mechanisms will lead to some degree of stirring as denser (more salty or colder) water is formed at the surface and billows down in a convective manner.

It can be easily shown however, by applying relevant formulae to predict velocity scales associated with these processes (Imberger and Patterson, 1981), that neither evaporative heating or penetrative convection due to cooling could overcome the vertical gravitational stability between the fresh surface plume and underlying marine water during streamflow periods. These mechanisms may become important as mixing agents during low streamflow periods in summer, and this is investigated in Chapter 5.

4.5.5 Wind mixing

In this section we investigate the ability of wind forcing to break down the stratification that occurs during discharge periods. This stratification is typified by the contour plots in Figures 4.2 and 4.3 of section 4.2, above.

The response of stratified enclosed or semi-enclosed water bodies to wind stress can be predicted according to a Wedderburn number, W, classification scheme (Imberger and Hamblin, 1982; Monismith, 1986). W is given by

$$W = (g'h/u_*^2).(h/L) \qquad 4.11$$

where, g' is the reduced acceleration due to gravity of the density jump at the base of the surface layer which has a depth h, and L is the fetch length . The parameter u* is the water shear velocity induced by the wind at the surface, given by (Fischer *et al*, 1979):

$$u* = (\rho_A C_d/\rho)^{1/2} U_{10}, \qquad 4.12$$

where, ρ_A is the density of air, approximately equal to 1.2kg m^{-3}, ρ is the density of the water, C_d is a drag coefficient that depends on atmospheric conditions and sea-surface roughness but can be approximated as 0.0013 (Fischer *et al*, 1979), and U_{10} is the wind speed at 10 m height.

The Wedderburn number was developed for the idealised case of a two-layer fluid in a uniform rectangular basin. When the wind acts, the surface water is advected downwind where it piles up and forces the bottom fluid to advect in the reverse direction, resulting in a tilted interface. W is essentially a balance between the pressure force arising from the longitudinal density gradient (formed by the tilted interface) and the pressure force due to the free surface slope that is set up by the applied wind stress. The interface will oscillate, but given the correct combination of wind stress, fetch length, upper mixed layer thickness, and vertical stratification this interface could surface as an upwelling region at the upwind end. This type of dynamical behaviour in lakes has been studied numerically (Thompson and Imberger, 1980), analytically (Imberger and Hamblin, 1982), experimentally (Monismith, 1986), and in the field (Imberger, 1985; D'Adamo, 1985; Csanady, 1975; Mortimer, 1974).

Based on laboratory and field experimental verification in lakes, as reviewed by Imberger and Patterson (1990), a W greater than order 1 implies that the stratification will be only slightly perturbed by gentle wind forces. As W approaches and becomes less than order 1, the surface stratification will become progressively more severely perturbed by downwind surface advection, with upwelling of bottom waters at the upwind end and strong vertical mixing.

Two main mechanisms are now recognised as energising entrainment at the base of a surface layer (Imberger and Patterson, 1990). The first is termed ***stirring*** (Kraus and Turner, 1967) and uses the turbulent kinetic energy generated at or near the surface by external energy inputs originating from the wind. The second process is ***shear*** induced mixing (Pollard *et al.*, 1973) and describes the entrainment arising from the locally produced kinetic energy contained in the shear across the interface between the surface and lower density layers. Often the two sources combine; the stirring motion from the surface sharpens the interface sufficiently to allow shear instabilities to mix the two fluids.

An indication of the relative importance or either stirring or shear to upper mixed layer deepening can be obtained from a consideration of the value of the Wedderburn number. Spigel and Imberger (1980) pointed out that for values greater than 1 deepening is energised by surface processes (stirring) whereas for values less than 1 interfacial mixing (shear) dominates.

Hence, stirring will dominate the mixing whenever the wind stress is too weak, the duration too brief, or the fetch too short to allow appreciable shear to build up across the interface. Sherman *et al* ., (1978) integrated the turbulent kinetic energy equation vertically over the mixed layer and Spigel and Imberger (1980) isolated the individual contributions from stirring and shear mixing to arrive at the following deepening formulas.

For deepening dominated by stirring (W > 1) the entrainment law, as originally introduced by Kraus and Turner (1967), for a two-layer fluid with a homogeneous upper layer and a linearly stratified lower layer, is:

$$h(t) = \eta u*(6C_k/N_o^2)^{1/3}\, t^{1/3} \qquad 4.13$$

where N_o^2 is the buoyancy frequency squared at the initial background density distribution, the initial density gradient is assumed to be linear, z is the vertical coordinate (positive downwards), $C_k = 0.13$ and $\eta = 1.23$ are constants that determine the efficiency of energy conversion (Imberger and Patterson, 1990) . For the case of stirring in a two-layer fluid where the upper and lower layers are homogeneous but of differing densities, the following deepening law, based on Equ. 4.13, applies:

$$h(t) = (C_k \eta^3 u*^3 t)/(g_o' h_i) \qquad 4.14$$

For deepening dominated by shear (W < 1), the deepening law, as originally introduced by Pollard *et al.*, (1973), for a two-layer fluid with a homogeneous upper layer and a linearly stratified lower layer, is:

$$h(t) = (2C_S/N_O^2)^{1/4}\, u* \, t^{1/2} \qquad 4.15$$

where $C_S = 0.24$ is a constant that determines the efficiency of energy conversion (Imberger and Patterson, 1990). For the case of shear in a two-layer fluid where the upper and lower layers are homogeneous but of differing densities, the following deepening law, based on Equ. 4.15 applies:

$$h(t) = [C_S/(g_o' h_i]^{1/2} u*^2 \, t \qquad 4.16$$

Using the above formulae, calculations are performed to predict the potential of winds of varying strength and direction to mix the surface freshwater layer in Oyster Harbour down through the water column during typical flood discharge situations (as shown in the stratification contour plots of Figures 4.2 and 4.3, section 4.2).

Two extremes for the fetch length, L, are considered, and these are a minimum of 3000 m for lateral (east or west) winds and a maximum of 5000 m for longitudinal (north or south) winds. The initial stratification is approximated from the data collected on June 29 and July 20 1988 (Figures 4.2 and 4.3) and comprises a linearly stratified surface region with a $(d\rho/dz)_o$ of 24kg m^{-3} per m and a homogeneous region below with a density of 24kg m^{-3}. The surface of the harbour is assumed to be freshwater.

To calculate W for a particular value of mixed layer depth, h, it is necessary, for the present analysis, to assume some initial step discontinuity in the surface stratification. Based on the calculation of the surface buoyant discharge thickness in section 4.4, an initial value of 0.3 m is chosen for h.

A range of curves of surface mixed layer depth, as a function of time, under different wind speeds and directions are presented in Figure 4.6. Figure 4.6a contains the curves for north or south winds, and Figure 4.6b contains the curves for west or east winds. These results have been calculated using the four deepening formulae of Equations 4.13 to 4.16. Allowance has been made in the calculations for the change in W that occurs as the mixed layer increases and the density difference decreases.

As shown in Figure 4.6a, mixing is most rapid for north or south winds because they blow over the longest fetch. The curves indicate that winds less than about 4 m s^{-1} can mix down to a maximum depth of about 1 m in 10 hours and 2 m in 20 hours. As the wind speed increases the rate of deepening also increases, with 10 m s^{-1} winds predicted to be capable of mixing down to 8m in 10 hours and to the bottom (12m) in about 15 hours. The abrupt changes in the slope of the curves for winds less than 5m s^{-1} indicates where the value of W has changed from being less than 1 to greater than 1 as a consequence of increasing the upper mixed layer depth, h, during the deepening process.

The predicted deepening behaviour for the harbour under west or east winds (Figure 4.6b) is somewhat different to that for north or south winds. As shown in Figure 4.6b wind mixing is not as effective in mixing the harbour when winds blow across the shorter fetch. This is noticeable for the case of 10m s^{-1} winds where it can be seen that for L = 3000m the maximum depth of wind mixing is about 8m. On the other hand for L = 5000m a similar wind is predicted to mix to the bottom (12m) in just 15 hours. The reason for this difference lies in the shape of the curves. As is evident in Figure 4.6b the deepening curve changes in slope at a time of 9 hours; it is at this point that h increases sufficiently to cause W to change from being less than 1 (indicating that the deepening was shear dominated) to being greater than 1 (when the deepening became stirring dominated). In contrast, the curve in Figure 4.6a shows no change in slope, indicating that W remains below 1, with deepening dominated throughout the process by shear.

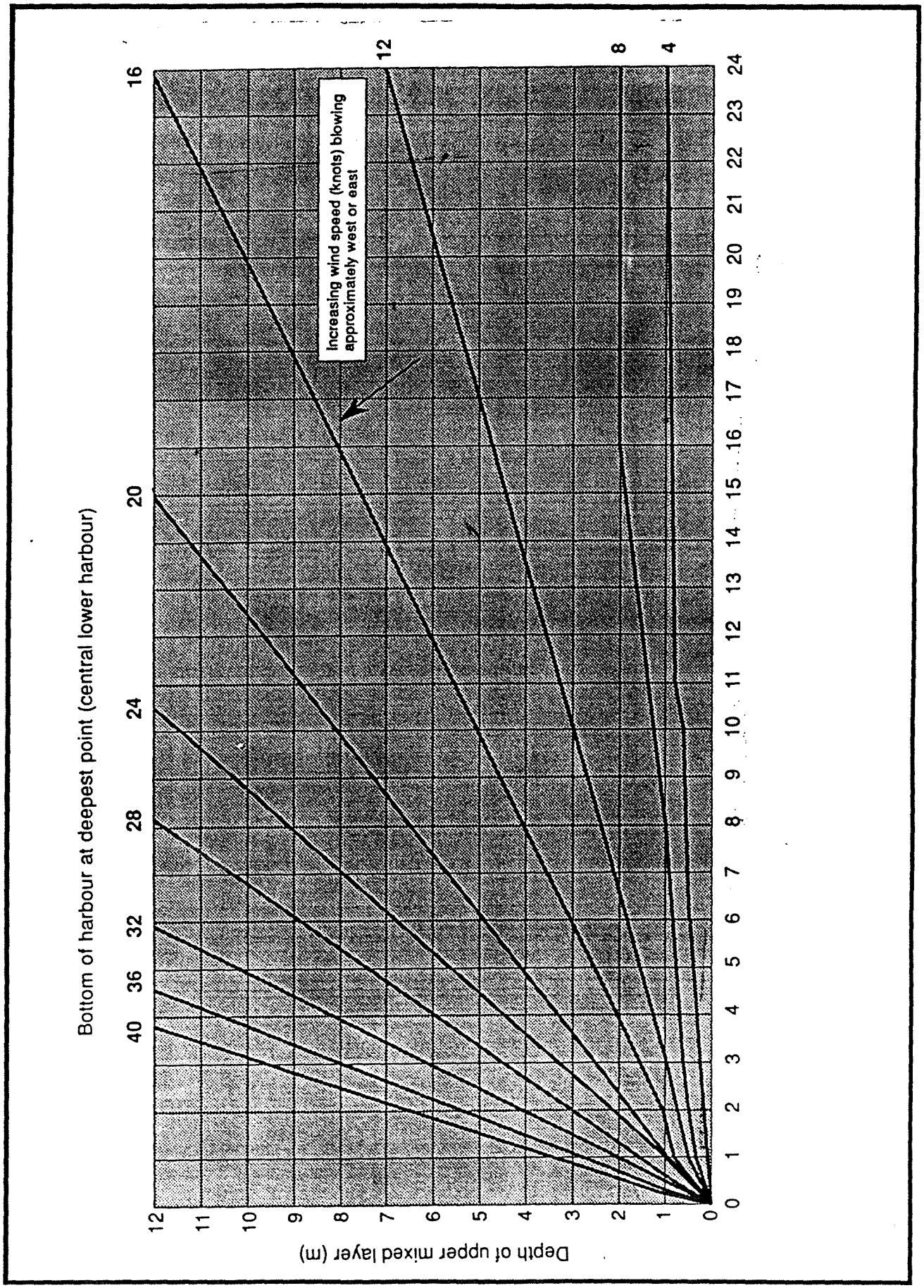

Figure 4.6a Theoretically predicted family of upper mixed layer deepening curves for a typical winter stratification in Oyster Harbour subjected to winds blowing approximately north or south during a flood discharge event.

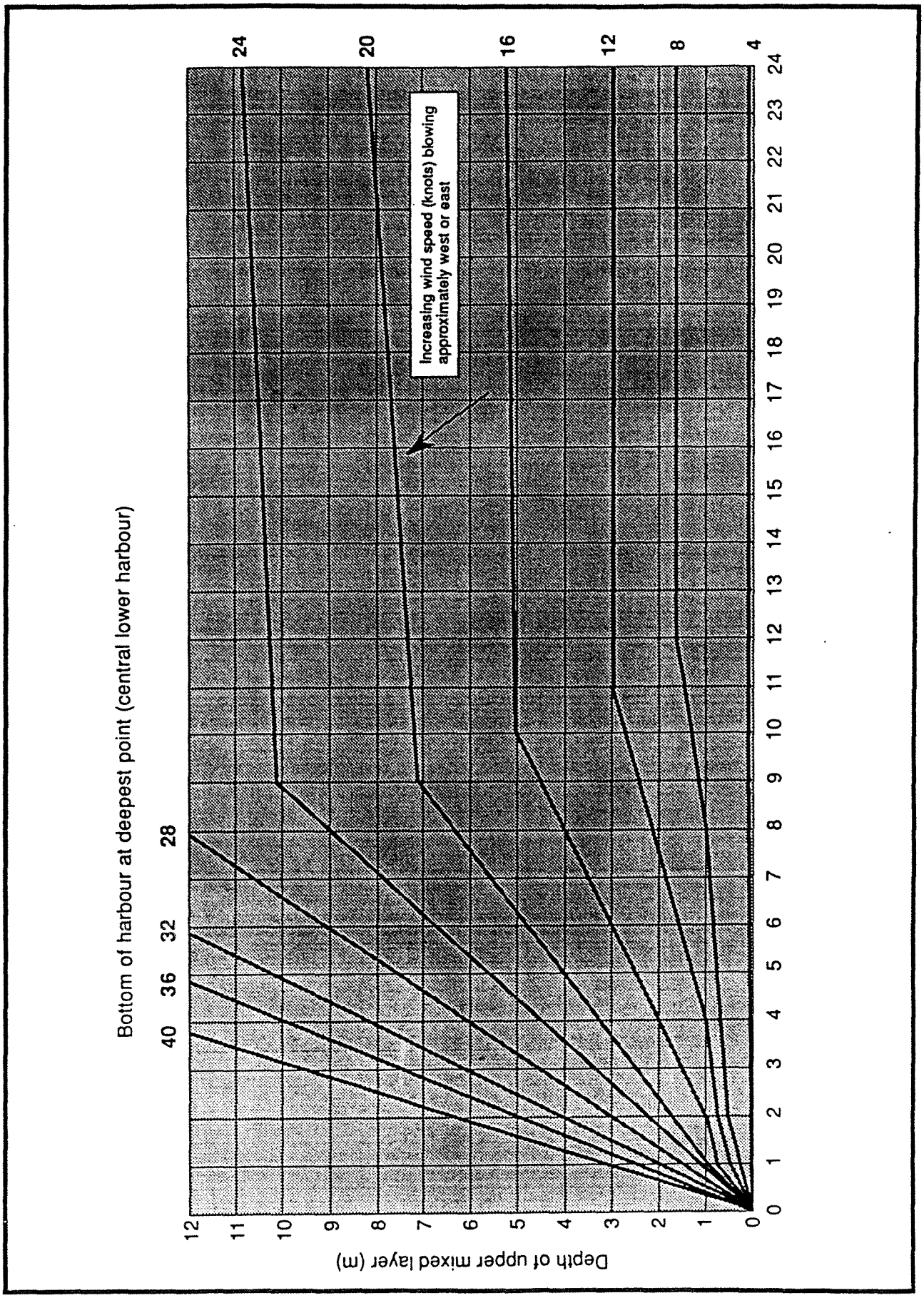

Figure 4.6b Theoretically predicted family of upper mixed deepening curves for a typical winter stratification in Oyster Harbour subjected to winds blowing approx. west or east during a flood discharge event.

In general, the wind mixing calculations suggest that during winter flood periods winds less than about 4m s^{-1} mix the surface buoyant layer down to a maximum depth of only 2m, and this takes 15 hours. In 10 hours wind mixing penetrates down to only approximately 1m. However, as winds become stronger and rise above 5m s^{-1}, the rate of vertical mixing increases. For example, winds of approximately 10m s^{-1} could mix the surface layer down to the bottom (12m) in just 15 hours.

It is unlikely that strong storm winds (greater than 5m s^{-1}), which often accompany a rainfall event, will persist during the subsequent river discharge period. The strongest winds are commonly associated with meteorological frontal features that also bring the rainfall, but these winds subside in intensity as the front passes the region. The time series plots in Figure 4.7, of rainfall and winds at Albany for the winter of 1988, exemplify this point. Peak river discharge rates arrive at Oyster Harbour between 12 and 48 hours after heavy rainfall (Simpson and Masini, 1990). In addition, it is worth recalling the results of the wind analysis for the winter 1988 data set in Chapter 3. Those results indicated that winds are likely to be less than or equal to 5m s^{-1} for 75 % of the time in winter. Hence, the likelihood of strong winds (greater than 5m s^{-1}) persisting during the period of peak discharge is low.

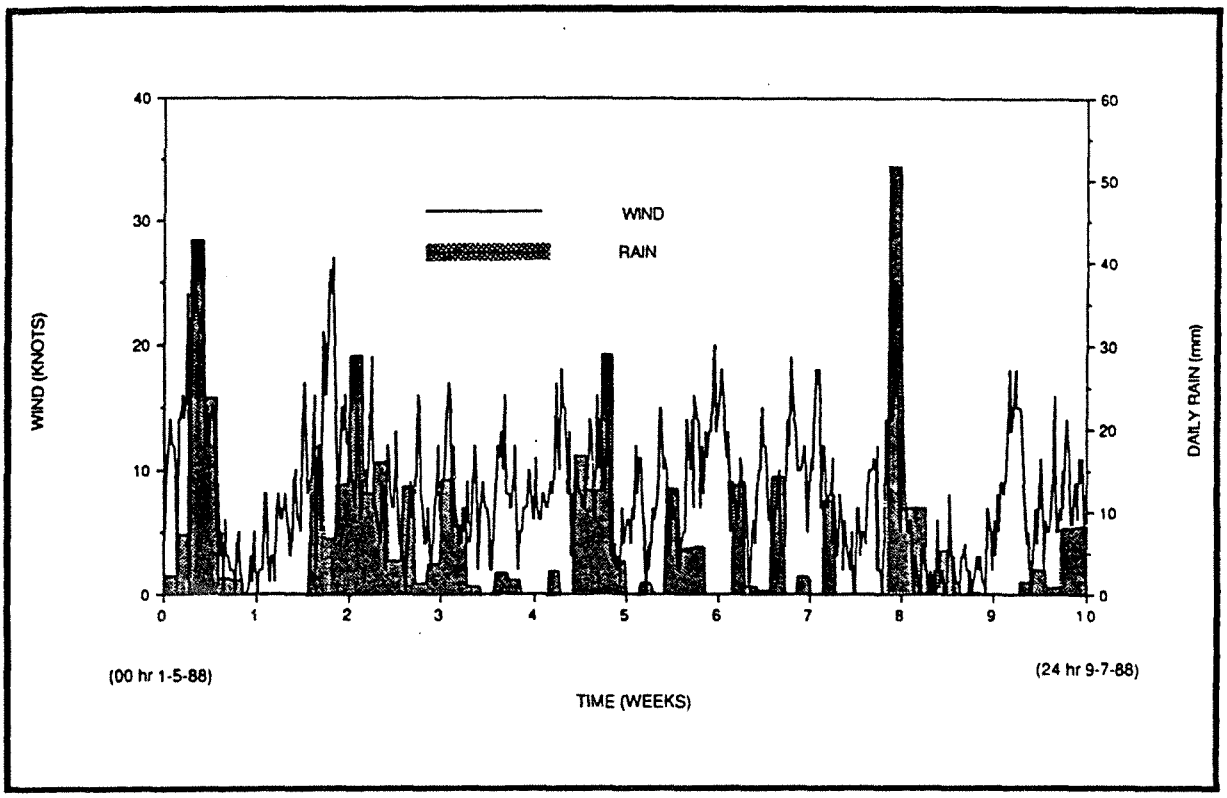

Figure 4.7 Daily rainfall and 3-hourly wind time series for Albany from 1 May to 9 July, 1988 (10 week period).

4.6 Nutrient flux through Oyster Harbour during flood flows

On the basis of the above hydrodynamic analysis it is concluded that during winter the flow of riverine discharge through Oyster Harbour occurs as a relatively thin buoyant surface layer that is unlikely to be mixed down to below about 1m depth by typical strength atmospheric forcings (such as wind). This surface layer is ejected out into King George Sound as a buoyant jet and the residence time of the buoyant river flow within Oyster Harbour is calculated to be of the order of 1 day.

Given these hydrodynamic characteristics it is possible to draw some conclusions regarding the biological assimilation of nutrients contained in these flows during winter.

Simpson and Masini (1990) reported that about 85 percent of the total phosphorus load and 50 percent of the total nitrogen load from the rivers that discharge into Oyster Harbour is soluble and therefore potentially available for plant growth. It is generally considered that eutrophication may be controlled in the Albany harbours by reducing the availability of phosphorus (Simpson and Masini, 1990). The first major winter flush of the Kalgan River through Oyster Harbour in 1988 occurred during 4-6 May (Simpson and Masini, 1990). This flood comprised only 5 percent of the Kalgan's annual discharge but over 40 percent of that river's annual phosphorus load. If we assume, based on the mixing analysis above and on the stratification data for the flood flows in section 4.2, that the nutrient-rich buoyant surface layer during a discharge event is well-mixed to a depth of at most 1m, then the benthic harbour area in contact with this layer is about 50 percent of the total harbour area. If the nutrients contained in the water over this shallow benthic area were to be completely assimilated by benthic plants then about 50 percent of the total incoming nutrient load in the surface buoyant layer mass would remain. It is unlikely however, that all nitrogen and phosphorus will be converted to biomass, especially in view of the relatively low water temperatures in winter. Although nutrient uptake by phytoplankton may also occur throughout the surface layer, given the low residence time in the harbour (one day or less) it is likely that most would be retained in this layer and be advected out to King George Sound in buoyant jets. Hence under these physical conditions a significant proportion (probably over half) of the nutrients in the surface flow are unavailable to the benthic plants and likely to be advected out into King George Sound during early winter discharge flow periods.

Based on the above hydrodynamic calculations, vertical mixing is unlikely to be sufficiently strong, on average, to facilitate a complete availability of nutrients to benthic macroalgae during the winter flood discharge periods when nitrogen and phosphorus loadings to Oyster Harbour are greatest.

The stratification in winter governs the vertical availability of nutrients, with the buoyant jets into King George Sound being responsible for the efflux of a significant percentage of nutrients that enter the harbour in streamflow during winter.

Hence, the winter stratification probably restricts over half of the annual load of nutrients into Oyster Harbour from reaching the benthic macroalgae.

5. Summer dynamics

5.1 Mean structure during spring tides and mild winds

In contrast to winter, the net discharge of freshwater into Oyster Harbour during summer is small, with baseflows being of the order of $0.1 m^3 s^{-1}$ (Mr G. Bott, pers. comm.). Diurnal heating by short-wave radiation also adds buoyancy to the water column.

Rainfall is limited in summer and most of the time salinity differences between the surface and bottom are typically less than about 1 ppt, with the bottom water being essentially marine and the surface water only slightly diluted with freshwater that enters the harbour from groundwater baseflow and minor discharge events that may follow relatively infrequent summer rainfall periods. If we add surface variations in temperature, due to solar heating, of up to about 1 °C to vertical salinity differences of up to 1 ppt, vertical density differences of up to $1 kg m^{-3}$ are calculated. Measurements of the stratification during low wind periods (winds less than about $5 m s^{-1}$), conducted in February 1989, show clearly that such vertical salinity, temperature and therefore density differences are typical for summer during low wind periods, and these data are presented in the following discussion.

As described in Section 3.2, an intensive field survey of the three-dimensional salinity, temperature and density structure of Oyster Harbour was conducted from 13 to 17 February 1989. The transect paths, with associated conductivity-temperature-depth (CTD) profiling stations, are shown in Figure 5.1 and labelled T1, T2, T3, T4 and T5. These measurements were complemented by current velocity data inferred from drogue-tracking

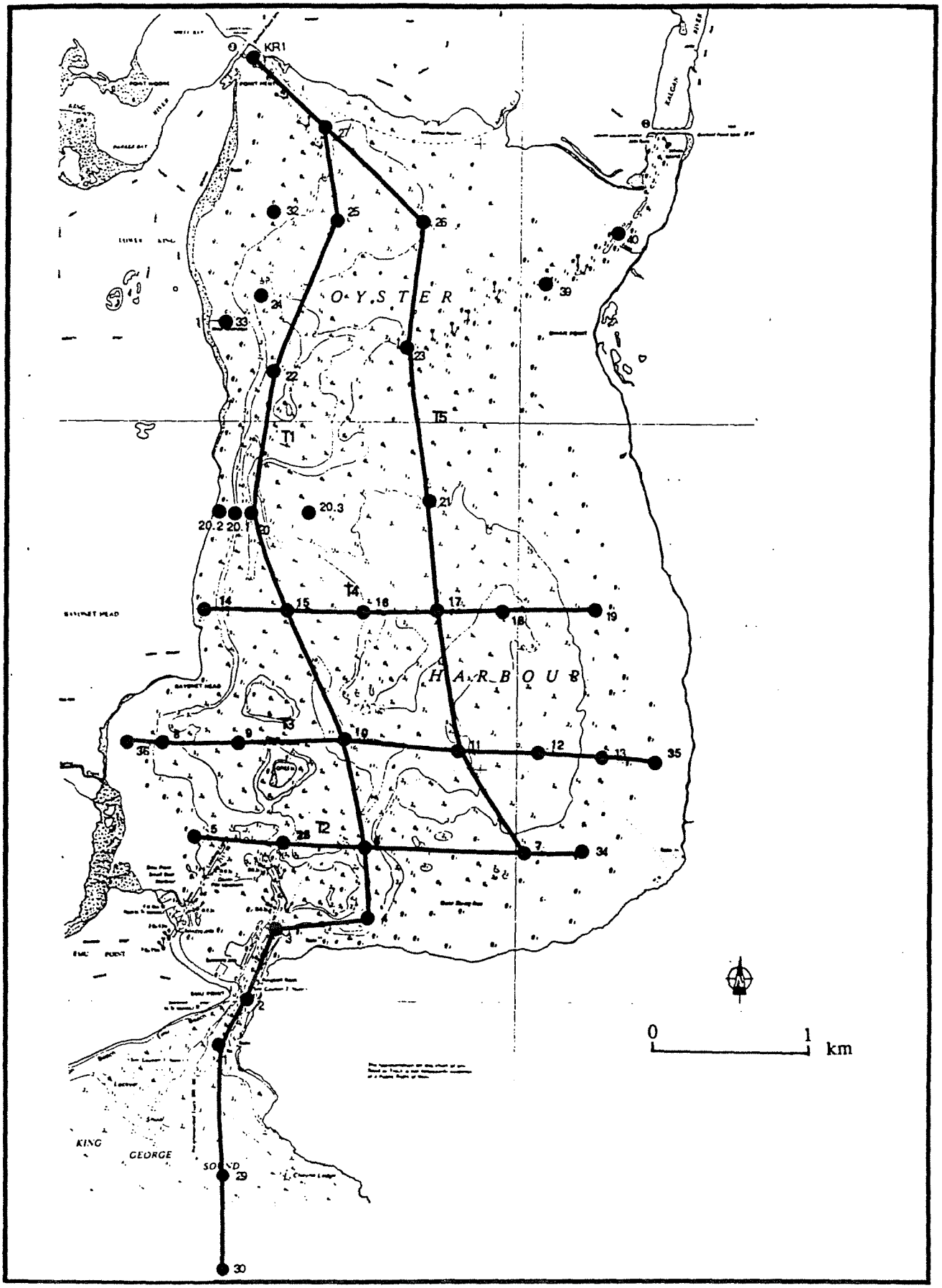

Figure 5.1 CTD data stations and transect paths T1, T2, T3, T4, T5.

The CTD data are reduced and plotted as vertical contour sections of salinity, temperature and density along the transect paths. All contour diagrams presented in this report have the format described in Figure 5.2.

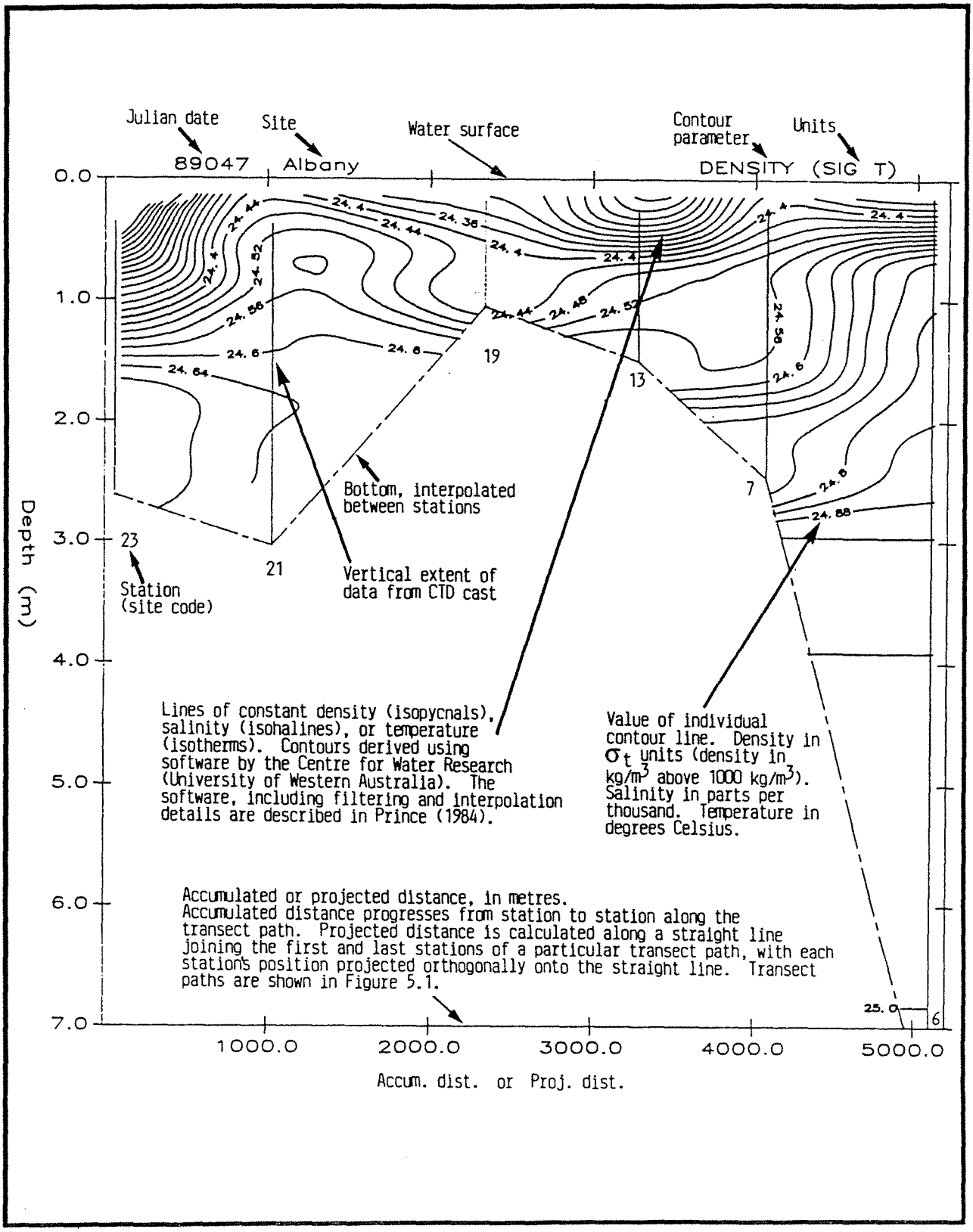

Figure 5.2 Description of a typical vertical contour diagram, as used to represent density, salinity or temperature stratification throughout this report.

In summer, marine water penetrates into the harbour on each flood tide as a bottom wedge. This salt-wedge structure was monitored by CTD profiling throughout five continuous diurnal tidal cycles. The mean features of the physical structure of the water during summer in Oyster Harbour are described in this section. More detailed discussions of individual hydrodynamic mechanisms in Oyster Harbour during summer are reserved for proceeding sections of this chapter.

The mean basin-scale structure of the water in Oyster Harbour during summer spring-tide conditions, when winds are relatively mild (less than about 5m s^{-1}), was captured on many occasions during the 5-day CTD survey from 13 to 17 February 1989. One such typical data set is presented in Figure 5.3, which contains the density, salinity and temperature contour plots from longitudinal transect T1 and lateral transect T4, performed between 1252 and 1504 on 16 February 1989. The tide had been in flood for over six hours. As shown in Figure 5.3, the harbour was stratified both vertically and horizontally as a salt-wedge estuary. There was a relatively thin (less than 2m thick) surface plume of buoyant water lying above the intruding marine wedge. A short burst of rainfall fell the preceding night and local runoff was the cause of this pronounced buoyant discharge plume, which had a strong frontal region at station 2.

Transect T1 from this survey stretched from the King River mouth (station 27) to station 30, nearly 2km out into King George Sound. It is interesting to note the differences in the strength of the vertical stratification in the waters of King George Sound, the entrance channel and the inner harbour. As is evident in Figure 5.3, the water in the Sound (stations 29 and 30) was strongly vertically stratified in temperature, with surface temperatures higher than bottom temperatures by about 0.5 °C due to solar heating by short-wave radiation, which ranged between 400 and 800 W m^{-2} throughout the day. The salinity contours show that the water in that region of the Sound was of constant salinity and hence the vertical density stratification, shown by the isopycnal contour plot, is a reflection of the temperature stratification. Once in the entrance channel (stations 1, 2 and 3) the stratified water of King George Sound underwent significant turbulent mixing due to the strong tidal inflow, and this is why the temperature and therefore density stratification in the channel is relatively weak. This conclusion was also supported analytically in Section 4.5.2, in which the mixing law for bottom mixing (Equation 4.9) was applied to a weakly stratified flow over a rough boundary for the Oyster Harbour entrance channel. After travelling through the channel the intruding marine water flows in as a relatively dense bottom current and enters Oyster Harbour as a salt-wedge.

Intensive measurements of the three-dimensional stratification of Oyster Harbour were conducted throughout approximately a 24 hour period from 2335 on 14 February to 2218 on 15 February. These data revealed the temporal characteristics of the salt-wedge structure in the harbour during a typical spring tidal cycle under relatively low wind conditions. Net discharge into Oyster Harbour was approximately 0.3m^3 s^{-1}, as shown in the hydrograph of Figure 5.4, and this is slightly higher than typical summer baseflows as a result of a discharge event on 26 January 1989. The tide was in ebb at the beginning of the data period (0000, 15 February) and then in flood thereafter (until 2218 hrs). Winds were relatively mild, ranging from about 3 to 6m s^{-1} and blowing from the northeast during the morning and swinging to west-northwest for the remainder of the day, as shown in the meteorological data set in Figure 5.5 containing wind, air temperature and solar radiation data from the the Green Island station and tide data from the Albany station (see also Chapter 3).

Six individual CTD profiling runs were performed along transect T1, throughout the day, starting at 2335 of 14 February during ebb, going through the low water period between 0430 and 0600 and ending at 2218 just before high water on 15 February. Transect T1 follows the longitudinal harbour alignment from the mouth to the head, with each station located in approximately the deepest part of the harbour along that alignment. A representative selection of these data sets have been presented as salinity, temperature and density contours in the following discussion. The exact transect paths for these runs are indicated by the grid presented in Figure 3.1, but in general they begin near the mouth of the King River and end in or near the channel at Emu Point.

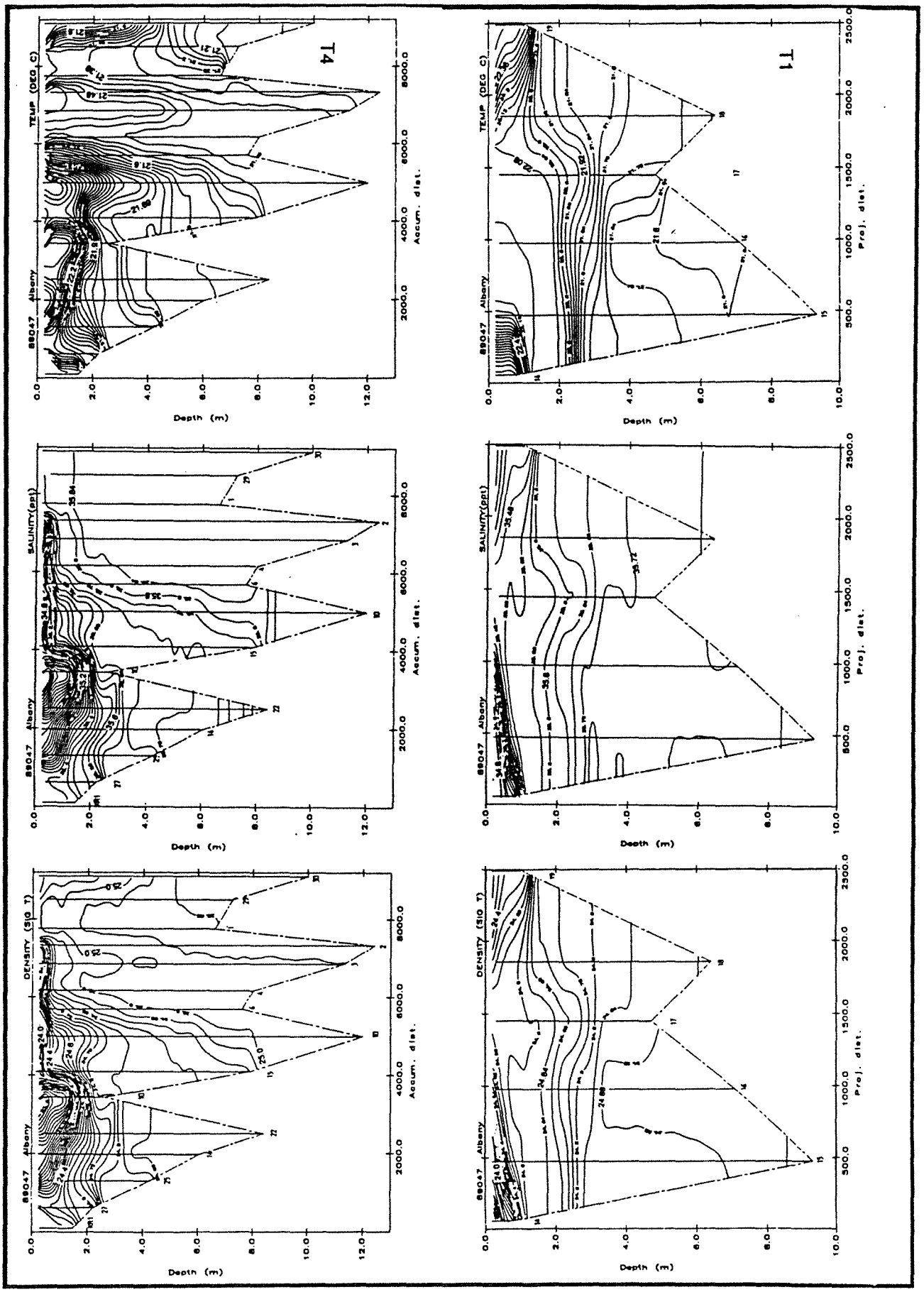

Figure 5.3 Density, salinity and temperature contour plots for transects T1 and T4, 1252-1504, 16 February, 1989.

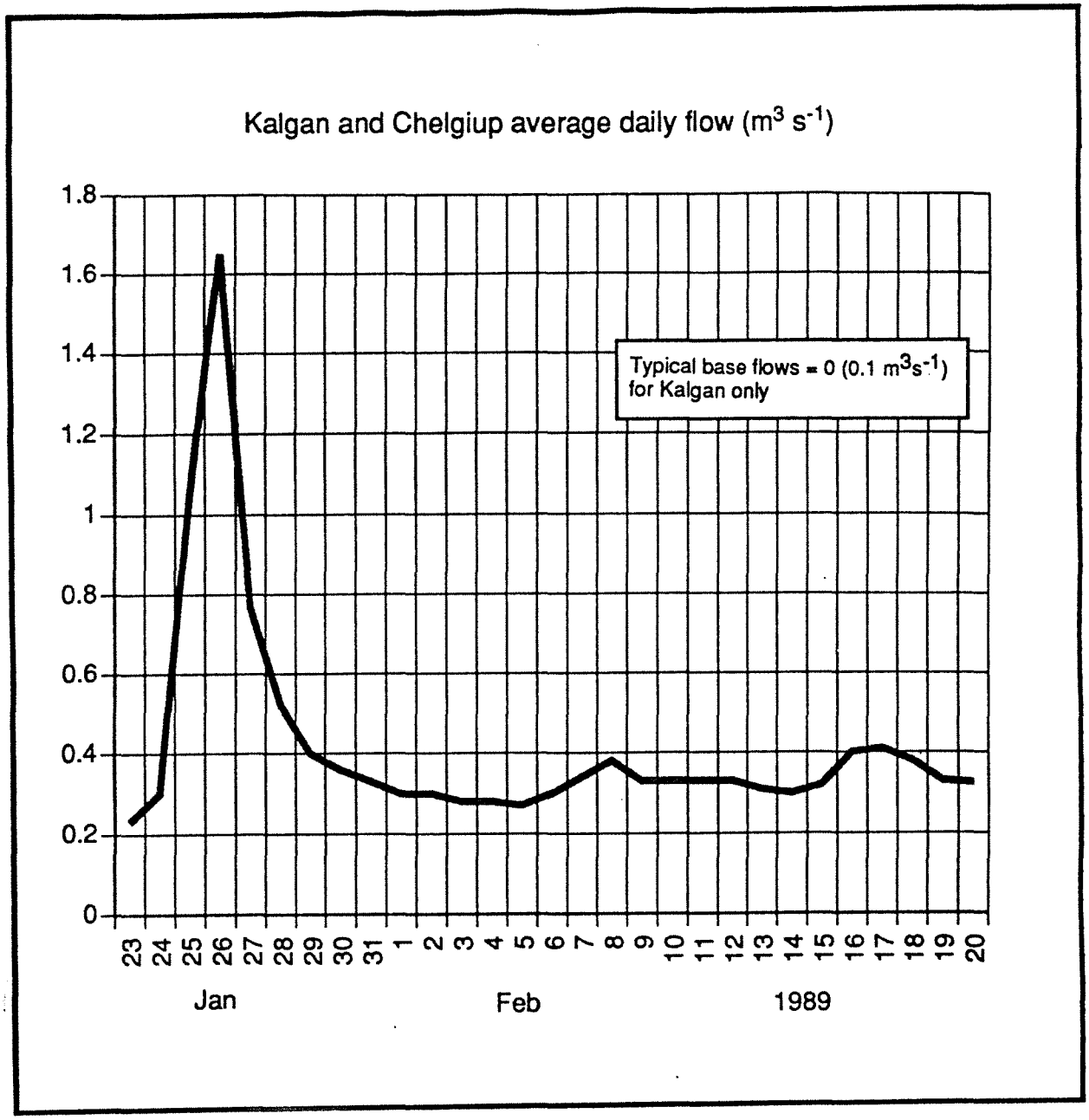

Figure 5.4 Kalgan River and Chelgiup Creek flows.

It is revealing to follow these contour plots through in chronological order. All discussion related to the meteorology can be referenced to the data presented in Figure 5.5.

Figure 5.6. Transect T1; 2335, 14 February - 0145, 15 February. Tide: ebb.

During this transect run the tide was strongly ebbing. Winds were about 3m s^{-1} and from the northeast. As the contours of salinity show (Figure 5.6), the harbour was stratified as a salt-wedge estuary. The temperature and density contours mirror those of salinity. Important features of this data set, with respect to the mean physical structure of the estuary, are described below.

(i) A buoyant surface plume of riverine water lies over the marine-wedge, and this represents the density-driven (baroclinic) flow of buoyant water towards the mouth.

The CTD measurements returned salinities as low as 5 ppt for the surface plume. The outflowing tide created a barotropic pressure gradient, due to the falling head at the mouth. This pressure gradient was directed downstream (southward) throughout the water column.

However, horizontal density gradients due to the salt-wedge structure resulted in an upstream (northward) directed baroclinic pressure gradient near the bottom and a downstream directed baroclinic pressure gradient near the surface. Hence, during this situation the tidal outflow is reinforced by density difference near the surface, but is opposed by density difference near the bottom. This interplay, between barotropic and baroclinic pressure gradients, manifested itself hydrodynamically by producing the shooting flow of a thin plume of buoyant water at the surface, heading towards the mouth. A similar mechanism was identified to operate in the intricate channel network around the inner periphery of the estuarine Venice Lagoon, Italy, during ebb tides, and was shown to be very important in enhancing mass transport to the adjacent Adriatic Sea (Imberger, D'Adamo and Oldham, 1990). This is important for Oyster Harbour, in terms of the basin-scale flushing, because it represents a residual transport mechanism that enhances the tidally driven ejection of resident upper harbour waters out into King George Sound. Vertical mixing will, of course, alter this picture, and this is discussed further in this Chapter.

The mild northeast wind that was blowing during this period would have reinforced this downstream surface flow by superposing a downstream surface wind-drift up to approximately 5cm s^{-1}.

A quantitative analysis of the relative importance of tidal and density driven flushing in Oyster Harbour can be performed.

From the tidal plot of Figure 5.5, it is evident that the water level of the harbour falls at a rate of up to approximately 5 x 10^{-5} m s^{-1}. The surface area of the harbour and adjoining rivers up to the King and Kalgan River upper bridges, is approximately 18 square kilometres. A tidal discharge rate through the mouth of up to 900m^3 s^{-1} is therefore calculated. The cross-sectional area of the central harbour is approximately 18000 square metres and hence a cross-sectionally averaged tidal outflow velocity through this region of approximately 4cm s^{-1} is calculated. It is to be noted that the momentum of tidal flows will be significantly damped over the shallows due to bottom friction, hence the flow may tend to be weaker over the shallows and stronger in the central deeper regions. Currents of 2-10cm s^{-1} were measured during a strong ebb by drogue-tracking in the lower harbour. The strongest flows were in the central regions, and the weakest over the eastern shallows. The current data from drogue-tracking are discussed more fully in the proceeding section (5.2).

Differences between the spatially averaged densities of the upper and lower harbour regions are typically of the order of 1kg m^{-3} in summer, as the contour plots in Figures 5.6, and 5.7 to 5.9 (following), indicate. The simplest way to estimate densimetric velocities driven by such density differences in a basin is to assume lock-exchange flows. These are produced by the removal of a gate separating two fluids of different density. Chen (1980) reviewed the literature on lock-exchange flows and presented a relation, giving the scale of the current velocity in lock-exchange flows:

$$u \sim (g'H)^{1/2}, \qquad 5.1$$

where H is the depth of the basin. A proportionality constant of approximately 0.5 can be applied to equation 5.1 (Simpson, 1982). Hence, for a density difference of 1kg m^{-3} and a basin depth range of 1 to 10m a densimetric velocity range for lock-exchange flow of approximately 5 to 15cm s^{-1} is calculated. This analysis indicates that density current flows could be as important as tidal flows in transporting mass horizontally in the inner regions of Oyster Harbour. This argument may not be valid in regions where the harbour narrows, such as through channels, in which case tidal flows would be accelerated.

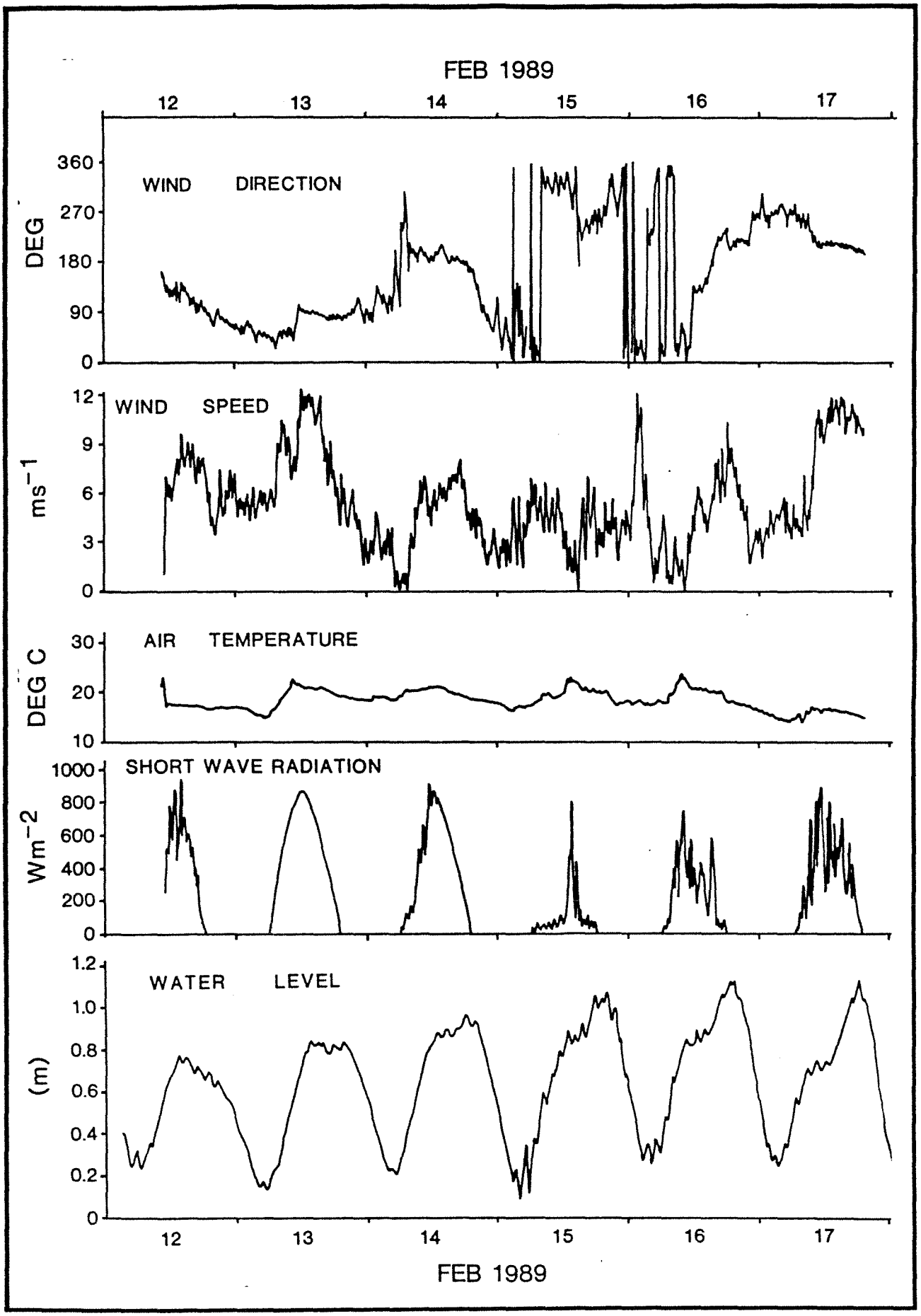

Figure 5.5 Meteorological data. Green Island, Oyster Harbour, 12 - 17 February, 1989.

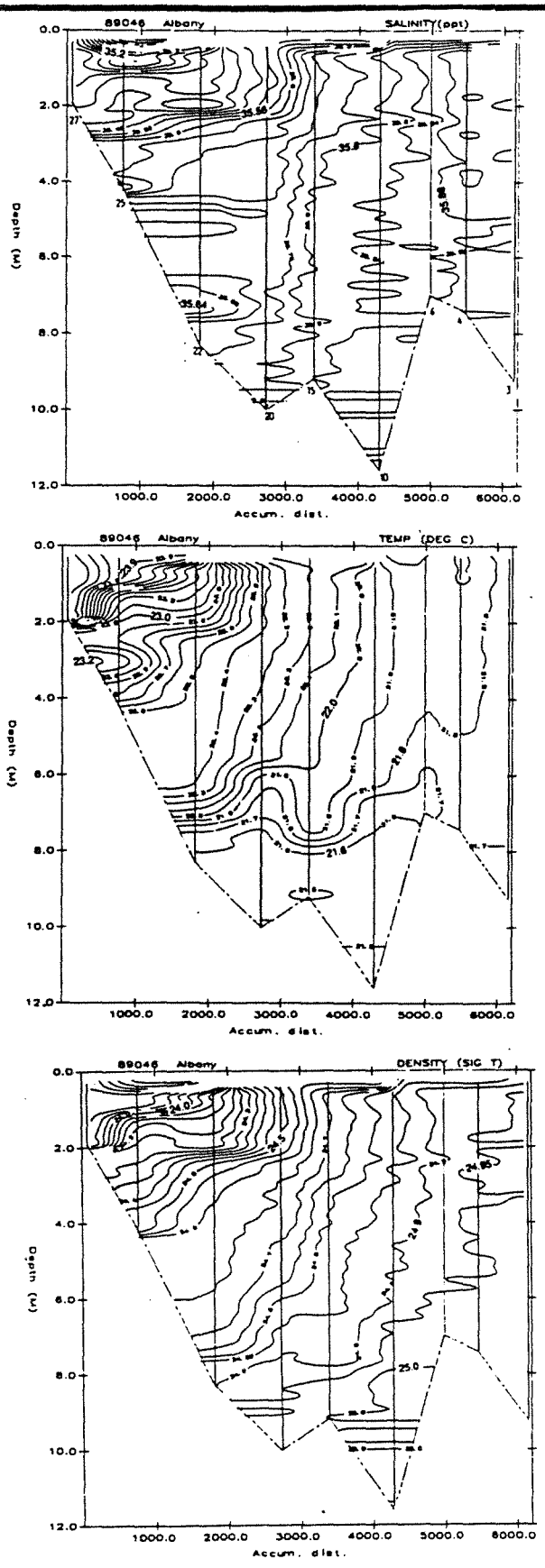

Figure 5.6 Salinity, temperature and density contour plots for Transect T1 2335 14 February - 0145 15 February, 1989.

If we assume that during flood tides downstream density currents are restrained by the opposing barotropic force of the tide, but that during ebb periods thin surface flows of less than 1m thickness (see Figure 5.6) are driven toward the mouth by a superposition of density and tidal forcing , then surface transport rates in a 12 hour ebb phase of the order of 10 to 20cm s^{-1} are calculated. This flow velocity results in a downstream directed surface advection of 4 to 8km per tidal cycle, which is sufficient to drive surface water from the northern periphery of Oyster Harbour to the mouth in less than one day. Hence, flushing times for surface waters in Oyster Harbour of the order of one day are calculated. Bottom waters in Oyster Harbour will have longer residence times, because they are subjected to a residual baroclinic forcing which is directed upstream. Vertical mixing processes will, however, lead to an upward transport of bottom water. Downstream directed baroclinic currents, in conjunction with ebb flows, can then drive this water out toward the mouth. Both the density-driven surface flow mechanism and the potential of environmental forcings to mix the water column is investigated further in this chapter.

(ii) A strong frontal region lies between stations 20 and 15, and this represents the main front of the buoyant harbour water that had been forced to pile up at the northern end under the upstream barotropic forcing of the preceding flood tide. The thin lens of buoyant water ahead of this front at the surface is the gravitational overflow emanating from the surface mass of buoyant water that lies behind the frontal region. The mean structure of this gravitational overflow was presented in (i), above.

(iii) The water under the thin gravitational overflow is weakly stratified between stations 15 and 3. This water represents the relatively well-mixed mass of marine water that had been advected into the harbour as a bottom wedge during the preceding flood tide. Salinities in this mass of water are greater than about 35.8 ppt, being close to oceanic salinities, as identified by CTD measurements in King George Sound throughout the study.

Figure 5.7. Transect T1; 0612 - 0803, 15 February. Tide: Start of flood.

The contours in Figure 5.7 are from transect T1 conducted immediately after low water on 15 February. As the tidal plot in Figure 5.5 shows , the low water period had four minor troughs. Transect T1 was performed from 0612 to 0803 hrs and included the last of these four troughs. The tide had risen by about 30cm with respect to low water by the end of this transect run.

Winds were still blowing from the north-northeast but had strengthened, compared to those during the previous transect (Figure 5.6), to about 5m s^{-1}. During the night air temperatures fell to about 15 °C, about 6 °C cooler than the day-time maximum. The tide fell about 1m in 8 hours during the preceding ebb.

The salt-wedge structure is evident in Figure 5.7, and on a basin-wide scale the stratification resembles that measured during the preceding ebb phase (Figure 5.6). The main hydrodynamic features of a surface buoyant flow, emanating from a general region of relatively less saline water in the upper harbour, over a general mass of weakly stratified marine water in the lower harbour, are still evident.

The intruding mass of marine water in the entrance channel is characterised by its well-mixed nature. The density of the marine water is close to 1025kg m^{-3} (or 25.0kg m^{-3}, expressed as sigma-t units). In Figure 5.7, the wedge-like structure can be seen to be established as soon as the marine water leaves the entrance channel and enters the larger expanses of the lower harbour, around stations 4, 6 and 10, for example.

Apart from in the entrance channel, the vertical stratification in the harbour resisted vertical mixing during what was a relatively intense preceding spring ebb tide. The mechanisms of wind mixing through the surface, wind-induced upwelling, penetrative convection due to surface cooling, tidally induced bottom boundary turbulence, interfacial shear between the bottom wedge and shooting buoyant surface flow, or lateral density currents driven by density gradients caused by differential cooling, were not able to break down the vertical density structure.

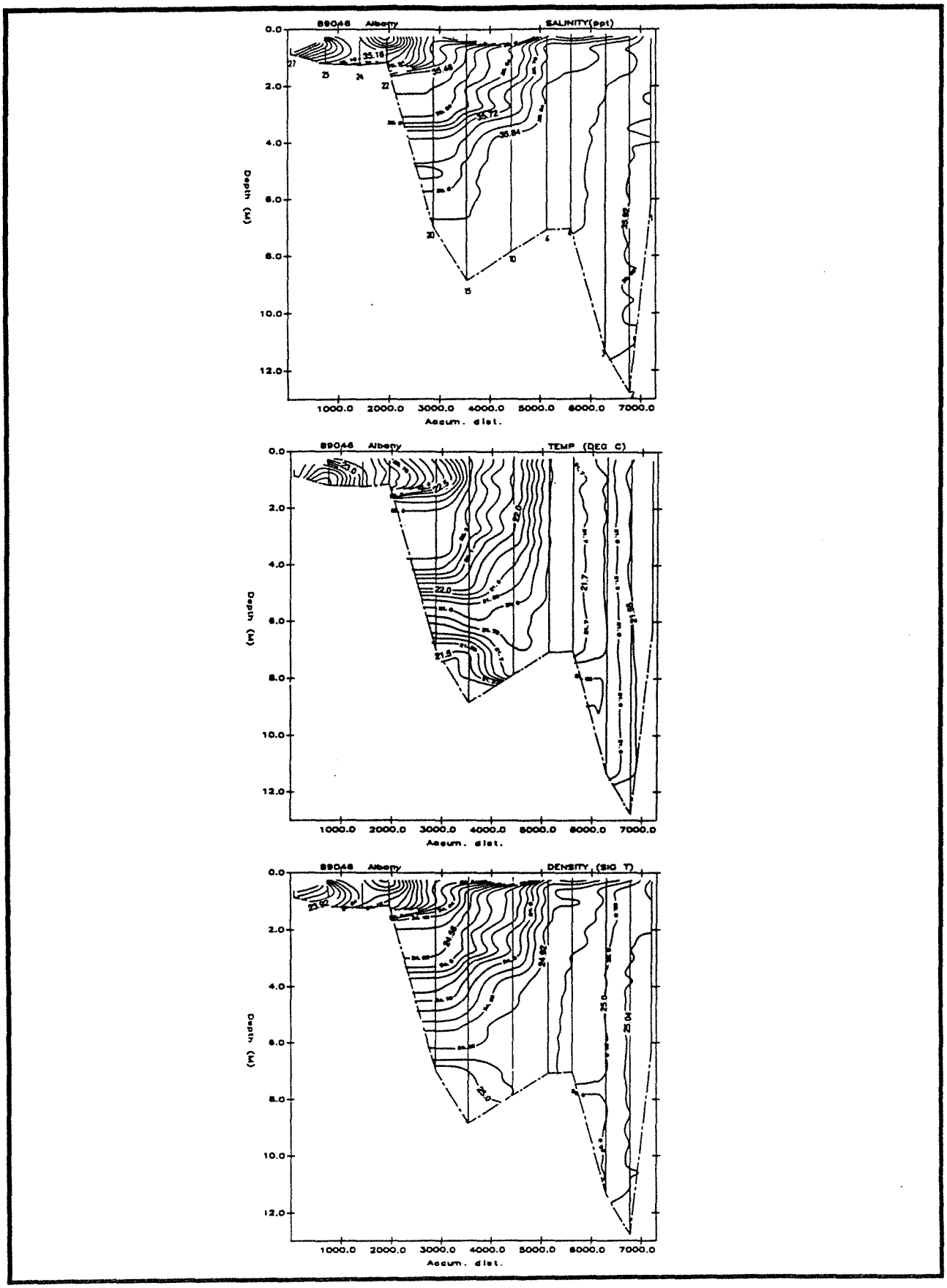

Figure 5.7 Salinity, temperature, density contour plots for transect T1, 0612 - 0803 15 February, 1989.

Figure 5.8. Transect T1; 1204 - 1246, 15 February. Tide: Fully developed flood

The contours in Figure 5.8 are from transect T1 conducted 8 hours into the flood tide on 15 February. The tide had risen 70cm since low water at about 0430 of that morning. The salinity, temperature and density contours all indicate an intruding bottom wedge of marine water, entering through the mouth. The marine front, indicated by the 1025kg m^{-3} isopycnal, had reached station 10, about 2km in from station 3 in the channel. This rate of entry corresponds to a mean speed for the intrusion of the marine-wedge of the order 10cm s^{-1}

In the period between the times of this and the previous transect (Figure 5.7) winds were from the north-northeast at about 3-5m s^{-1}. Air temperature had reached about 20 °C and solar radiation was low before 1200 due to cloud cover but increased to about 600-1000 W m^{-2} between 1200 and 1400 as the skies cleared of cloud cover.

The stratification shown in Figure 5.8 represents the typical salt-wedge nature of the harbour water under low wind conditions. Again, none of the environmental forcings (wind, tide, heating, streamflows, density currents) were able to initiate any appreciable vertical mixing in the harbour, except in the strong tidal current region near the mouth where the water column is homogeneous.

Drogues were deployed during this period in the central regions of the lower harbour and show that relatively large horizontal eddies were formed in the central harbour during the flood period. The northwest wind field of 3-5m s^{-1} would have caused surface drift currents in the upper metre of about 4-7cm s^{-1} and these were oppositely directed, but of the same magnitude in speed, as tidally induced currents in the same region. The dynamical interplay between opposing wind and tidal forcings probably caused the eddying, and this is discussed more fully in the proceeding section (5.2).

Figure 5.9. Transect T1; 2113-2218, 15 February. Tide: Towards end of flood.

The contours in Figure 5.9 were from transect T1 conducted 17 hours into the flood tide on 15 February. The tide had reached its first major peak at 1930, fell slightly, and then rose again to high tide level at 2150 (Figure 5.5).

The tide had risen almost 1 metre since low water at about 0430 of that morning. The salinity, temperature and density contours all indicate an intrusive bottom wedge of marine water, entering through the mouth. Again the water in the entrance channel (up to approximately the position of station 4) is well-mixed due to boundary turbulence along the channel bottom and sides. Winds were relatively weak (approximately 3m s^{-1}) and from the northwest. Air temperatures had fallen to about 18 °C. The bottom nose of the marine wedge, indicated by the 1025kg m^{-3} isopycnal, had reached approximately station 20, about 4000m in from the mouth, by 2140 hours. This corresponds to an average inflow speed, since the beginning of the flood tide, of the order of 7cm s^{-1} and this is within the same order as that calculated from Figure 5.8, above, when the stratification was measured at approximately 1200 hours.

In Figure 5.9, it is interesting to note the surface front of relatively less saline water between stations 27 and 4, and extending vertically down about 3m from the surface. This mass of water represents resident harbour water, that is separated from the intruding marine wedge. The strong density gradient zone at the interface between this surface mass of water and the intruding wedge, suggests that little exchange of mass between these two water bodies had occurred during the flood phase of the tide. The characteristic salt-wedge structure of that day (see the previous contour plots in Figures 5.6, 5.7 and 5.8) is still evident, even at the very end of the spring flood tide. Again, none of the available environmental forcings were able to break down the vertical or horizontal stratification. This suggests that little mixing occurred between the intruding marine wedge and the slightly less dense mass of buoyant resident harbour water.

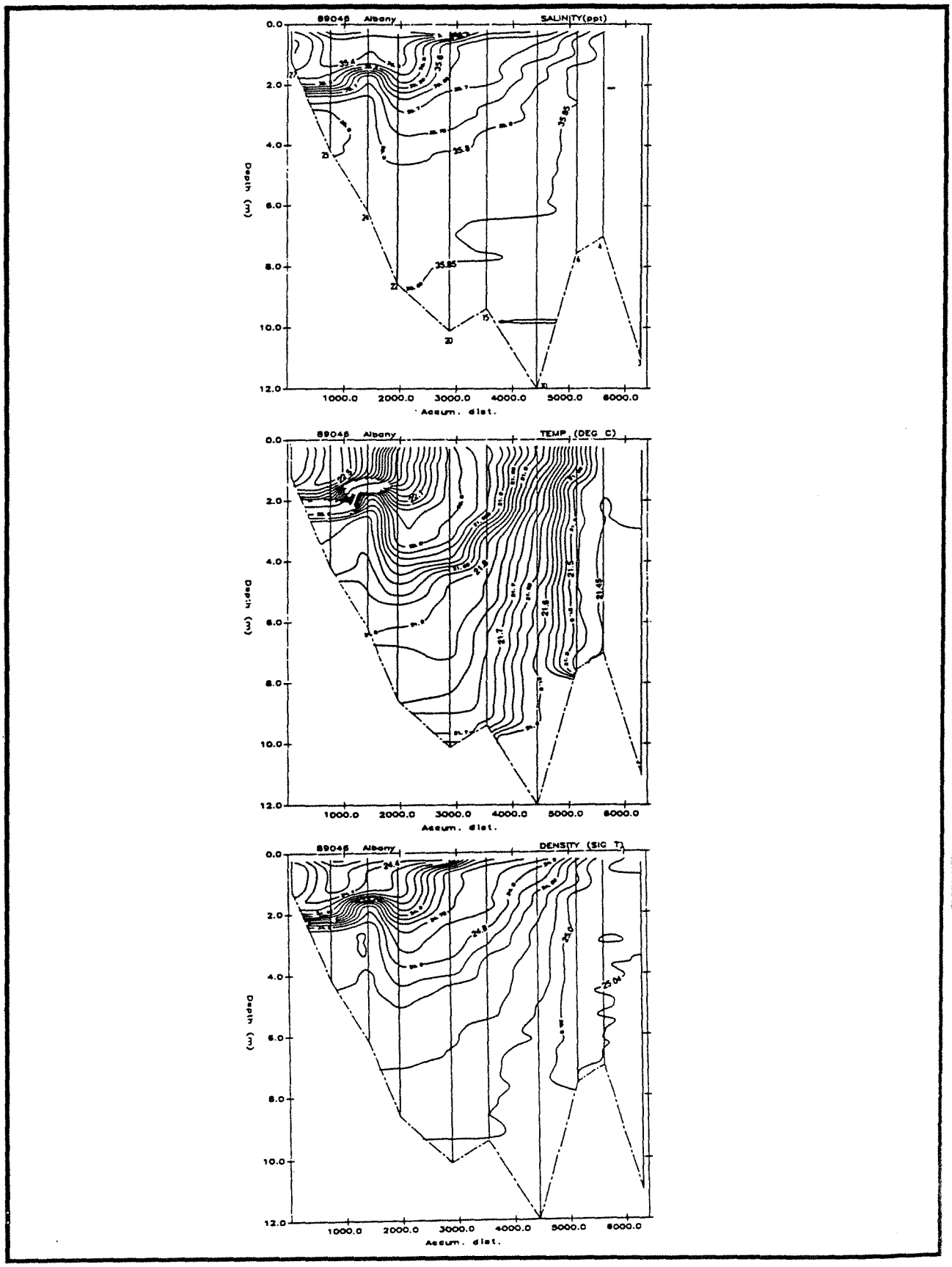

Figure 5.8 Salinity, temperature and density contour plots for transect T1, 1204 - 1246 15 February, 1989.

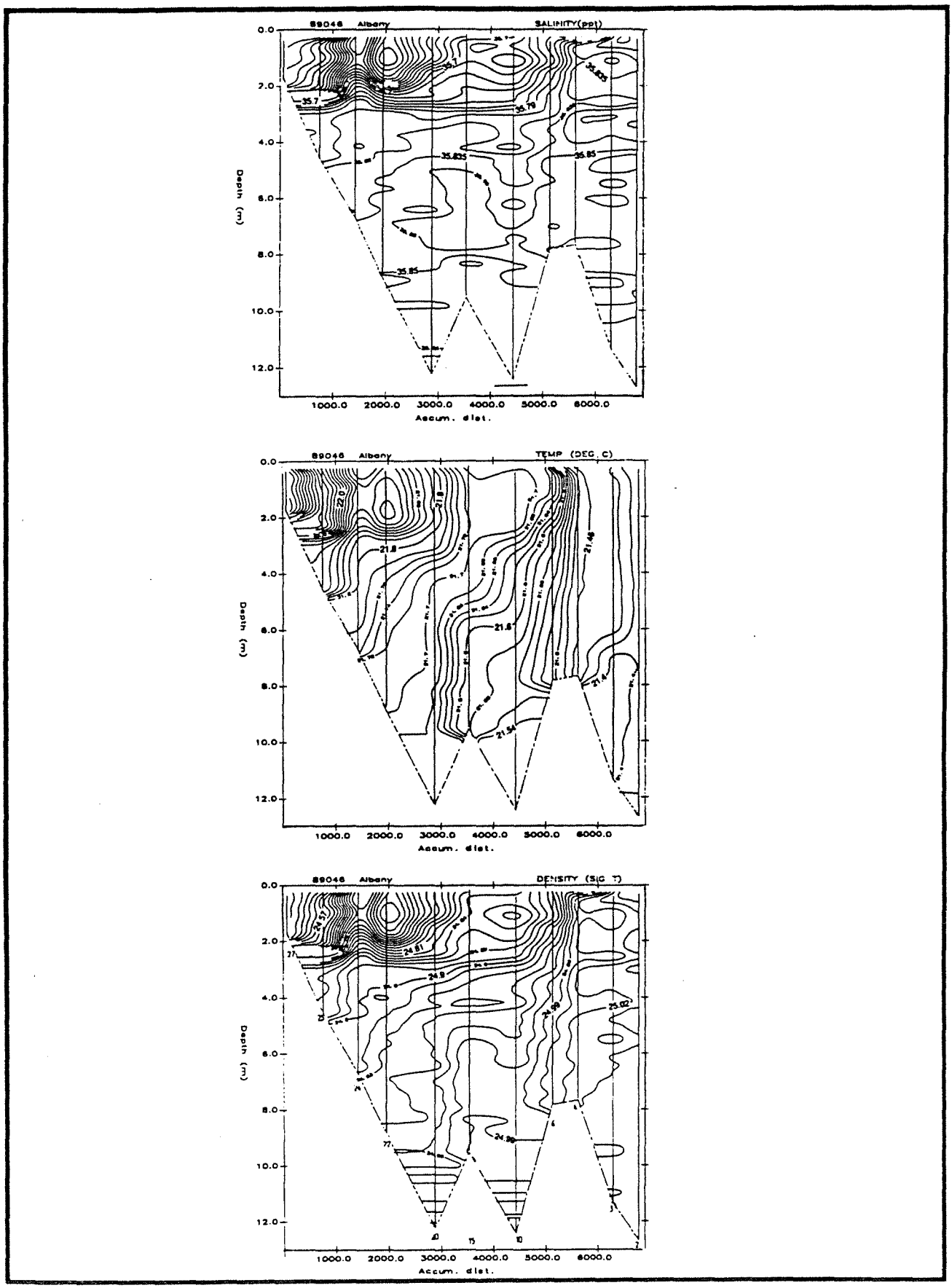

Figure 5.9 Salinity, temperature and density contour plots for transect T1, 2113 - 2218 15 February, 1989.

Summary

In summary, the CTD data from 14 and 15 February 1989, discussed above, have indicated that the mean structure of Oyster Harbour during mild wind conditions in summer is that of a salt-wedge.

The tide drives a relatively saline marine wedge into the harbour via the entrance channel. The marine water was found to be well-mixed in the entrance channel due to boundary turbulence during spring flood tides

Once through the channel, the marine water intrudes under, and displaces upstream towards the northern bank, the resident harbour water that is slightly less dense than marine water due to dilution with freshwater inputs.

When winds are weak, wind mixing between these two individual masses of water is negligible. As a result, by the end of the flood tide, the relatively less saline resident harbour water is forced to 'pile-up' against the northern boundary of the harbour.

Upon the turn of the tide, this buoyant surface mass propagates as a thin (less than 1m thick) surface gravitational overflow down the harbour at speeds of the order of 10 to 20cm s-1, under a superposition of baroclinic forcing due to density difference and barotropic forcing due to the falling tide. Bottom water propagates out toward the mouth during ebbs at lower velocities than the surface front because, at depth, the horizontal density gradient is reverse to that at the surface, with more saline (and therefore denser) water residing in the lower harbour.

The influence of individual hydrodynamic mechanisms that superpose to yield the mean summer structure of the harbour, as shown above, is discussed in the proceeding sections. In addition, the important influence of wind mixing over a wide range of speeds and directions will be investigated.

5.2 Tidal inflows and outflows

5.2.1 Salt-wedge propagation

Drogue-tracking during spring flood and ebb periods was performed between 13 and 17 February 1989 in three regions of the study site, comprising the entrance channel, the lower central harbour and a region outside of the channel in King George Sound. The drogues that were deployed were of the cross-vane type, having projected areas, in elevation view, of 2 or 4 square metres. The drogues were tracked (as described in Chapter 3) and currents inferred from the relative displacements of each drogue with respect to time. In addition, basin-wide CTD surveys in this same period enabled the displacement of individual isohalines (lines of constant salinity), isotherms (lines of constant temperature) and isopycnals (lines of constant density) to be followed as indicators of water movement.

The stratification data in section 5.1, above, has shown that the harbour has a residual salt-wedge structure in summer. During spring tides, when water level varies diurnally by up to about 1m, the tidal prism is of the order of 18×10^6 m^3, as compared to the harbour volume at low water of 40×10^6 m^3. During neaps, when water level varies diurnally by as low as about 0.3m, the tidal prism reduces to about 5×10^6 m^3. Clearly, the tide introduces a significant mass of oceanic water into Oyster Harbour during floods. The drogue results to be discussed in this section show that, on a basin-wide scale, the tide drives a cyclic barotropic flow field in Oyster Harbour that is directed upstream during floods and downstream during ebbs. The extent to which the marine wedge is driven into and out of the harbour during typical diurnal tides is now investigated.

Flood flows by drogue tracking

Drogues were released both at 1 and 4m depths and tracked in the central regions of the lower harbour during the flood tide of 14 February 1989. The drogue tracks from this survey are shown in Figure 5.10. On that day both the tide and wind were in the same direction (heading

north in Oyster Harbour) and hence the tidal inflows were reinforced by surface wind drift. Winds on that day ranged from about 0-3m s^{-1} in the morning to about 5m s^{-1} in the afternoon (see Figure 5.5). All drogues tracked in the central regions of the lower harbour moved upstream at speeds of order 5-10cm s^{-1}, however over the eastern shallows the drogues moved at about 2-5cm s^{-1}. The tidal currents over the shallows were relatively weak due to frictional damping.

These data indicate that the salt-wedge is driven upstream during spring tides at a time-averaged rate of up to 10cm s^{-1}. This would result in the salt-wedge penetrating upstream as far as approximately 4km with respect to the mouth during a 12 hour flood period. This result is confirmed by isopycnal tracking (discussed below).

Ebb flows by drogue tracking

Surface drogues were tracked during a spring ebb tide, in the central regions of the lower harbour from 2200 16 February to 0500 17 February 1989. The drogue tracks from this survey are presented in Figure 5.11. Winds were from the west at about 2-6m s^{-1}. As shown, all drogues, with the exception of that over the eastern shallows, headed southwards, towards the mouth. The centrally released drogues were advected in the tidal ebb flow, and had speeds of approximately 4-10cm s^{-1}. However, the drogue over the eastern shallows headed towards east, which was in the downwind direction. As for the flood tide drogue data (above) it would appear that tidal flows are appreciably damped over the shallows. In this case it is apparent that the circulation over the eastern shallows was dominated by wind drift.

One of the drogues (No. 5 in Figure 5.11) exhibited an interesting behaviour; it was released at 2203 16 February in the deep alignment near Green Island and was tracked to exit through the mouth and be approximately 1500m into King George Sound by 0317 17 February, at which point it was lost sight of, only to re-appear again just outside of the mouth at 1117 17 February presumably re-advected in towards the harbour by the flood tide. The average propagation speed of the drogue through the channel was about 40cm s^{-1}. This raises the possibility that at times a significant volume of the tidal jet of an ebb tide can be effectively re-advected back into the harbour on the subsequent flood tide. This is discussed more fully in Section 5.2.4 (below).

Tidal oscillations of the salt-wedge by tracking isopycnals

The upstream propagation of the tidal wedge is also revealed by tracking the displacement of individual density contour lines as a function of time. Sixteen longitudinal CTD transects along transect T1 were made throughout the survey period from 13 to 17 February 1989. The density of the channel water at low water on 15, 16 and 17 February was measured with the CTD probe to be close to 1025kg m^{-3}. The longitudinal CTD transects enabled the upstream extent of this marine water to be determined throughout the five-day period. Figure 5.12 presents a chronological sequence of isopycnal contour plots for transect T1 from the sixteen CTD data runs, performed between 0950 13 February and 1533 17 February 1989. Table 5.1 summarises the results of tracking the 1025kg m^{-3} isopycnal.

The results in Table 5.1 indicate that the salt-wedge has a greater rate of inflow than outflow. From the sixteen isopycnal tracks it is evident that the bottom nose of the wedge intrudes during spring flood tides at rates that range from 3 to 20cm s^{-1}, with an average of all measurements being 12cm s^{-1}, and during spring ebbs it retreats at rates that range from 3 to 10cm s^{-1}, with an average of all measurements being 7.5cm s^{-1}.

These results are fairly consistent with the speeds inferred from the drogue tracking data, however the drogues indicated slightly lower velocities on average. The reason for this is probably that the drogues tracked currents at 1 and 4m depths, whereas the isopycnal tracking was for the upstream extent of the intruding marine water along the bottom. Nearer the surface, the wedge is retarded during flood tides by the opposing baroclinic force of the resident, less saline, harbour water. In contrast, near the bottom the density gradient is in the reverse direction with the densest water near the entrance channel reinforcing, in a baroclinic sense, the

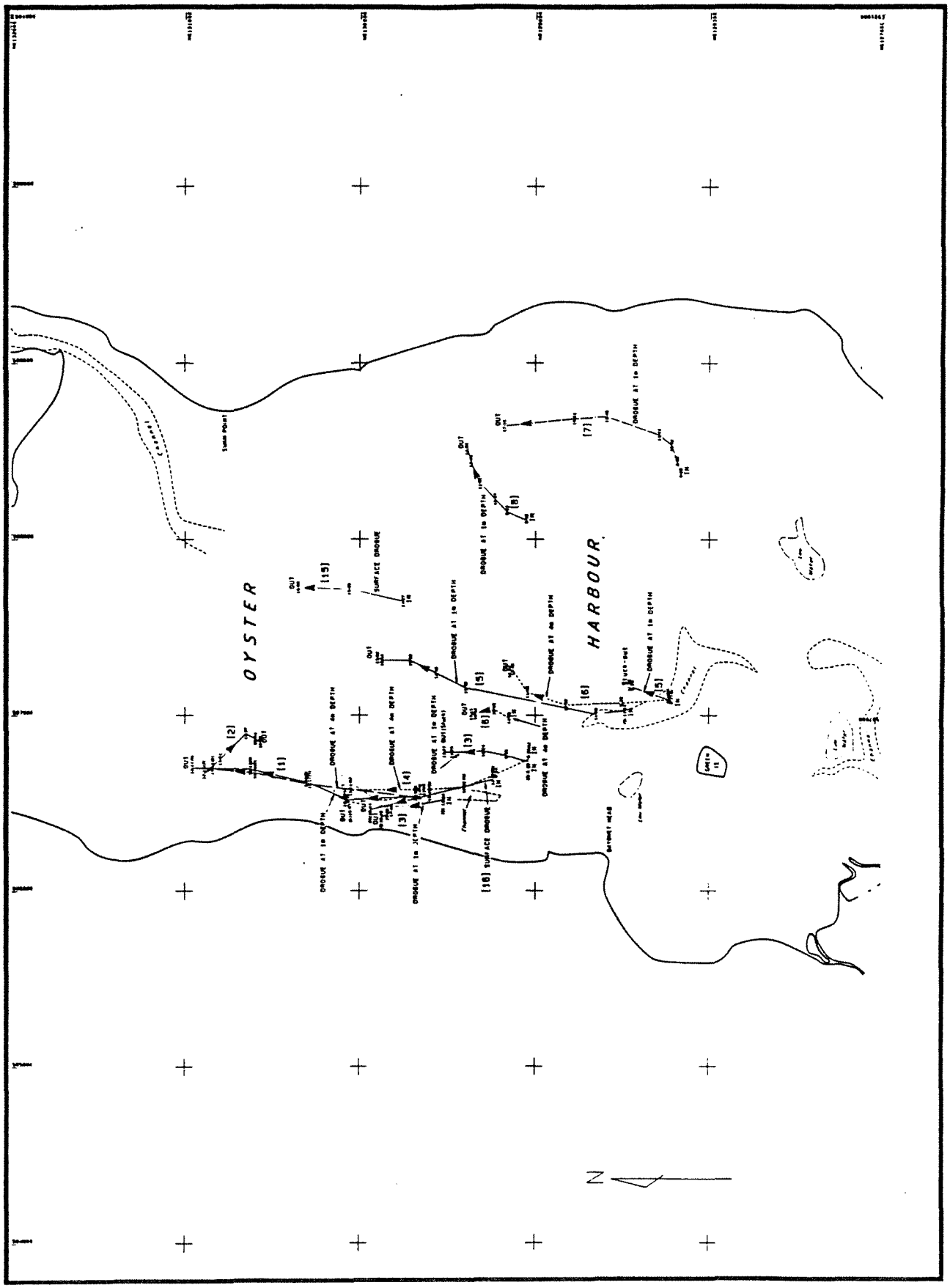

Figure 5.10 Drogue tracks from drogues released in Oyster Harbour during spring flood tide between 0800 and 1500 14 February 1989.

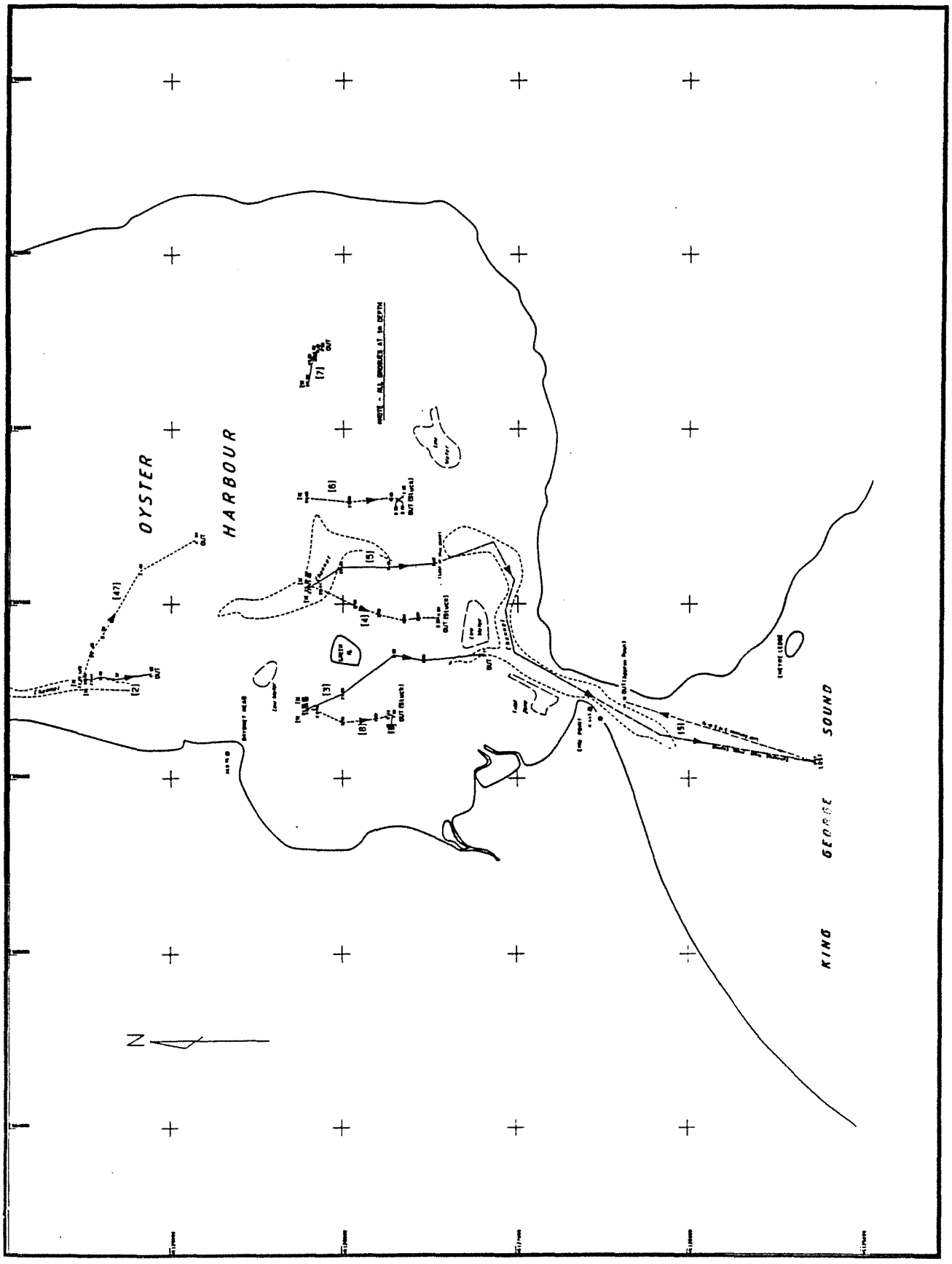

Figure 5.11 Drogue tracks from drogues released in Oyster Harbour during spring ebb tide between 2200 16 February and 0500 17 February, 1989.

upstream barotropic tidal forcing during floods and opposing the downstream barotropic forcing during ebbs.

Table 5.1 Tidal propagation of the salt-wedge in Oyster Harbour in summer during spring tides. The propagation of the wedge is inferred by the displacement of the 1025kg m^{-3} isopycnal near the bottom, representing the nose of the salt-wedge. The data were collected with the CTD probe (see Chapter 3). The average speed of propagation between individual measurements has been calculated, with the turn of the tide used as a datum where possible.

DATE FEB 1989	TIME (HRS)	TIDE	DISTANCE (APPROX) WITH RESPECT TO MOUTH (STN 2) OF THE NOSE OF THE WEDGE ALONG THE BOTTOM (m)	TIME-AVERAGED SPEED OF WEDGE +=upstream (inflow) -=downstream (outflow) cm s^{-1}	COMMENTS/TIDAL INFORMATION	FIG No.
13	1020	flood	+3900	+20*	Tide in flood since 0448. During a strong storm	5.12a
14	1209	flood	+2000	+8*	Tide in flood since 0536	5.12b
15	0145	ebb	0	>-10*	Remnant bottom pool of marine water at Stn 10. Tide had been ebbing since 1912, 14 Feb	5.12c
15	0645	flood	+1500	+36**	The wedge was very thin along the bottom upstream of Stn 10, probably due to the series of minor ebbs at low water (LW). First LW at 0536, then again at 0848, then flood	5.12d
15	1233	flood	+2350	+4*		5.12e
15	1432	flood	+3300	+13*		5.12f

DATE FEB 1989	TIME (HRS)	TIDE	DISTANCE (APPROX) WITH RESPECT TO MOUTH (STN 2) OF THE NOSE OF THE WEDGE ALONG THE BOTTOM (m)	TIME-AVERAGED SPEED OF WEDGE +=upstream (inflow) -=downstream (outflow) cm s^{-1}	COMMENTS/TIDAL INFORMATION	FIG No.
15	1853	flood/ slack	+3000	-2	Minor tidal oscillations (three ebbs) occurred between 1400 and 1700	5.12g
15	2146	high water (HW)	+3280	+3*	First HW at 1910, then again at 2126, then ebb	5.12h
16	0900	flood	+1000	+10*	Three LWs: at 0424, 0600 and 0712 (lowest LW at 0600)	5.12i
16	1311	flood	+3875	+19*		5.12j
16	1725	flood/ slack	+2810	-7	Minor slack between 1200 and 1624	5.12k
16	2213	HW	+2333	-3*	HW at 2024, slack until 2200, then ebb	5.12l
16	2332	ebb	+2000	-6*		5.12m
17	0600	LW	-500	-10*	Tide in flood since 0536	5.12n
17	1042	flood	+2500	+18*		5.12o
17	1520	flood/ slack	+2350	-1	Minor slack between 1136 and 1600	5.12p

* indicates that high confidence is placed in using this value as a measure of the tidally forced propagation speed of the salt-wedge nose in the harbour. The other values are considered unrepresentative because they occurred at times when the tide was in a period of temporary slack.

** indicates that this value was unusually high, compared to all other values, and the reason is that this was the average velocity of flow through the narrow entrance channel, which is much higher than the velocity of the wedge when it subsequently enters the wider cross-section of the lower harbour at the end of the channel.

Approximate statistics

Average of all inflow speeds = 12cm s^{-1}

Average of all outflow speeds = 7.5cm s^{-1}

Calculations earlier in this report (Section 5.1) estimated the residual two-layered velocity regime that is present due to horizontal stratification by performing a simple lock-exchange calculation. Using the stratification data in the sixteen contour plots of Figure 5.12, a longitudinal density difference of 0.5kg m^{-3} is used. By applying Equation 5.1 a baroclinic velocity of the order of 5cm s^{-1} is calculated. This is the likely explanation why the drogue and isopycnal tracking exercises returned higher inflow propagation speeds for the bottom nose of the wedge when compared to outflow speeds.

There is evidence that during ebbs some of the dense marine water remains trapped as a bottom pool in the lower harbour (see Figure 5.12c, for example). This indicates that outflows can over-ride the densest water at the bottom, with shear between the two layers insufficient to completely entrain bottom waters up into the outflowing upper layer. This 'trapping' can be expected to be even more pronounced during weaker tides, especially during neaps.

A simple first order estimate of exchange between the harbour and ocean can be made on the basis of the results of the isopycnal tracking, described in Table 5.1, above. These results indicate a residual (tidally averaged) upstream (northward) intrusion of marine water of about 4.5cm s^{-1} for spring tides. If we assume the marine water intrudes upstream as a bottom wedge with an average vertical thickness of say 4m and an average width of say 750m then a tidally averaged inflowing volumetric flux for a spring tide period of 135m^3 s^{-1} is calculated.

This flux would result in an introduction of the equivalent of a harbour volume (calculated at spring high water) in a time of about 4 days. If we allow for much reduced inflow rates during neap tides then higher values, closer to about 10 days, are calculated for the time taken to introduce the equivalent harbour volume into Oyster Harbour by the tidally averaged upstream propagation of marine water via the mouth. Hence, this analysis can be extended to conclude that on the basis of the results of the tracking of isopycnals (Table 5.1) flushing times for bottom waters of the harbour are greater than about 4-10 days.

Some of the contour plots in Figure 5.12 (in particular 5.12 l and m) indicate a relatively fast downstream (southward) propagation of surface water (in the upper 0.5m), compared to deeper waters, during ebb tides. The residual downstream baroclinic forcing due to density difference is responsible for this because it superposes its own downstream velocity field on the barotropic outflow during ebbs. For example, the 35.2 ppt isohaline near the surface has propagated downstream a distance of approximately 2000m in about 105 minutes, which equates to a time-averaged speed of 30cm s^{-1}. This measurement is consistent with the theoretical predictions performed earlier (Section 5.1) for this transport mechanism. At mid-depth, the downstream propagation of the wedge is slower than at the surface. For example, the 35.6 ppt isohaline has moved only 750m in the same amount of time, with a time-averaged speed of about 10cm s^{-1}.

Summary

In summary, the intensive measurements of both density structure and currents by drogue-tracking have shown that the harbour has a typical salt-wedge structure that responds directly to tidal forcing, but with its dynamical characteristics significantly influenced by baroclinic mechanisms due to vertical and horizontal density gradients.

During floods the wedge intrudes up to 4km along the bottom in from the mouth at mean speeds of the order of 12cm s^{-1}. As a consequence resident harbour water is driven towards the northern end.

During ebbs the retreat of the wedge along the bottom is slower than during flood tides, having mean speeds of the order of 7.5cm s^{-1}. This is because during ebbs the tidal flow field opposes the residual baroclinic inflow of oceanic water in through the mouth, this water being more saline and therefore denser than the resident harbour water.

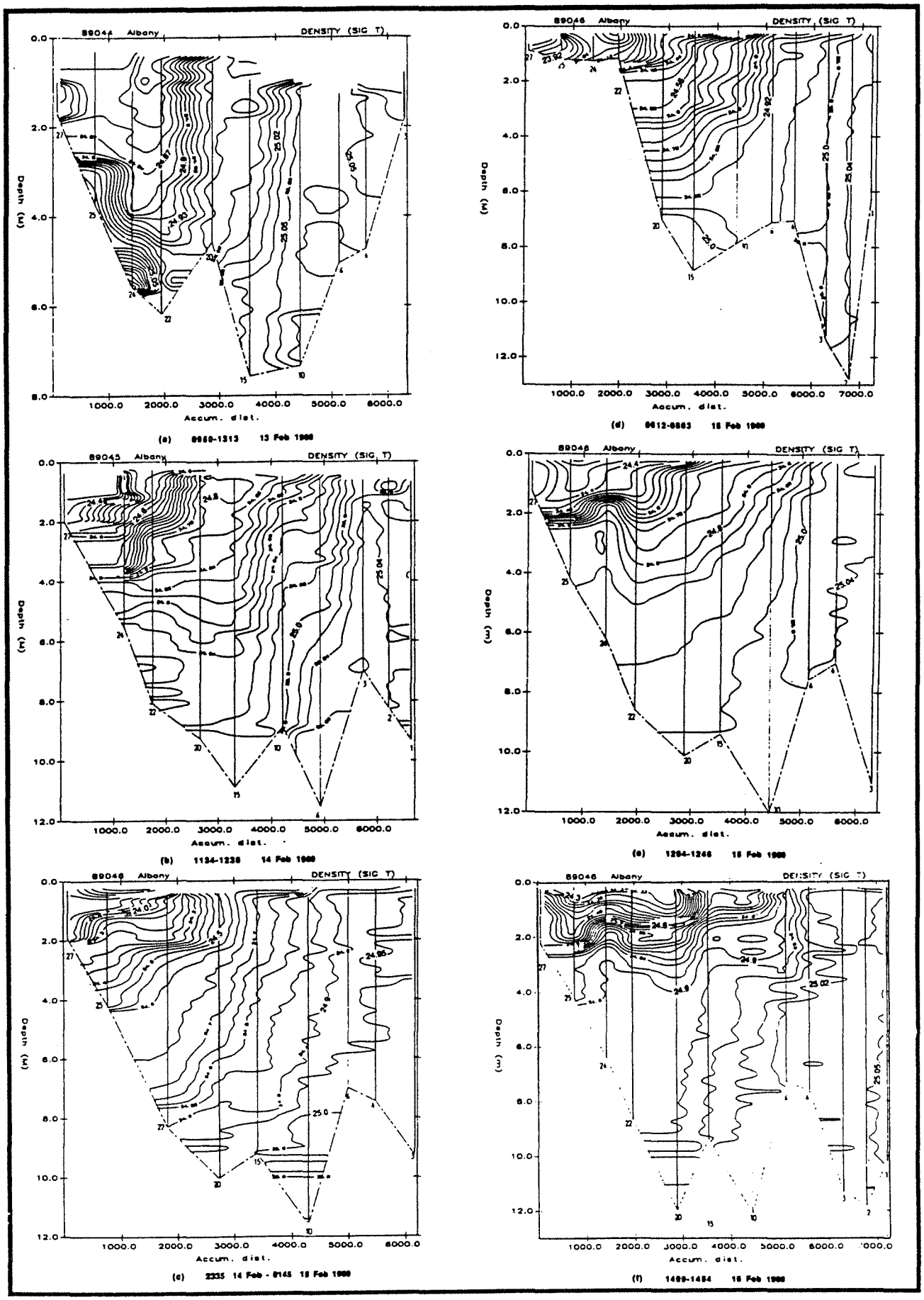

Figure 5.12 (a,b,c,d,e,f) Density contour plots for transect T1. Data period: 0950 13 February - 1454 15 February, 1989.

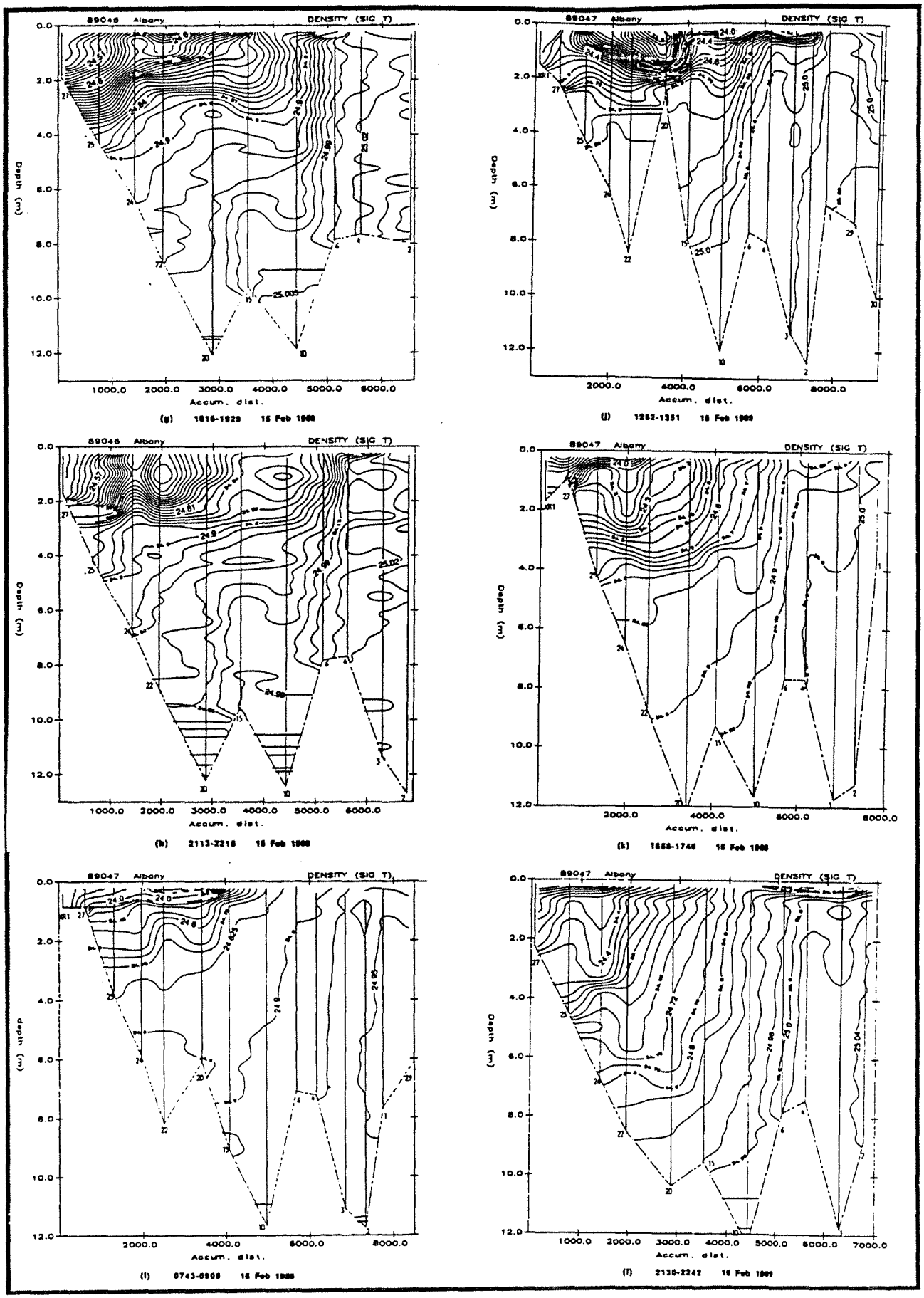

Figure 5.12 (g,h,i,j,k,l) Density contour plots for transect T1. Data period: 1816 15 February - 2242 16 February, 1989.

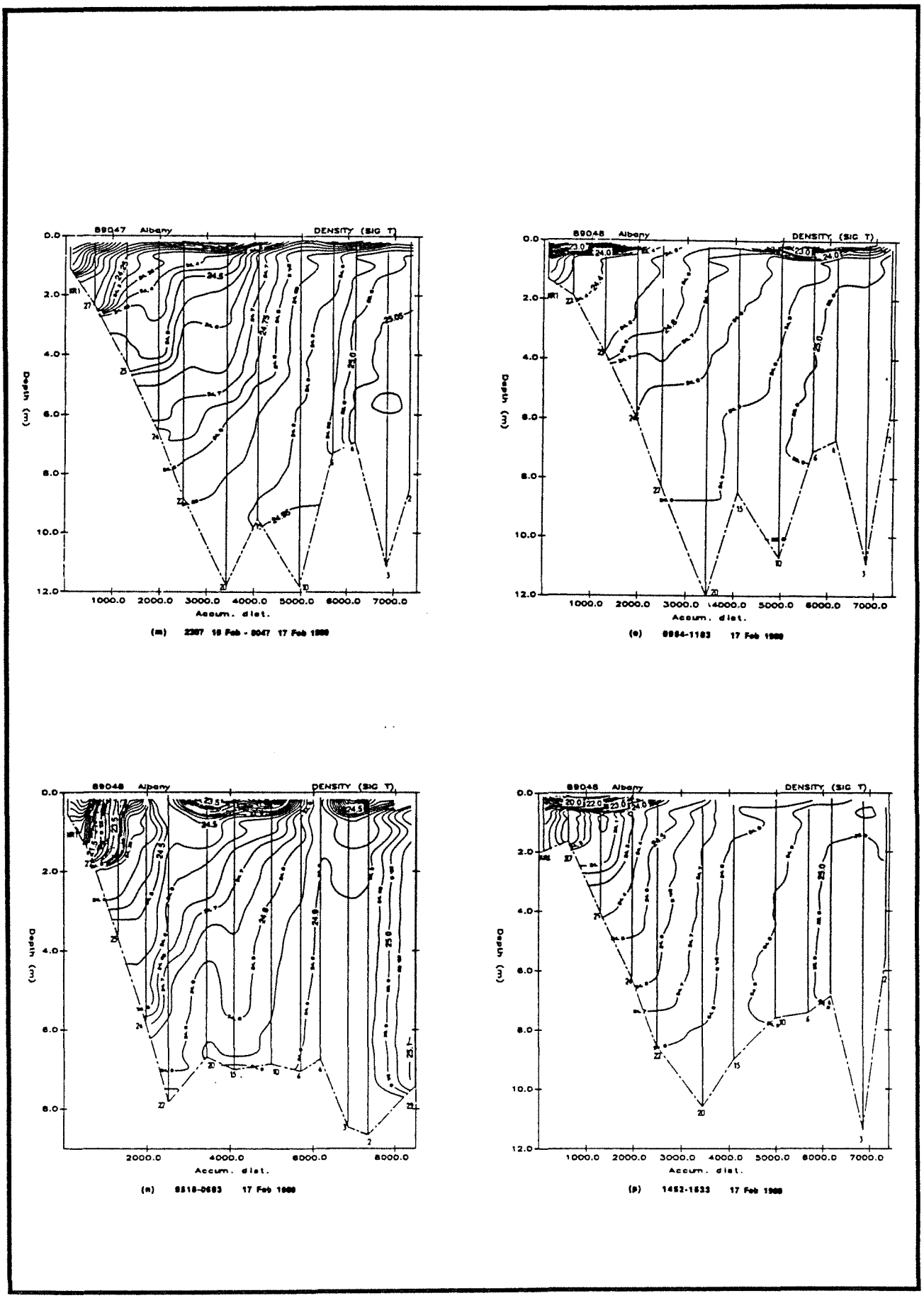

Figure 5.12 (m,n,o,p) Density contour plots for transect T1. Data period: 2307 16 February - 1533 17 February, 1989

contains density, salinity and temperature contour plot sets for transects T3 and T4, from CTD data collected between 0955 and 1033 on 16 February 1989. During that particular morning winds were very weak (averaging 1-2m s^{-1}) and from the north. Hence, the possibility of lateral upwelling due to winds is excluded. The contour plots in Figure 5.13 show that water along the western side of the harbour was, on average, more dense, more saline and colder than water on the eastern side. The density, salinity and temperature characteristics of the water on the western side were indicative of the marine wedge that was propagating into the harbour at that time through the entrance channel, as revealed by CTD measurements along transect T1 (see the density contours in Figure 5.12i, for example). Figure 5.13 also indicates the occurrence of less saline buoyant water at the surface along the eastern margin, which was probably deflected towards that bank by the earth's rotation during the ebb of the preceding night. It is to be noted that the data set collected during this study are not sufficiently conclusive to give clear evidence of anti-clockwise deflections of inflows and outflows. However, both the theoretical calculations and the measurements of the basin-wide stratification indicate that rotation is likely to be important.

5.2.3 Interaction of tidal flows and wind drift

When the wind blows on the water surface, it sets in motion, by the action of a surface shear stress, a downwind surface drift. Wu (1969) has shown that very near the surface this drift is approximately equal to 3 percent of the wind speed. Wu (1969) suggests that this drift quickly reduces to about 1 percent of the wind speed within the first meter of the surface. Hence, we adopt an average wind-induced drift speed for the upper 1m of the water column of 1 percent of the wind speed. Hence, for a 5m s^{-1} wind a vertically averaged surface wind drift of 5cm s^{-1} is calculated for for the upper 1m of the water column.

Surface drogues, with their centres at 1m depth, were tracked during the morning and early afternoon of 15 February 1989. The drogue-tracks are plotted in Figure 5.14. As shown, appreciable rotation of the surface currents occurred during that period. Winds were from the northerly direction at 4-6m s^{-1} during the morning and surface wind drift would have been in opposition to the incoming tidal currents. Hence, at the surface a complicated interaction between tidal and wind currents was produced. The rotating currents in the central harbour indicate that the influence of the wind in altering the barotropic tidal flow field is strongest near the surface, with drogues released nearer the bottom showing a more consistent upstream flowing nature. The tide had a minor ebb in the early afternoon of 15 February and this may explain why even the 4m deep drogues exhibited downstream displacement during that period.

In addition, the surface salinity gradients would also have driven downstream surface flows of the order of 5cm s^{-1} and these would have enhanced the surface wind drift. It is interesting to note the paths of the two drogues over the eastern shallows, which indicate a southerly current of about 5cm s^{-1} with no eddying. This exemplifies the role that the wind had in surface transport, because bottom tidal currents in the shallows would have been small due to frictional damping along the bottom.

The role of the wind in driving surface transport was highlighted in the drogue-track plots that were presented in Figures 5.10 and 5.11, for 14 and 17 February, respectively. These data showed that currents in the central harbour regions were tidally driven and of the order of 5-10cm s^{-1} and heading either directly towards or away from the mouth, as the tide dictated. However, currents over the eastern shallows were relatively weak (of the order of 2-5cm s^{-1}) and headed directly downwind. These cases illustrate the point that tidal flows are significantly weakened over the shallows by frictional damping, and the wind induced circulation therefore assumes a relatively dominant role in these regions. Winds were on average about 2-5m s^{-1} during the two field surveys and the current speeds over the shallows therefore compare well with the predicted values of approximately 2-5cm s^{-1} (as can be calculated by applying Wu's (1969) method).

Very close to the surface, in the upper 0.5m, the downstream density gradient results in a 'shooting' flow of surface water out towards the mouth during ebbs. This surface flow can have speeds up to three times faster than that of water below. This is an important result with respect to flushing of the harbour, because it acts in superposition to the tidal flow field. It is a residual flushing mechanism that acts to drive surface waters out to the ocean at rates of up to 20cm s^{-1}. In a localised sense this baroclinic mechanism could cause surface water from the northern regions of the harbour to be advected to King George Sound as a surface buoyant current in times of the order of 1-2 days.

Bottom waters are likely to be retained for longer periods in the harbour, with simple estimates (above) indicating that bottom waters could have residence times in Oyster Harbour of 4-10 days or more.

The wedge retreats at much slower rates during ebb tides than it advances during flood tides. This is because there is a constant upstream directed density gradient field, which is alternately opposed and assisted by the tidally forced flow. There is evidence from the stratification data that the densest water at the bottom can remain as a benthic layer in the deeper portions of the lower harbour during ebb tides.

5.2.2 Influence of the earth's rotation

As Fischer *et al* (1979) describe, the earth's rotation can force currents to deviate within estuaries in an anti-clockwise manner in the southern hemisphere. A basin-scale mixing mechanism called tidal pumping can result (Fischer *et al*, 1979), where for the case of Oyster Harbour inflows during flood tides would be deflected towards the west bank and outflows during ebbs deflected towards the east bank. If an estuary is large enough then tidal pumping can cause a residual circulation.

The Rossby number, R, is a non-dimensional number that is used to indicate the potential of the earth's rotation to rotate currents. The Rossby number is given by:

$$R = u/Lf, \qquad 5.2$$

where u is the speed of the current, L the width of the basin and f is the Coriolis parameter (=4.2 x 10^{-4} s^{-1} at the approximate latitude of 35 ^{o} S for Oyster Harbour). When $R < 1$ rotational effects are important and the current will be appreciably deflected by the force of the earth's rotation. When $R > 1$ rotational effects are overcome by the fluid's momentum.

Applying this formula to spring tidal inflows in Oyster Harbour yields the following result. From the analysis of current data in 5.2.1, above, typical flood velocities are of the order of 12.5cm s^{-1}. An appropriate length scale, L, for this calculation is taken as the smallest across-basin dimension, and this is 3000m. A value of R of 0.4 is calculated, and this indicates that flood inflows should be deflected towards the western side of the harbour. During spring ebb tides average outflow velocities of up to 7.5cm s^{-1} are typical and an R of 0.25 is calculated. Again, rotational effects in outflows, with deflection towards the eastern bank, should be important. For weaker tidal situations, such as neaps, tidal velocities will be lower than during springs, and this will result in even lower Rossby numbers. Hence, it can be concluded that rotational effects are probably always acting to deflect tidal currents anti-clockwise in Oyster Harbour.

In addition, the same force of the earth's rotation should deflect riverine surface plumes counter-clockwise as they propagate through Oyster Harbour towards the ocean. As was calculated in Chapter 4, outflowing buoyant surface plumes of river discharges have velocities of the order of 10-30cm s^{-1}, which leads to R values less than or equal to 1, which in turn indicates that these flows should be deflected towards the eastern bank. Qualitative evidence that this probably happens is provided by the fact there there is a high deposition of riverine sediment along the entire eastern margin of Oyster Harbour. Over half of Oyster Harbour's area has a depth of less than 1m, and most of this area occurs on the eastern side, (see Figure 2.3).

Many lateral transects (transects T3 and T4) were performed throughout the 5-day CTD survey from 13 to 17 February 1989. Two such transects that suggest an eastward deflection of the marine wedge that is driven upstream during flood tides are presented in Figure 5.13, which

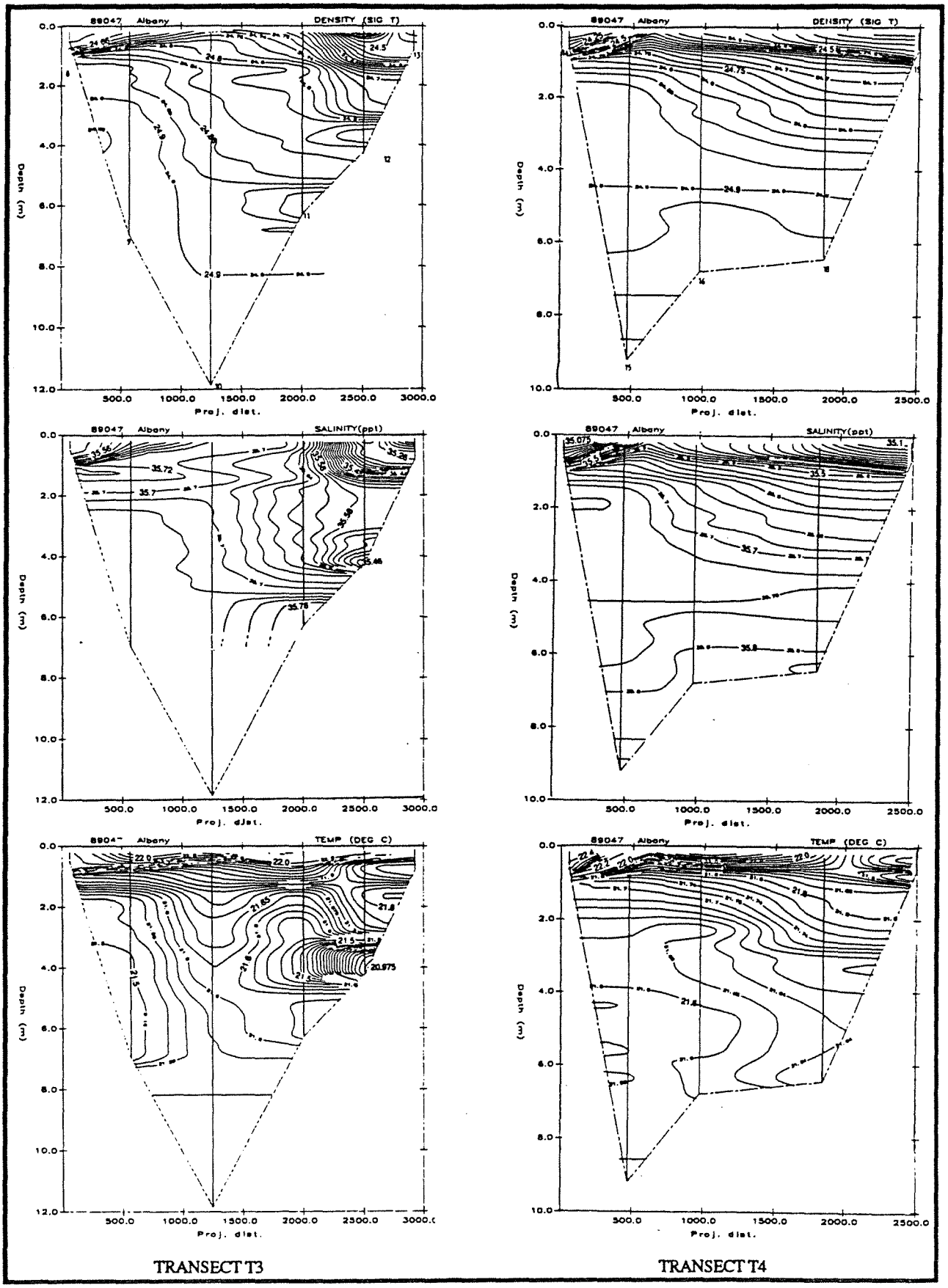

Figure 5.13 Density, salinity and temperature contours for transects T3 and T4. Data period: 0955 - 1033 16 February, 1989.

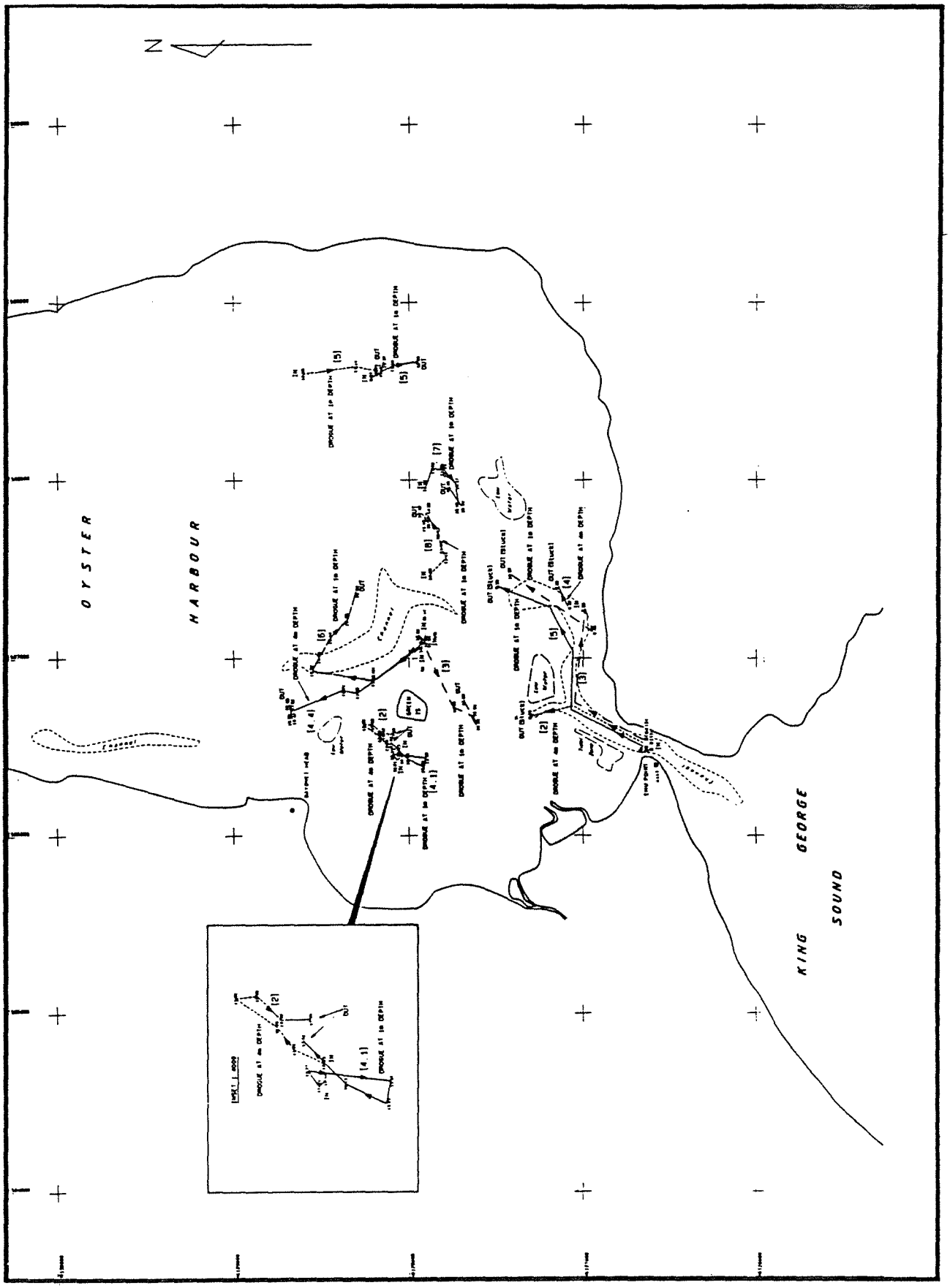

Figure 5.14 Drogue tracks from drogues released in Oyster Harbour during a spring flood tide between 0800 and 1500 15 February, 1989.

Summary

Tidal forcing dominates circulation in the central regions of the harbour, with strong upstream motion during floods and strong downstream motion during ebbs. Winds can influence the tidal flow field by enhancing flows when the wind and tide are in the same direction, and by opposing flows when the wind and tide are directed against each other. When winds are in opposition to tidal currents, eddying can occur in the central regions of the harbour, with radii of up to 500m. Eddying under such circumstances is most notable near the surface.

Tidal flows appear to be significantly damped over the shallows by frictional damping. In these regions the wind can therefore assume a dominant role in driving circulation patterns, with currents generally orientated downwind and having vertically averaged speeds in the shallows (which are less than 1-2m in depth) of the order of 1 percent of the wind speed.

The possibility that density currents could also become important in driving exchange between the shallows and deeper regions of Oyster Harbour during low wind conditions is investigated in sections that follow.

5.2.4 Entrance and jet dynamics

The hydrodynamic characteristics of tidal outflows and inflows between the harbour and King George Sound, during the period between 13 and 17 February 1989, were revealed by drogue-tracking during both ebb and flood tides.

During ebbs a tidal jet emanates out of the harbour and into the Sound. Drogues were released at 1 m depth in the entrance channel between 2000 and 2100 15 February, at the beginning of the ebb tide, and the drogue paths that were tracked thereafter are presented in Figure 5.15a. In the initial stages the drogues both advanced out of and retreated back into the channel as a result of the minor oscillations in the tide (see the tidal plot in Figure 5.5). However, after about 2300 all drogues headed out into King George Sound in a tidal jet. Velocities through the channel were 30-40cm s^{-1} and these reduced to about 15-30cm s^{-1} in the jet. No vertical CTD profiles of the jet were collected during the exercise and hence no comment can be made on the vertical structure of the jet. By 0300 16 February the jet had extended out 2.5km into the Sound, and had a width of about 1km.

The drogues were taken out of the water at about 0300 and placed back into the water at 1m depth at approximately 0500 hours in positions across the alignment between Cheyne Ledge and the opposite shore of Middleton Beach 1-1.5km out from the harbour mouth (see Figure 5.15b). The tide turned from ebb to flood during a prolonged low water period of minor oscillations from about 0400 to 0800 on 16 February. The drogue-tracks presented in Figures 5.15a and b reveal the flow field in front of the mouth during the period of low water and early flood of 16 February. As shown, during the initial flood phase the influence of the outflowing jet, generated during the preceding flood, is still evident in the Sound. The drogues in the central regions well out from the mouth (about 1km or more) maintained their outflowing momentum, which was obviously strong enough to overcome the barotropic onshore flow field due to the flood tide. However, nearer the shore the drogues exhibited movement towards the mouth. By about 1000 the drogues in the jet had slowed to have almost zero velocity and the radially inflowing drogues had inflow speeds in the entrance channel of up to about 55cm s^{-1}. Hence, the barotropic tidal flow field dominated circulation five hours after the start of the flood.

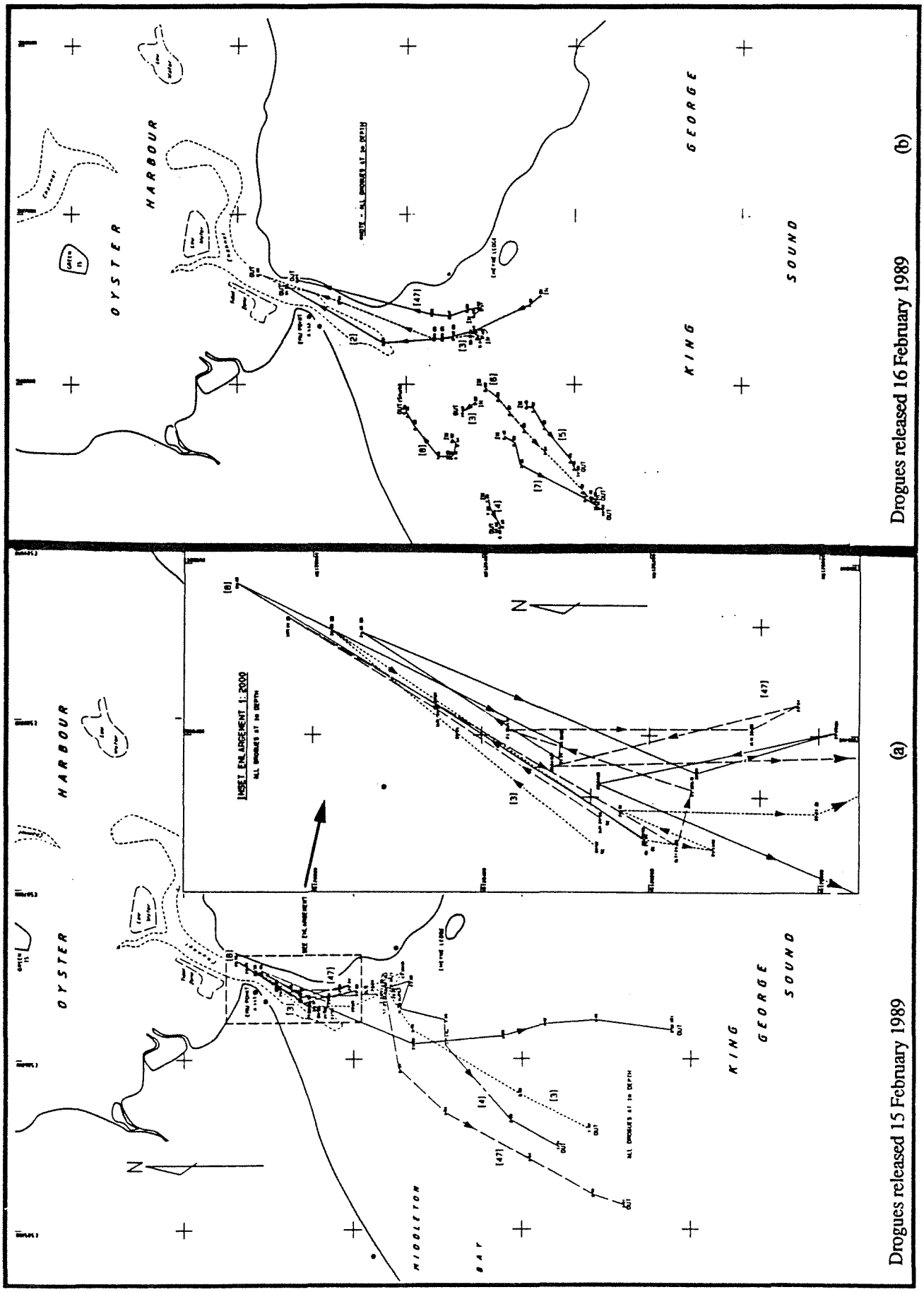

Figure 5.15 (a),(b) Drogue tracks from drogues released in Oyster Harbour entrance channel and King George Sound during a spring ebb and subsequent flood tidal period between 2000 15 February and 0500 16 February, 1989.

A similar drogue-tracking exercise during a period of flood immediately following low water was conducted between about 0600 and 1200 17 February. The tide was in flood from 0530 onwards. The drogue tracks from that survey are presented in Figure 5.16. The drogues were placed in the water approximately radially about the entrance 1.5km out from the mouth of the harbour. These results again show the dominance of the outflowing jet momentum during the early flood stages along the alignment directly out from the entrance channel (see the tracks for drogues 2, 47 and 7, for example). At about 1000hr, approximately 4.5 hours into the flood phase, the radially inflowing velocity field was able to overcome the residual momentum in the jet that was generated during the preceding ebb phase.This behaviour was similar to that described above for the previous day. Inflow velocities through the channel were again of the order of 50cm s^{-1}.

The present analysis assumes both that the tidal jet from Oyster Harbour is barotropic and that there are no currents in the Sound that could advect the tidal jet volume away from the influence of the radial flood inflow. Further, the outflow is slightly less dense than the water of the Sound, as shown by the CTD data from within the harbour (section 5.1, above), and hence the possibility that the jet lifts off the bottom and then becomes baroclinically driven exists. A method to predict the likelihood of lift-off was presented by Luketina (1987), who referenced the work of Hearn *et al* (1985) and Safaie (1979) and applied the theory to the Koombana Bay jet of southwest Australia. The Koombana Bay jet exhibited many similar structural properties to that of Oyster Harbour. Following Luketina (1987) a lift-off depth of the order of 10m is calculated for the Oyster Harbour jet during spring ebb tides. This implies that the jet is attached to the bottom for at least the first 2.5km of its propagation with respect to the mouth. Hence, the assumption that the jet is predominantly barotropically driven is valid. For neap ebb periods, when outflow velocities are weaker, the calculation of lift-off depth yields a value of the order of 1m, and this means that the jet is probably detached from the bottom for most of its length and is particularly prone to surface wind drift movements.

As was calculated above, the tidal prism volume varies from 5 to 18 x 10^6 m^3. If we assume that during floods water from the Sound enters from a semi-circular area into the harbour, then the radius of this region is of the order of 1.5km for neap floods and of the order of 2.25km for spring floods. As the drogue paths in the tidal jets that were monitored on 15 and 16 February during spring ebbs indicate, the jet probably has a plan view shape resembling a simple cone, with the width of the 'cap' of the cone 2.5km out from the mouth being of order 1000m. This implies that about a third of the volume of water that flows into the harbour during spring floods in summer was that ejected out from the harbour in the preceding tidal ebb jet. The re-entrainment of ejected harbour water back into the harbour during floods was highlighted in Figure 5.11 by the path of travel of drogue No. 5. That drogue was released in the central lower harbour during an ebb and observed to undergo significant ejection out to King George Sound only to be then found in the entrance channel later during the subsequent flood tide.

Obviously, wind drift, regional oceanic and tidal currents and baroclinic forcings will influence the general circulation pattern in the Sound and may therefore deflect the tidal jet away from and out of the radial inflow region of flood flows. Current meter data from the four King George Sound stations (as described in Section 3.5, and discussed in Pattiaratchi *et al* (1991)) indicates that residual currents in summer are of the order 3-5cm s^{-1} around the Sound. From the calculations of probable lift-off depths for the jet it appears that during spring tides the jet is predominantly barotropic and attached to the bottom, hence wind effects will be of minor importance to its fate once in the Sound. However, during neaps the jet is probably detached for most of its length and will be strongly influenced by surface wind shear stress. A detailed analysis of circulation in King George Sound is not within the scope of this report. Hence, no further analysis of the behaviour of the jet volume during flood periods is undertaken. Such an investigation would be desirable and it is recommended for any future studies of the assimilative capacity of King George Sound to nutrient loading.

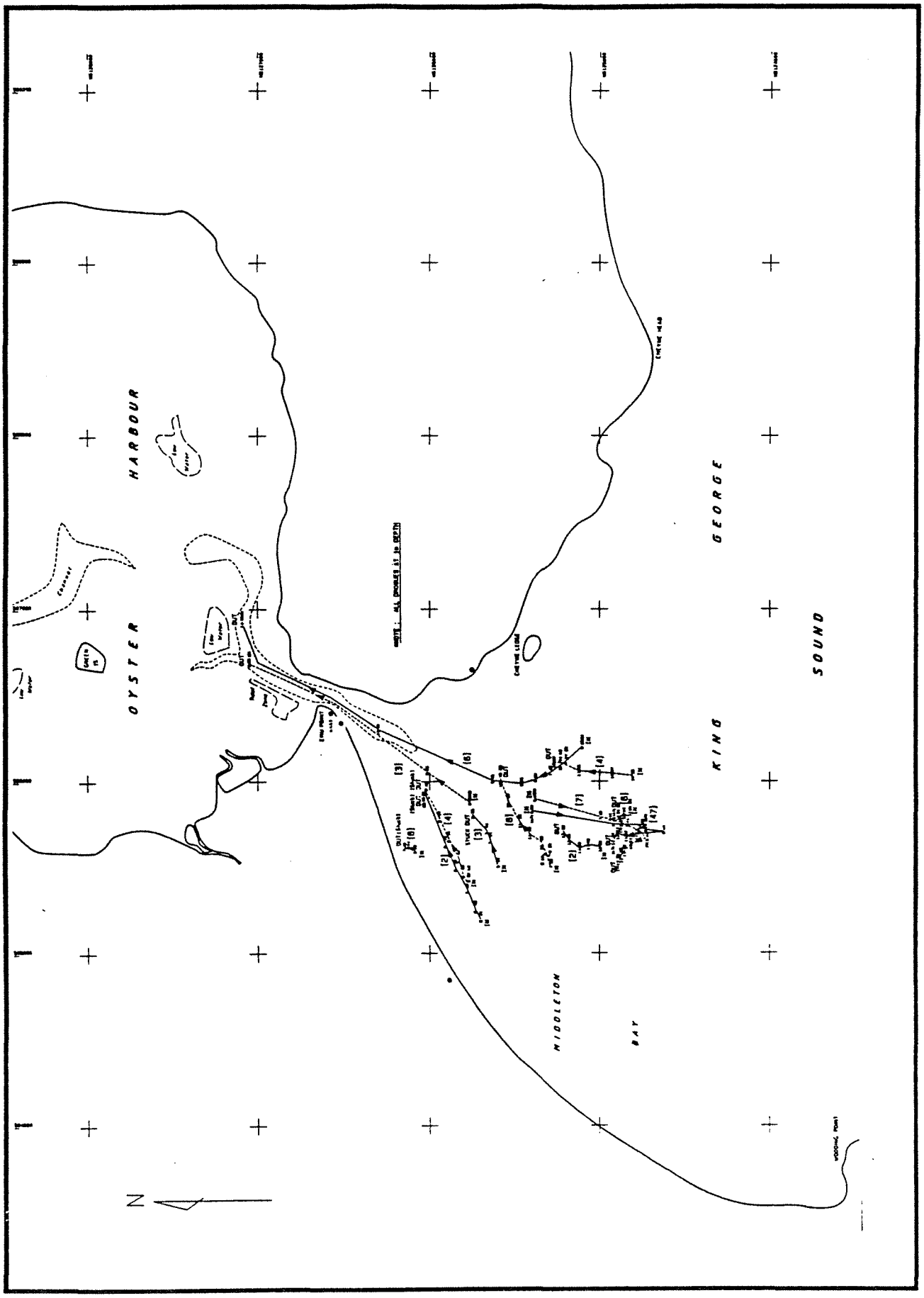

Figure 5.16 Drogue tracks from drogues released in King George Sound during a spring flood tide between 0600 and 1200 17 February, 1989.

Summary

In summer, ebb flow emanates out of Oyster Harbour as a tidal jet.

The vertical structure of the jet was not monitored. However, tidal mixing in the entrance channel is estimated to be sufficiently strong to ensure that the jet is homogeneous upon its exit into the Sound. Density differences between the jet and ambient waters of the Sound are typically up to about 0.2kg m^{-3} in summer.

The leading front of the jet penetrates out into King George Sound well past the radial inflow zone of flood flows in the Sound. Drogue tracking indicates that the jet penetrates at least 3km into King George Sound during spring flood tides, and has a width at its leading edge of the order of 1km. During springs it is likely that the jet remains attached to the bottom for at least the first 2.5km of its length with respect to the mouth. This is probably not the case during neap tides.

It is estimated that up to one third of the ebb outflow volume is re-advected back into the harbour during spring floods because, at the end of the ebb, a significant proportion of the tidal jet resides within the radial sink zone of flood flows from the Sound into the harbour. This proportion may be somewhat less during neaps because the jet is probably buoyant and more prone to advection out of the radial inflow region by surface wind drift currents, especially if winds are such as to cause surface currents to be directed away from the mouth.

5.3 Wind mixing and transport

5.3.1 Classification scheme for wind mixing

The aim of this section is to quantify the vertical transport of mass in the harbour as a function of wind speed and direction.

As we have highlighted previously in this report the salt-wedge during flood tides enters and propagates upstream as a bottom density current. In the absence of wind this wedge undergoes little vertical mixing with resident buoyant harbour water. The marine water has a relatively high water quality (low levels of pollutants or nutrients) compared to the eutrophic water in the harbour. An understanding of the mixing between marine and harbour waters is important to an understanding of the dilution of pollutants. As for the winter situation (see Chapter 4), the availability of nutrients to the benthic macroalgae and epiphytes, which smother and cause seagrass dieback, is highly dependent on the ability of vertical mixing agents to transport nutrient-rich freshwater from the surface down to the bottom. In addition, the flushing of nutrient-rich and polluted waters out to the ocean will be influenced by the nature of mixing between marine and resident harbour waters within the harbour.

The basin-scale three-dimensional density structure of Oyster Harbour was captured throughout many consecutive tidal cycles between 13 and 17 February 1989, as was described in Section 5.1. Wind speeds and directions throughout that period ranged widely from calms through to storms having wind speeds of the order of 10m s^{-1}.

A Wedderburn number classification scheme (Imberger and Hamblin, 1982) is used to indicate the potential of wind to both mix the estuary vertically and change its horizontal density structure. This approach was described in Section 4.5.5. Based on the many CTD measurements collected during the February 1989 survey, the vertical stratification in summer is approximated as two layers, with an upper layer of 2m having a linear density stratification of 0.15kg m^{-3} per m overlying water with a linear density stratification of 0.01kg m^{-3} per m. The deepening laws presented in Section 4.5.5 are now applied to this initial stratification for northwest, northeast, southeast or southwest winds (with a fetch of 4500m), having speeds from 2 to 20m s^{-1}. The results of this calculation are presented diagrammatically in Figure 5.17, which shows the predicted depth of surface mixing as a function of time for different wind speeds. As shown in Figure 5.17, when winds are less than about 2m s^{-1} vertical mixing is predicted to proceed relatively slowly. Winds of greater strength are predicted to break the stratification down quickly, with 10m s^{-1} winds, for example, estimated to mix the harbour to the bottom in just 6 hours. These predictions assume that the initial stratification is not

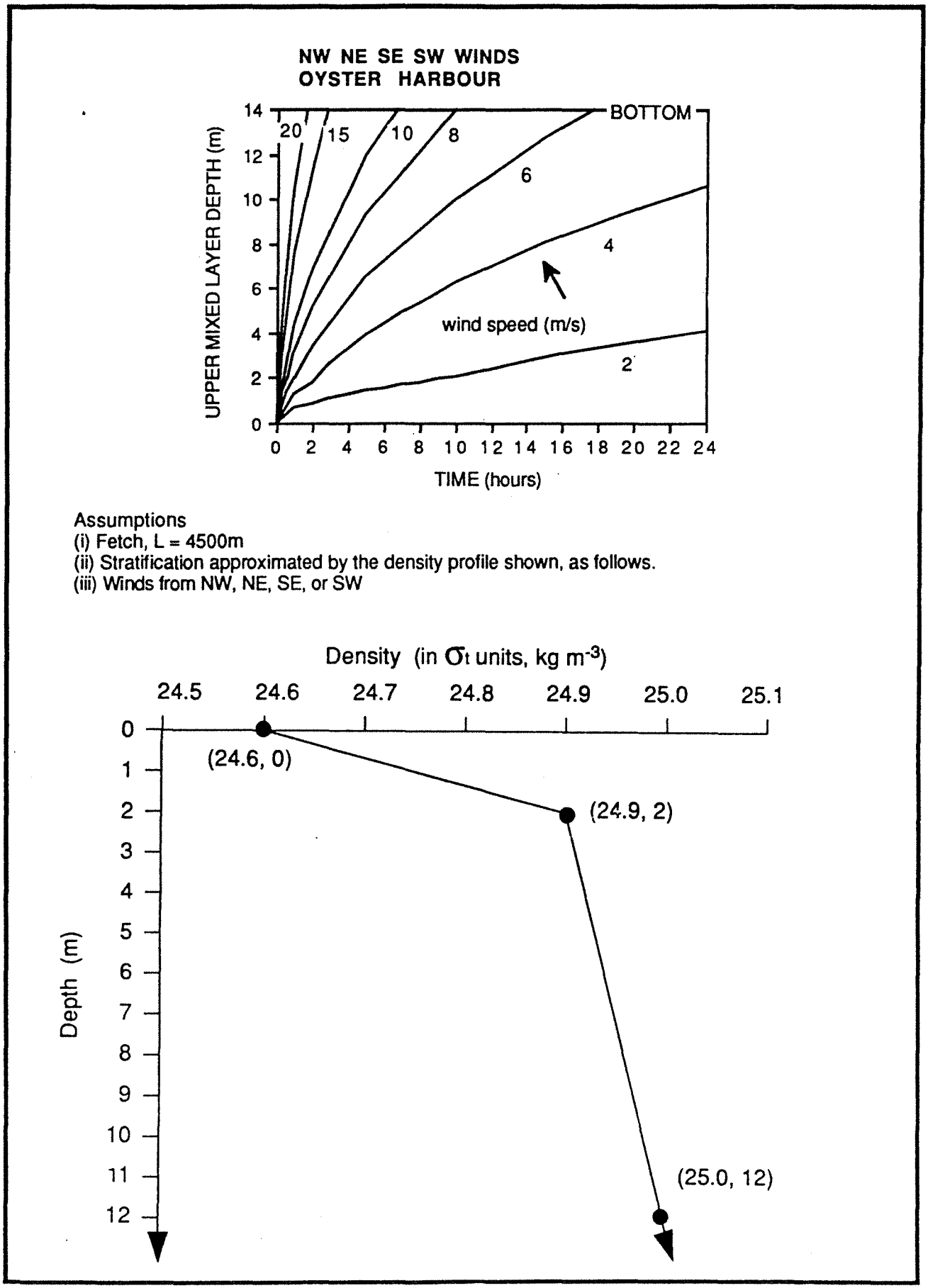

Figure 5.17 Predictions of the rate of increase of upper mixed layer depth for a range of wind speeds in Oyster Harbour during typical summer vertical stratification conditions.

reinforced by fluxes of buoyancy from sources such as solar heating or freshwater inputs. The validity of this assumption is addressed below.

The spatial characteristics of surface mixing and upwelling due to wind stress for events of varying intensity are investigated in the following sections by comparing measured rates of mixing with the above predictions.

5.3.2 Low wind conditions

Throughout the five-day field survey of stratification (13 to 17 February 1989) winds were predominantly less than about 5m s^{-1} (see Figure 5.5). As was discussed in Section 5.1, basin-scale stratification data showed clearly that such winds were not able to appreciably mix the harbour vertically. This point is exemplified by the time series contours in Figure 5.18 of vertical density stratification for stations 10, 15 and 20, constructed from consecutive CTD profiles collected between 13 and 17 February 1989. As shown in Figure 5.18, the harbour was vertically stratified most of the time during that period. According to the predictive curves in Figure 5.17 mixing should be rapid during winds greater than 2m s^{-1}. However, as the stratification data indicate, only winds stronger than about 5m s^{-1} were able to initiate appreciable mixing. The most likely reason for this is that as mixing proceeds there is a constant flux of buoyancy into the surface via solar heating and freshwater inputs due to river and creek flows and submarine groundwater discharge. The predictions in Figure 5.17 are calculated according to the assumption that additional buoyancy is not added to the water column during the mixing process.

Based on the February data set, low wind conditions are therefore defined as those when winds were less than about 5m s^{-1}. If we take a typical vertical stratification during low winds, such as that for Wednesday (1409-1631) 15 February 1989 presented in 5.19, then a W slightly greater than or equal to about 1 is calculated. Winds were from the northwest during the morning prior to the survey at 4-6m s^{-1}, and then weakened to 1-3m s^{-1} tending to a westerly at the commencement of the data collection. Hence, vertical mixing should have been weak with any upwelling being gentle and occurring on the western side of the harbour. The contour plots in Figure 5.19 present the lateral and longitudinal density structure and they show that the entire harbour was in fact stratified vertically, as predicted. The lateral transects (T3 and T4) present the density structure of the upper 4m of the water column and show that the isopycnals were tilted upwards along the western side of the harbour, and this probably indicates slight upwelling due to the mild west-northwest winds, as predicted for situations of W greater than or equal to 1. The stratification in the longitudinal direction (transect T1, for example) is typical of a gravitational overflow (Luketina and Imberger, 1987) sustained by a buoyancy flux from weak river discharge and solar heating

Care must be taken in applying the Wedderburn number to classify the potential of winds to mix the harbour in this case. This is because the Wedderburn number was originally developed (Thompson and Imberger, 1980) for the case of a lake with a fixed value of initial vertical stratification, and with any additional buoyancy flux from external sources other than wind being added at a rate less than the rate at which the mechanical energy of the wind is able to mix the surface layer down. In the present case a continual buoyancy flux is derived from solar heating and freshwater inputs via rivers and groundwater. An approximate quantification of the importance of these buoyancy fluxes is now made.

Solar heating

The effect of solar heating in raising the temperature of surface waters in Oyster Harbour is highlighted in Figure 5.20, which is the time series contour plot of vertical temperature stratification at station 10, spanning from 1222 13 February to 1604 17 February 1989. The diurnal heating that occurred during the afternoons of 15 and 16 February is shown clearly by the isotherms near the surface in Figure 5.20. The temporal resolution of CTD drops on 13 and

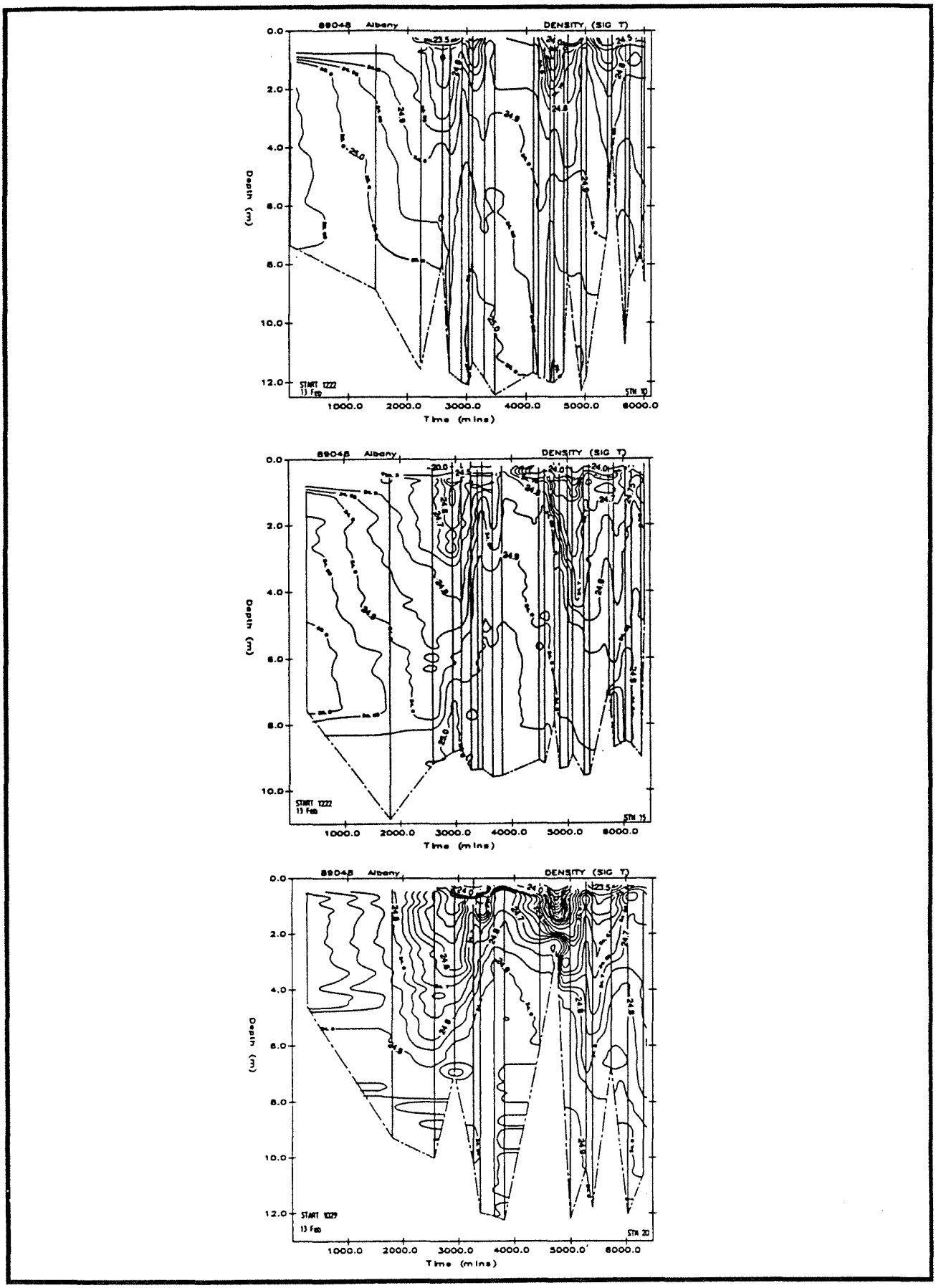

Figure 5.18 Density contour plots for time series of CTD drops at stations 10,15 and 20 during 13 to 17 February, 1989.

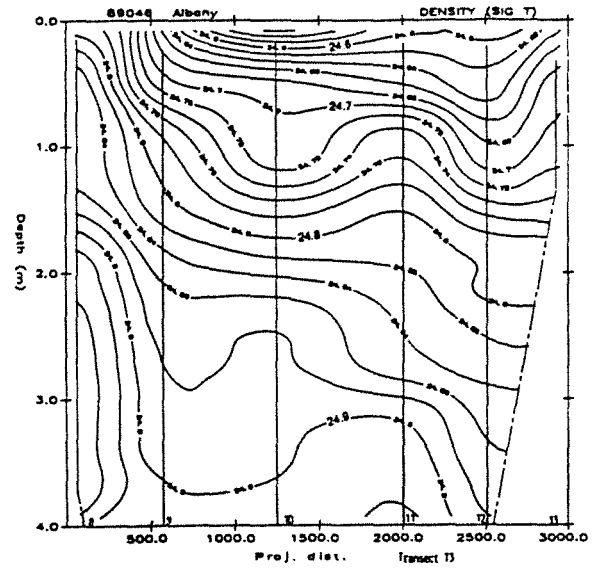

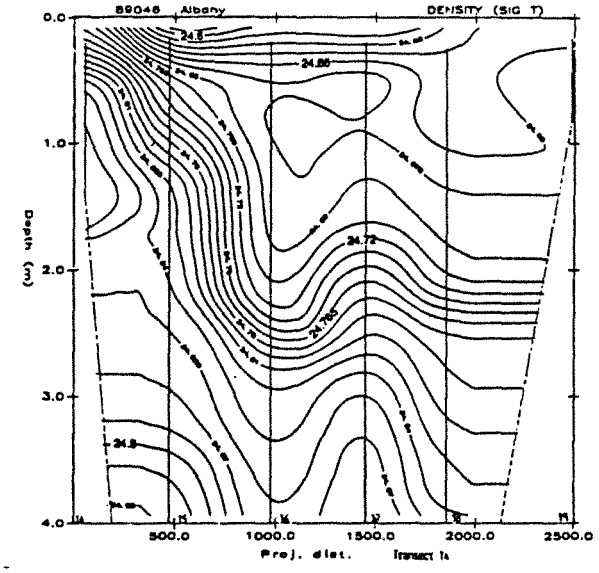

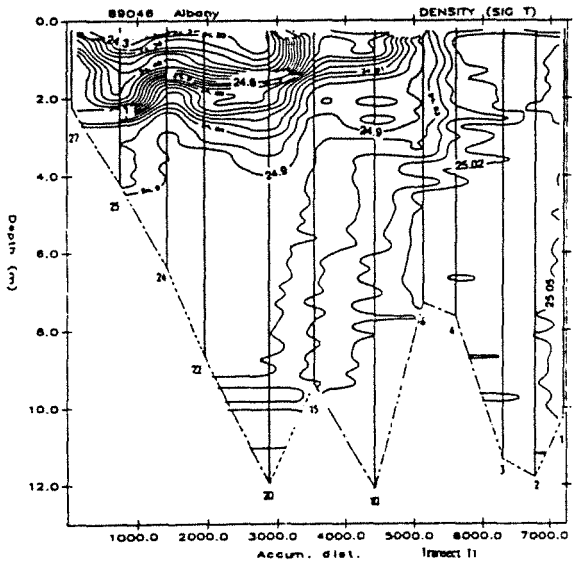

Figure 5.19 Density contour plots for the upper 4m along transects T3 and T4 and for the full depth along transect T1. Data period 1409 - 1631 15 February, 1989.

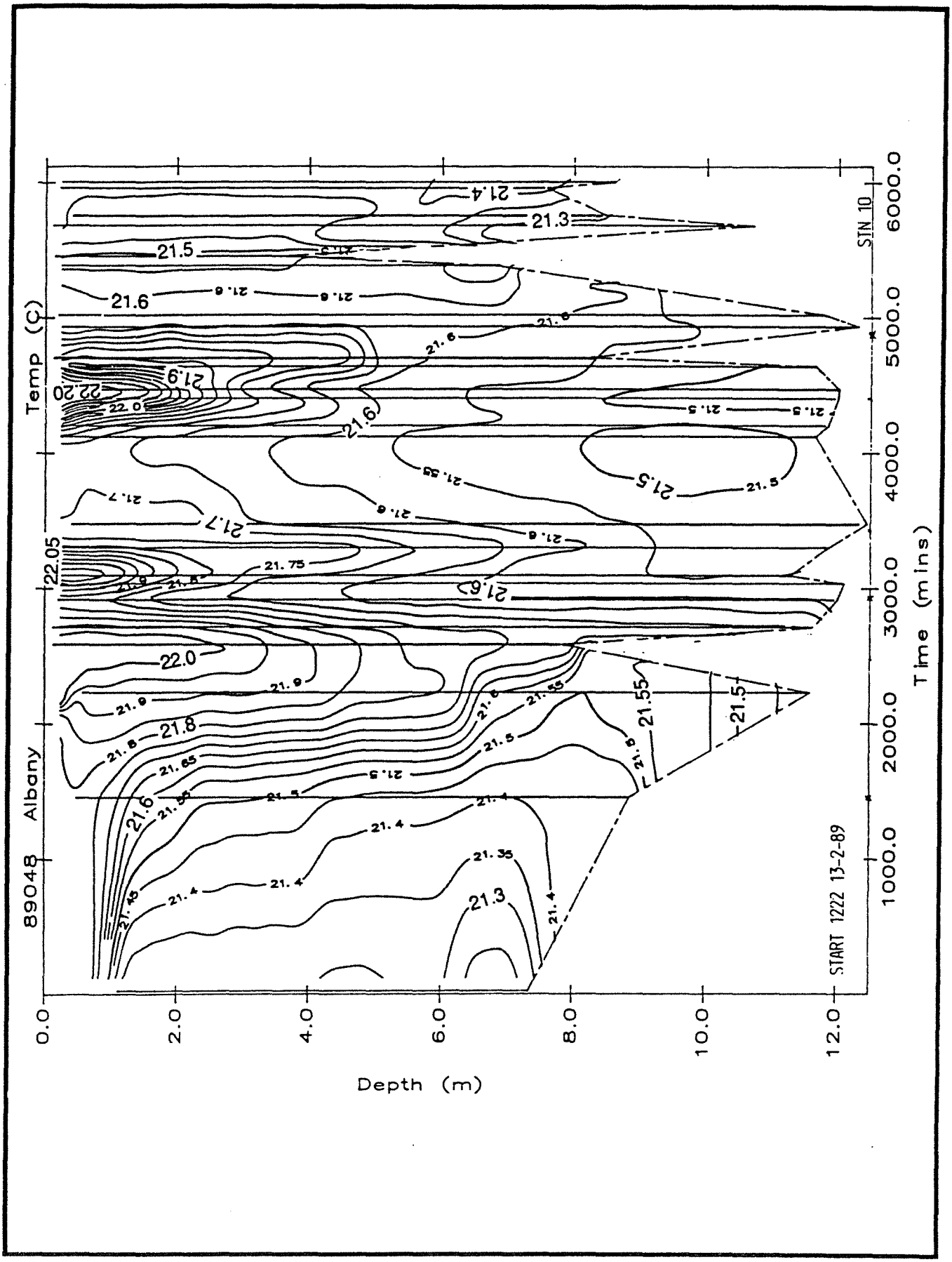

Figure 5.20 Temperature contour for a time series of CTD drops at station 10, during 1222 13 February to 1604 17 February, 1989.

14 February was insufficient to capture diurnal variations in surface temperature. The absence of a warmer upper layer on February 17 is due to the lower air temperatures and strong wind mixing of that afternoon. The data in Figure 5.20 indicate that mean temperature of the upper 3-4m of the water column can rise by about 0.5 °C during a typical summers day when winds are relatively mild and solar heating strong. This can lower the density of the surface water by about 0.15kg m^{-3}.

River discharges

The CTD profile data revealed the entry of freshwater inputs from rainfall that fell during the period between 13 and 17 February 1989. Table 5.2 contains details of the rainfall and subsequent streamflow for the Kalgan plus Chelgiup catchments.

Table 5.2 Total rainfall for 24 hour periods from 0900 to 0900 hours of successive days, and average instantaneous discharge rates for the 24 hour periods 0000 to 2400 hours for combined flow from the Kalgan and Chelgiup catchments.

RAINFALL		STREAMFLOW (KALGAN + CHELGIUP)	
Period	Total rainfall (mm)	Period	Average discharge ($m^3 s^{-1}$)
13 Feb 0900 - 14 Feb 0900	0	13 Feb 0000 - 2400	0.30
14 Feb 0900 - 15 Feb 0900	3.2	14 Feb 0000 - 2400	0.30
15 Feb 0900 - 16 Feb 0900	19.4 **	15 Feb 0000 - 2400	0.32
16 Feb 0900 - 17 Feb 0900	1.4	16 Feb 0000 - 2400	0.40
		17 Feb 0000 - 2400	0.42
		18 Feb 0000 - 2400	0.38
		19 Feb 0000 - 2400	0.34
		20 Feb 0000 - 2400	0.33

** Note: most of this rain fell during a storm between 0000 and 0300 16 February

As Table 5.2 shows, rain fell on 15 and 16 February, and streamflows rose slightly from 0.30 to 0.42$m^3 s^{-1}$ as a consequence. The stratification in the harbour was intensified vertically as a result of these increased streamflows. The density, salinity and temperature contour plots in Figure 5.21 from Transect T1, 1252-1351 16 February, show clearly a buoyant gravitational overflow of riverine water that resulted from the rainfall/runoff event of the previous night. The major sources of freshwater were the King and Kalgan Rivers, as indicated by the density contour plots in Figure 5.22 (a, b and c), which are synthesized from basin-scale CTD profiles collected on Friday 17 February. Figure 5.22 a contains a contour plot of longitudinal transect T1 (0518 to 0603 hours) showing surface regions of buoyant water indicating the King River discharge (stations KR1, 27 and 25) and the Kalgan River discharge (stations 20 and 15). Figure 5.22b contains contours from transect T5, which is longitudinally aligned along the eastern side of the harbour, and shows most clearly the two plumes of buoyant water from the King and Kalgan Rivers Figure 5.22c presents salinity contours of the upper two meters from transect T1 during a later stage of the morning (0954-1103), with the same surface stratification features of the King and Kalgan outflows evident. It is interesting to note that even though the tide had been in a strong flood mode since 0536 that morning the buoyant freshwater still occurred in the lower regions of the harbour. In addition, it is possible that there was a flux of freshwater to the lower harbour from the nearby Yakamia Creek.

Groundwater

No information currently exists on the flux of groundwater into Oyster Harbour. A first order estimate of groundwater flux can however be made by making some simple assumptions. Approximately 1000mm of rain falls annually at Albany. The first assumption made is that about 15 percent of this remains in the groundwater system as recharge, yielding an annual recharge of 150mm. Second, it is assumed that at least half of the local catchment that surrounds the harbour is of a porous material which carries groundwater flow all year round. Third, a catchment area around Oyster Harbour for groundwater recharge of approximately

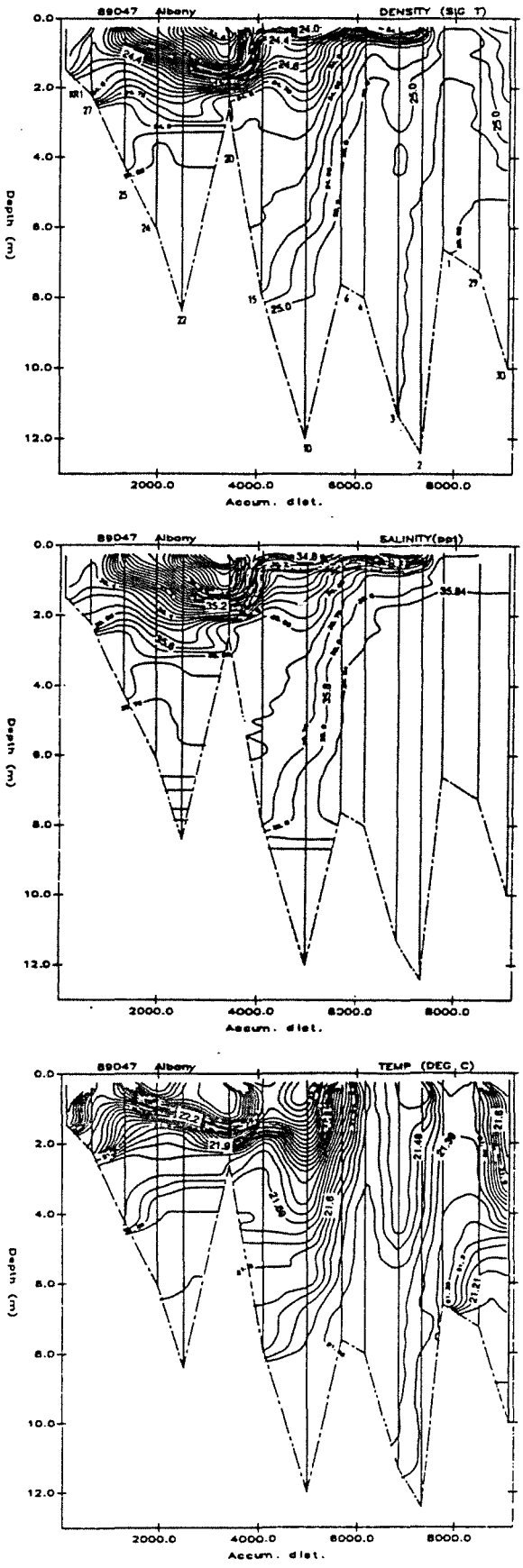

Figure 5.21 Density, salinity and temperature contour plots for transect T1. Data period 1252 - 1351 16 February, 1989.

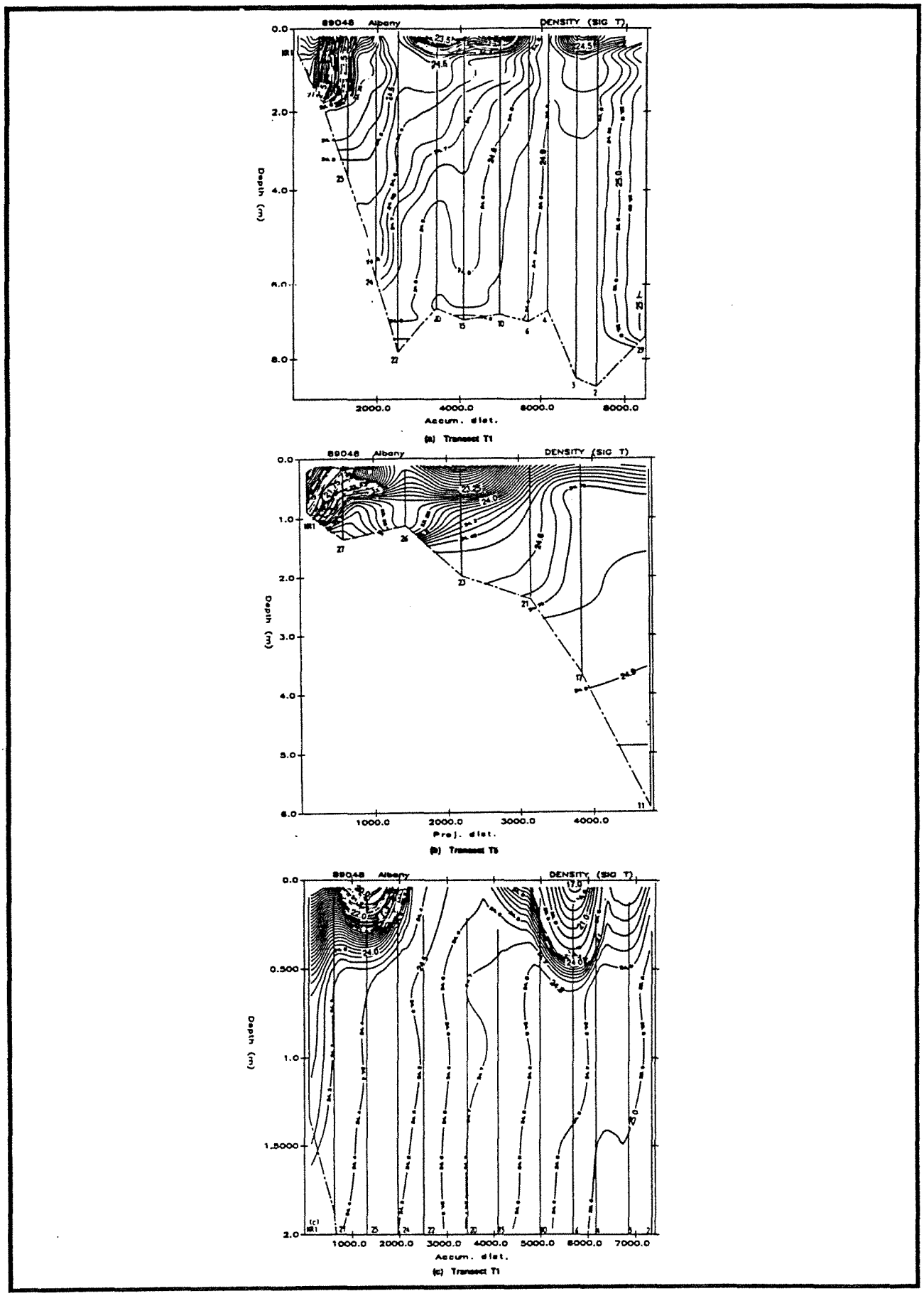

Figure 5.22 (a,b,c) Density contour plots (a) Transect T1 0518 - 0603 17 February, 1989; (b) Transect T5 0755 - 0650 17 February, 1989; (c) Transect T1 0954 - 1103 (Upper 2m) 17 February, 1989.

50 square kilometres is assumed. Using these values a volumetric groundwater flux into the harbour from submarine groundwater discharge of the order of $0.25m^3 s^{-1}$ is calculated. This equates to a submarine groundwater discharge flux along the inner shoreline of Oyster Harbour of the order of $1m^3$ per day per metre of shoreline, which is within the order of estimates made for the Perth metropolitan shoreline by Appleyard (1990). Since net baseflow from the rivers during summer is of the order of $0.1m^3 s^{-1}$ then the estimated contribution of groundwater in adding buoyancy to the harbour is likely to be hydrodynamically important.

Hence, the turbulence generated by the wind shear at the surface has to work continually against the stabilising influence of a steady flux of buoyancy to the upper layer from solar and freshwater inputs.

This may explain why even at wind speeds of order $5m s^{-1}$, when W values would be of order less than or equal to 1, the harbour still shows basin-wide vertical stratification. It appears that for typical values of vertical stratification in summer, the harbour resists full-depth mixing when winds are less than about $5m s^{-1}$. As was derived in Chapter 3, winds are probably less than or equal to this value for of the order of 50 % of the time. When winds climb above this value, the harbour can be well-mixed by winds. Mixing by strong winds is the subject of the following discussion.

5.3.3 Strong wind conditions

Upwelling can be expected when winds strengthen to reduce W below 1, and this occurred during the morning of 17 February 1989 when southwest winds rose to $10-12m s^{-1}$. The storm began at about 1100 hours and blew throughout the afternoon. A Wedderburn number of the order of 0.01 is calculated for that event, and hence appreciable upwelling and subsequent strong vertical mixing is predicted. A lateral CTD transect was performed along transect T4 between 1224 and 1254. The isopycnal contour plot from that transect is shown in Figure 5.23 and the initial stages of upwelling can be seen, with mid-depth waters surfacing between stations 15 and 16. The isopycnals along the western side (between stations 14 and 15) do not exhibit upwelling because the harbour was sheltered by the raised topography along the western bank.

Another CTD transect along T4 was performed about 4 hours later between 1617 and 1632. The resulting isopycnal contour plot is presented in Figure 5.24 and again shows upwelling of the density structure. This plot shows upwelling in the central harbour area between stations 16 and 18. The vertical stratification has been significantly weakened compared to that measured in the morning (Figure 5.23).

Figures 5.25a and b present the respective longitudinal density structures of the harbour along transect T1 during the morning (0954 to 1103), before the storm, and afternoon (1452 to 1533), about 4 hours into the storm. As shown in Figure 5.25a, the harbour exhibits a characteristic wedge-type structure, with a surface layer of buoyant water from river discharge caused by the preceding nights' rain (see section 5.3.2, above). By mid-afternoon (Figure 5.25b) the strong southwest winds mixed the harbour vertically downstream of station 22. The surface waters exhibited some weak vertical stratification and this may indicate the influence of buoyancy flux from freshwater discharges via the rivers, that resulted from the previous nights' rain. The entrance of relatively fresh riverine water during that afternoon is indicated by the vertical stratification between stations KR1 and 22 in Figure 5.25b which indicates the gravitational overflow of a buoyant surface front of King River water into Oyster Harbour.

The application of vertical mixing laws, as described in section 4.5.5, leads to a predicted upper mixed layer depth in the harbour of the order of 10m at 1500 hours of 17 February (see Figure 5.17). Figure 5.25b indicates that the waters of the central lower harbour were mixed down to at least 8m at that time. Near the bottom however the isopycnals are tilted towards the upper harbour and at the surface they tend to be tilted towards the mouth. This is probably due to the baroclinic forcing of the longitudinal pressure gradients resulting from the longitudinal density stratification set up by buoyant riverine water at the surface in the upper harbour and relatively dense marine water at the bottom in the southern half of the lower harbour. This again

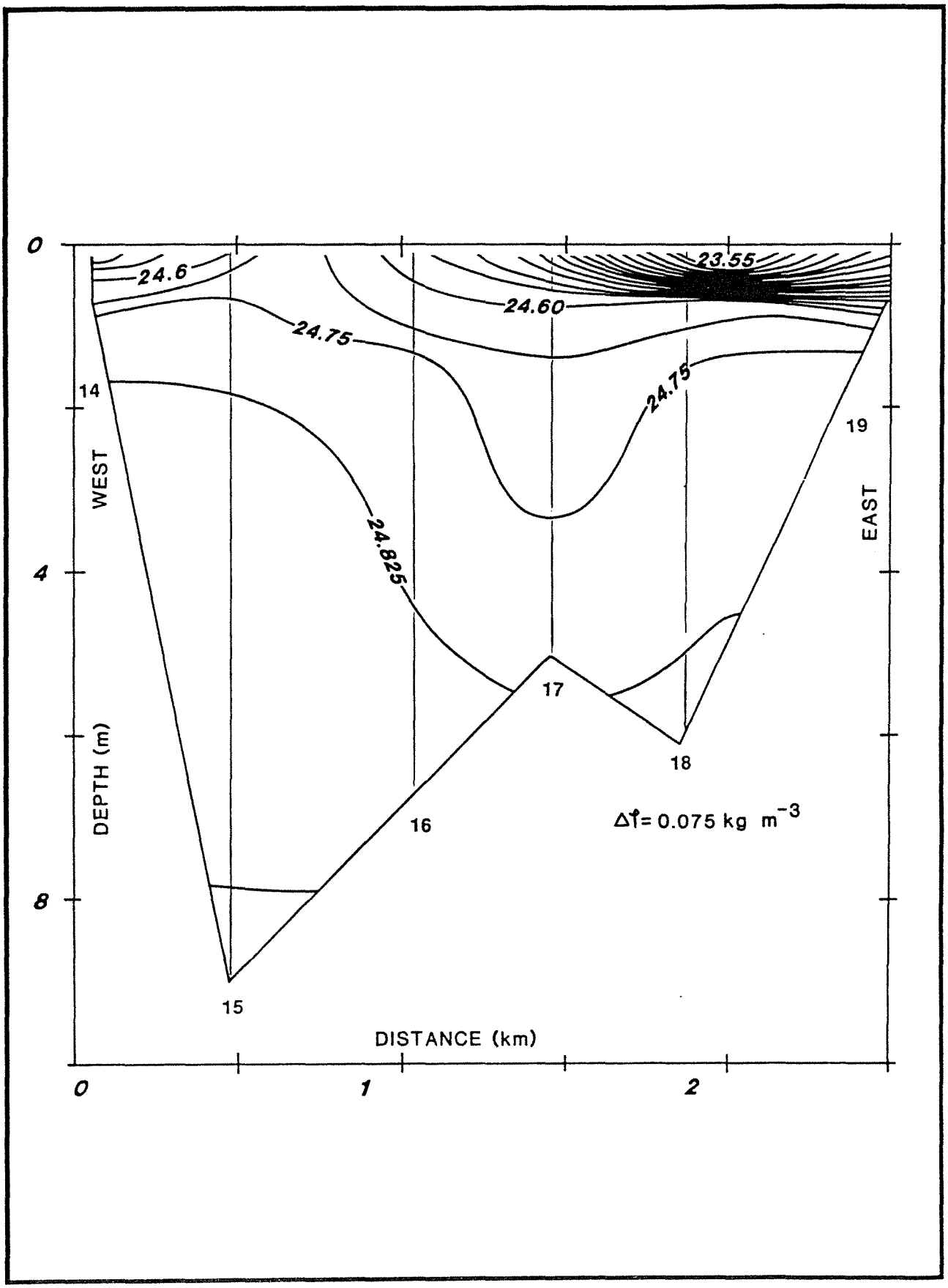

Figure 5.23 Density contour plot for transect T4. Data period: 1224 - 1254 17 February, 1989.

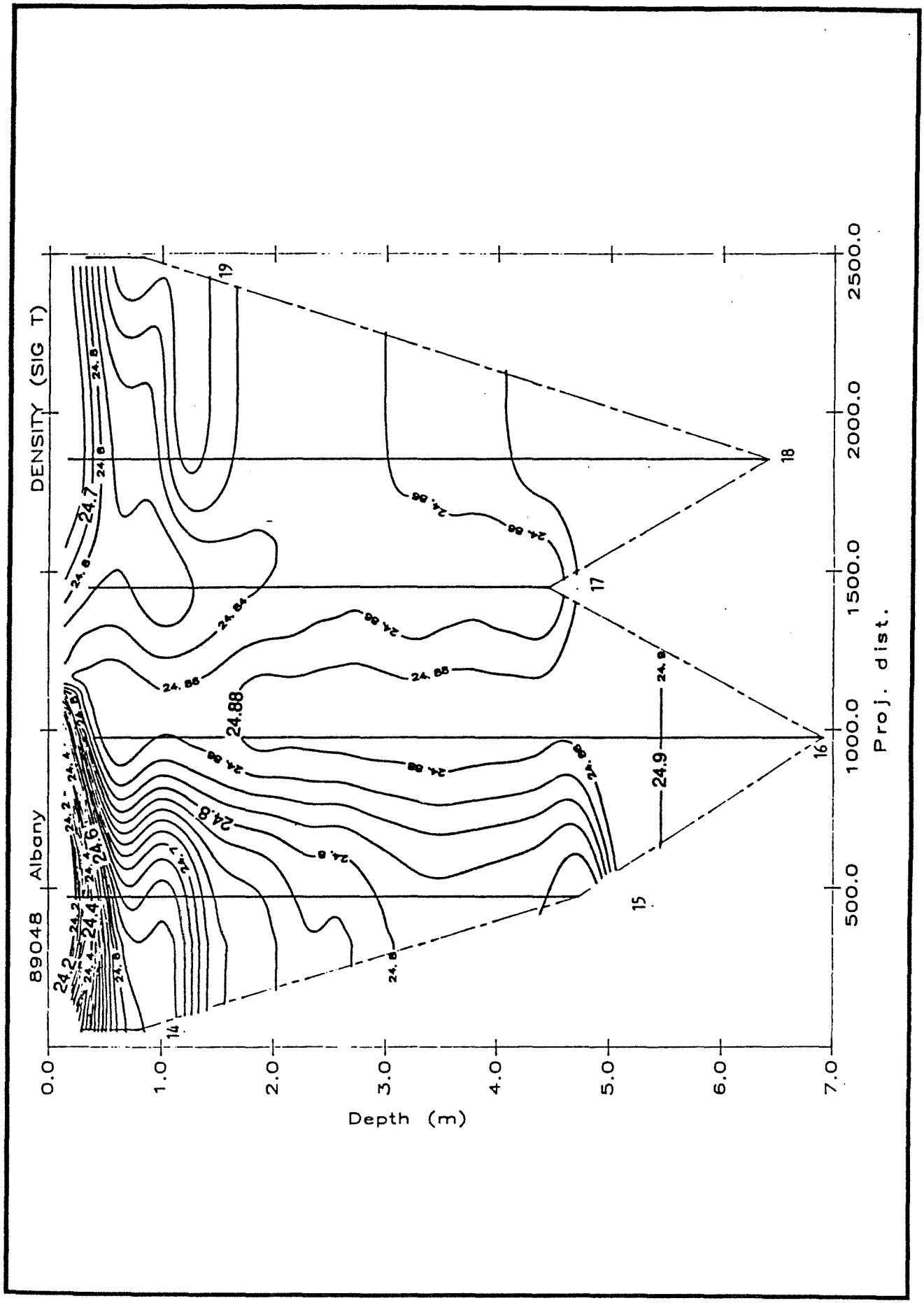

Figure 5.24 Density contour plot for transect T4. Data period: 1617 - 1632 17 February, 1989.

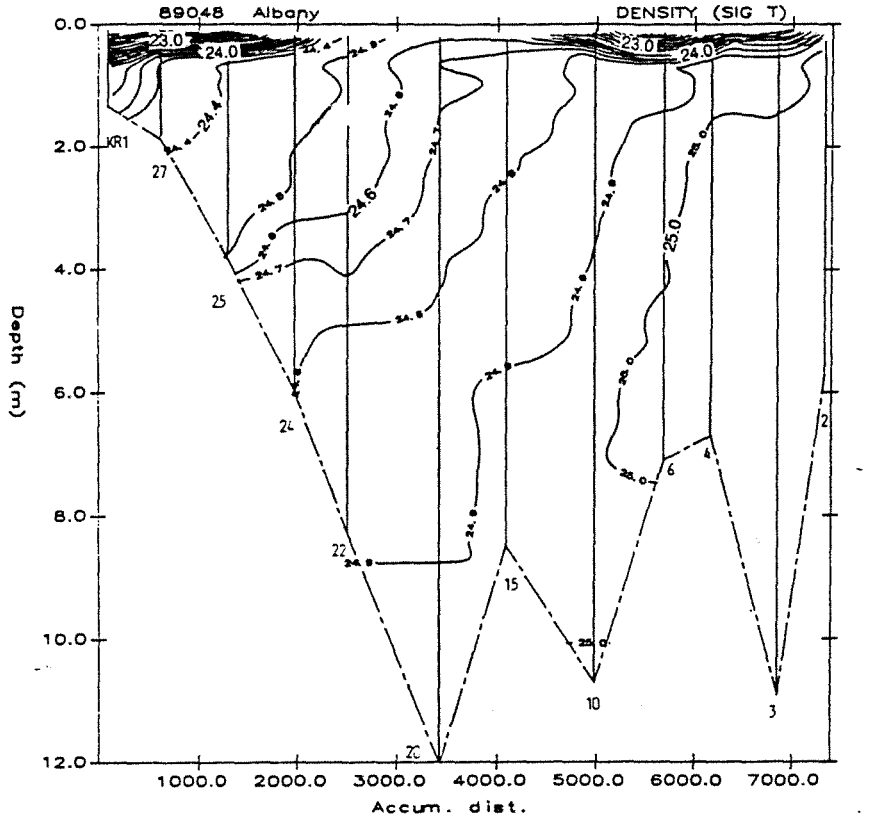

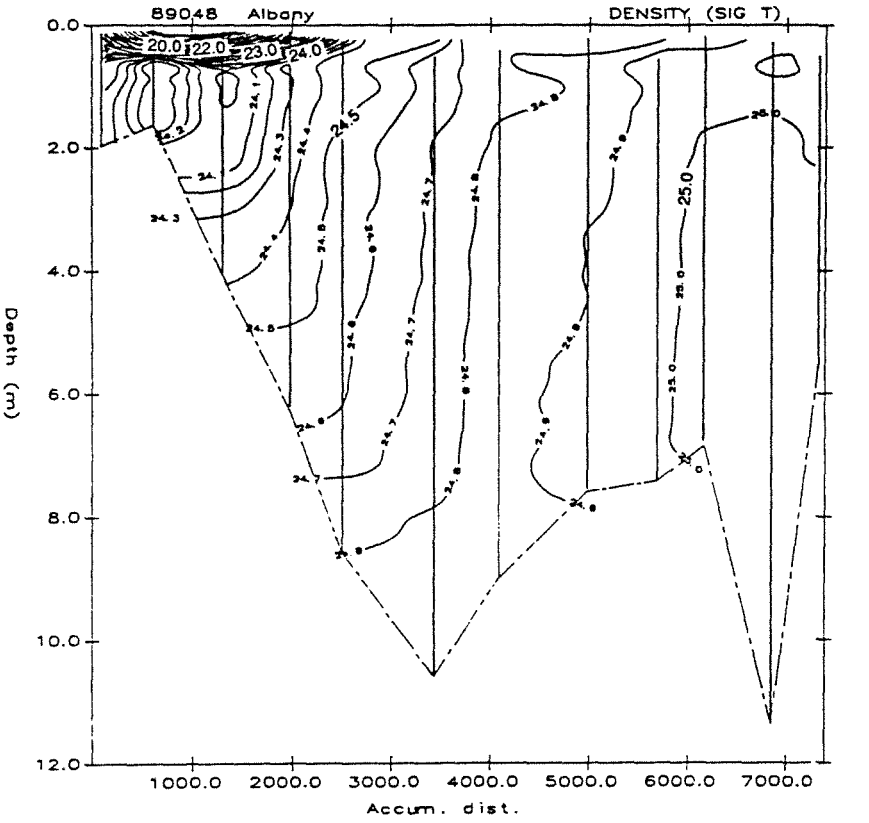

Figure 5.25 Density contour plots for transect T1. (a) 0954 - 1103 17 February, 1989; (b) 1452 - 1533 17 February, 1989.

reinforces the point made in section 5.3.2, above, that baroclinic circulation strongly influences the basin-scale density structure even during periods of strong storm winds.

Another clear example of storm mixing was provided by the basin-scale CTD survey of the afternoon of 13 February 1989. East-northeast winds of the order of 8-12m s^{-1} blew from about 0700 to 1600 on that day. The Wedderburn number for that period was of the order 0.01-0.1, and hence upwelling and severe vertical mixing is predicted.

The CTD survey captured the behaviour of the stratification along transect T4 between 1024 and 1127 and this is presented in the isopycnal contour plot of Figure 5.26, showing a clear upwelling structure with the most dense water at the upwind (eastern) end as expected. Approximately one hour later another lateral CTD transect was performed along transect T3 during the period 1208-1235. The resulting density, salinity and temperature stratification is presented in Figure 5.27, and this data shows the relatively well mixed central harbour region and the stratified areas nearer the banks, indicating differential deepening. The differential deepening is probably due to the sheltering influence of the peripheral topography at the upwind (eastern) end and the downwind advection and consequent set-up of buoyant surface waters against the western bank.

The stratification was also measured in the longitudinal harbour alignment during the storm and the resulting isopycnal, isohaline and isothermal contour plots along transect T1 have been presented in Figure 5.28. These plots are constructed from CTD data collected over a 5 hour period, from 0950 to 1317, with the data for the upper harbour (stations 27, 25 ,24 and 22) collected in the morning between 0950 and 1029 and the data in the lower harbour (stations 15, 10, 6, 4 and 3) collected between 1122 and 1317. The contour plots show that the lower harbour was mixed almost to the bottom.

The persistence of weak stratification near the bottom upstream of station 15 indicates differential deepening due to wind mixing, probably due to the lower fetch that the wind travelled over in the upper harbour. This characteristic of mixing in the harbour is consistent with that measured during the storm of Friday 17 February, discussed above.

5.3.4 Relaxation of the density structure after wind mixing

After a strong wind event that causes severe mixing in the harbour, the density structure is left relatively well mixed vertically but stratified horizontally in the longitudinal alignment. This is because the harbour has a characteristic salt-wedge structure before a mixing event with the most saline, and therefore densest, water residing in the lower harbour. In comparison, the average salinity of water in the upper harbour is slightly lower due to riverine inputs of freshwater.

A good example of the baroclinic re-adjustment of the density structure after a strong mixing event was provided by the basin-wide CTD survey before and after the storm of the evening of Thursday 16 February 1989. Winds gusted to 8-10m s^{-1} at about 1800 hours and lasted until about 2100 hours. Figure 5.29 shows the longitudinal density, salinity and temperature structure from 1656 to 1740, before the storm, along transect T1. All three parameters show the characteristic wedge structure of the harbour for summer conditions. The Wedderburn number characteristic wedge structure of the harbour for sum conditions. The Wedderburn number for the period of the storm is calculated to be of order 0.1 or less. Hence, strong and rapid vertical mixing is predicted. According to the mixing curves presented in Figure 5.17 the surface should have mixed down to about 8m depth.The stratification was again monitored from 2130 to 2242, immediately after the storm, and the density, salinity and temperature structure along transect T1 is presented in Figure 5.30. As shown, in the lower central harbour the water was relatively well-mixed down to about 8m depth near station 10. This is consistent with the predictions. The stratification at the surface exhibits relatively strong vertical gradients upstream and downstream of stations 10 and 15.

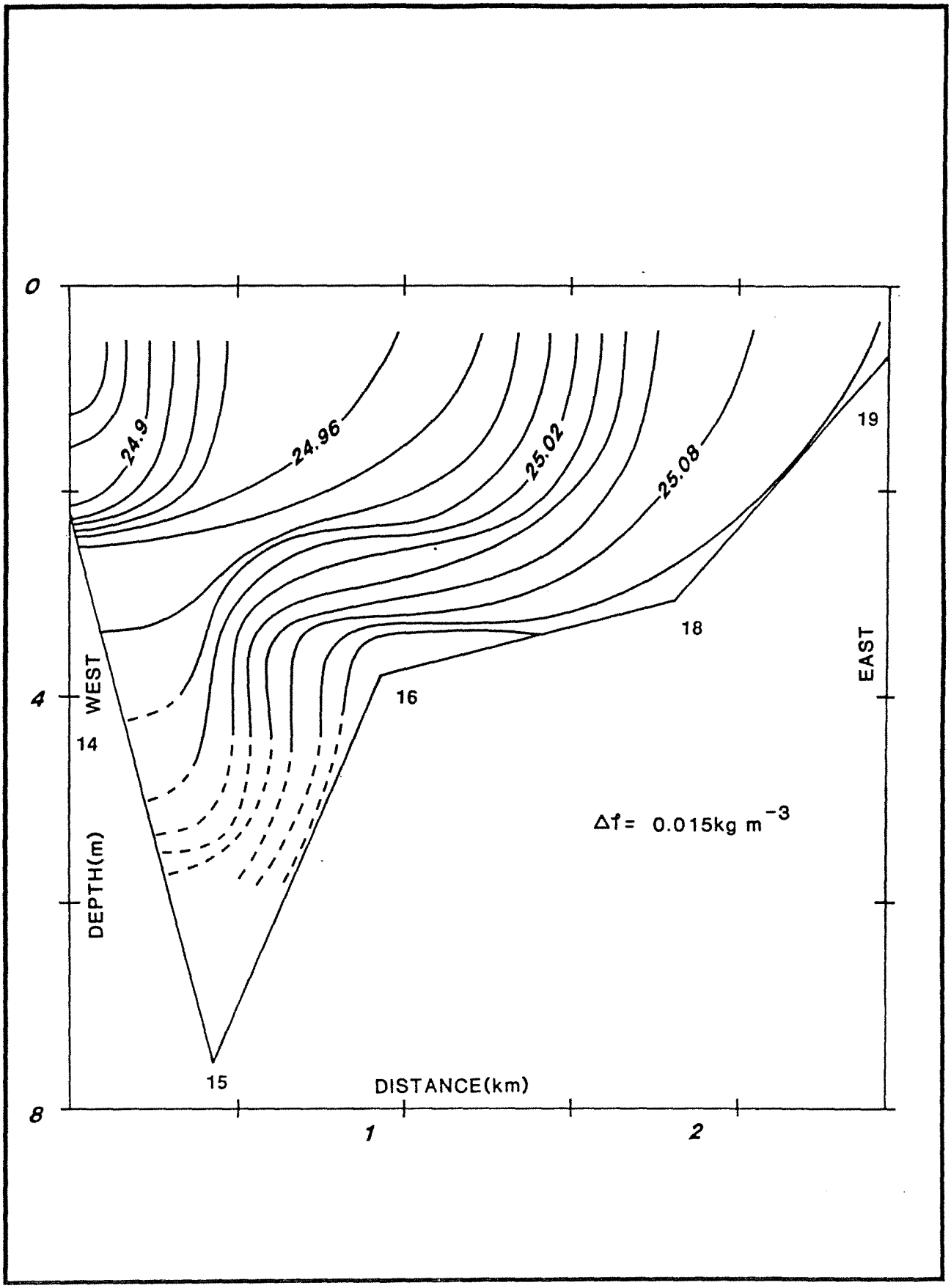

Figure 5.26 Density contour plot for transect T4. Data period: 1044 - 1127 13 February, 1989.

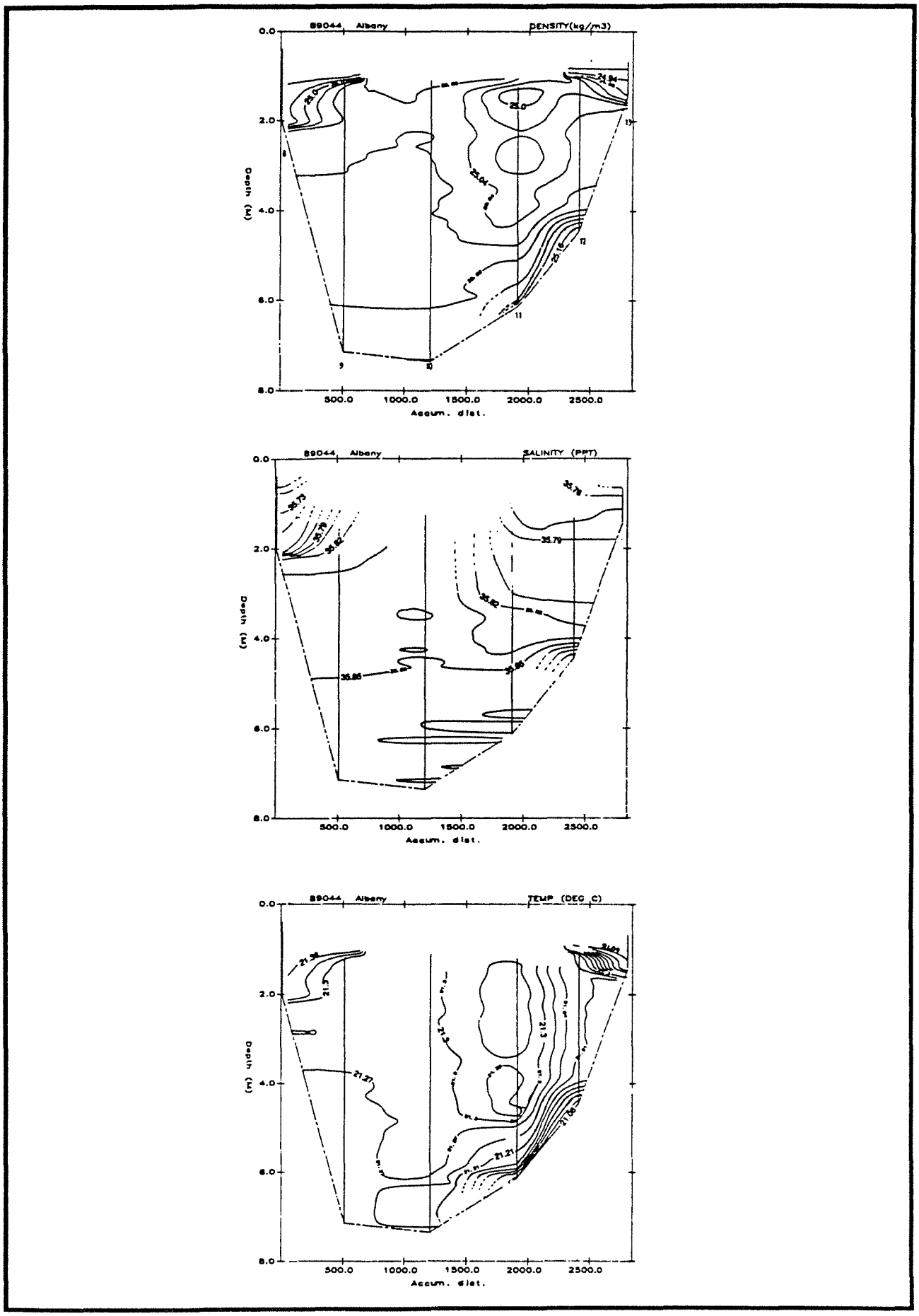

Figure 5.27 Density, salinity and temperature contour plot for transect T3. Data period: 1208 - 1235 13 February, 1989.

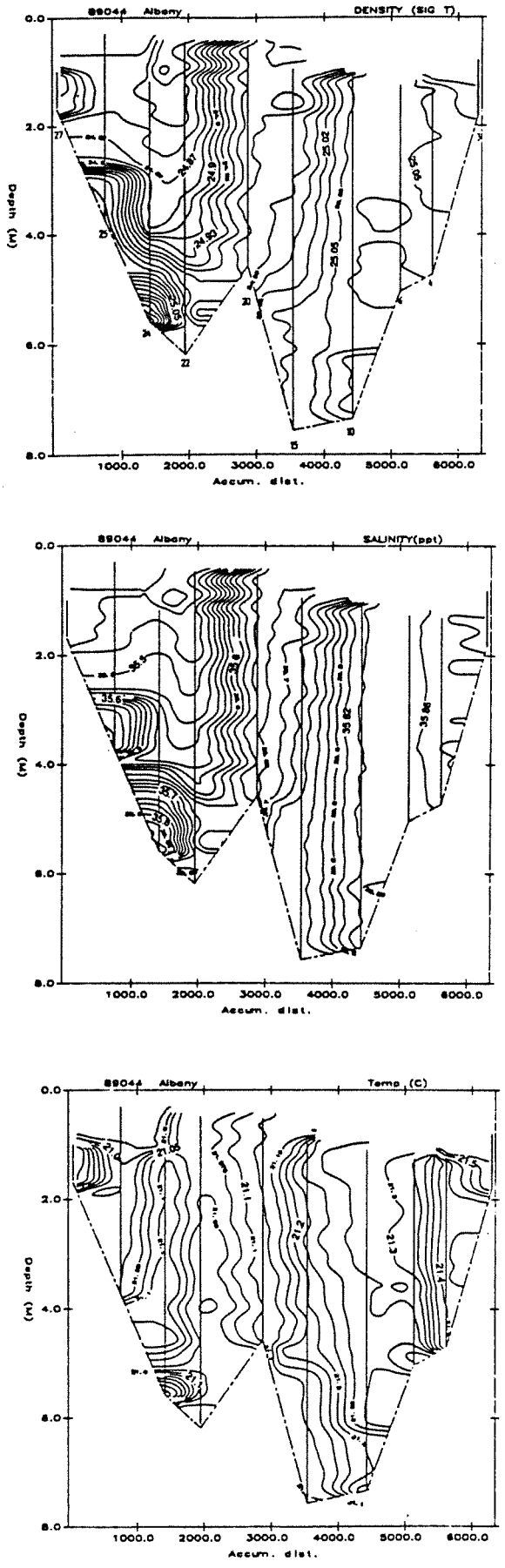

Figure 5.28 Density, salinity and temperature contour plot for transect T1. Data period: 0950 - 1317 13 February, 1989.

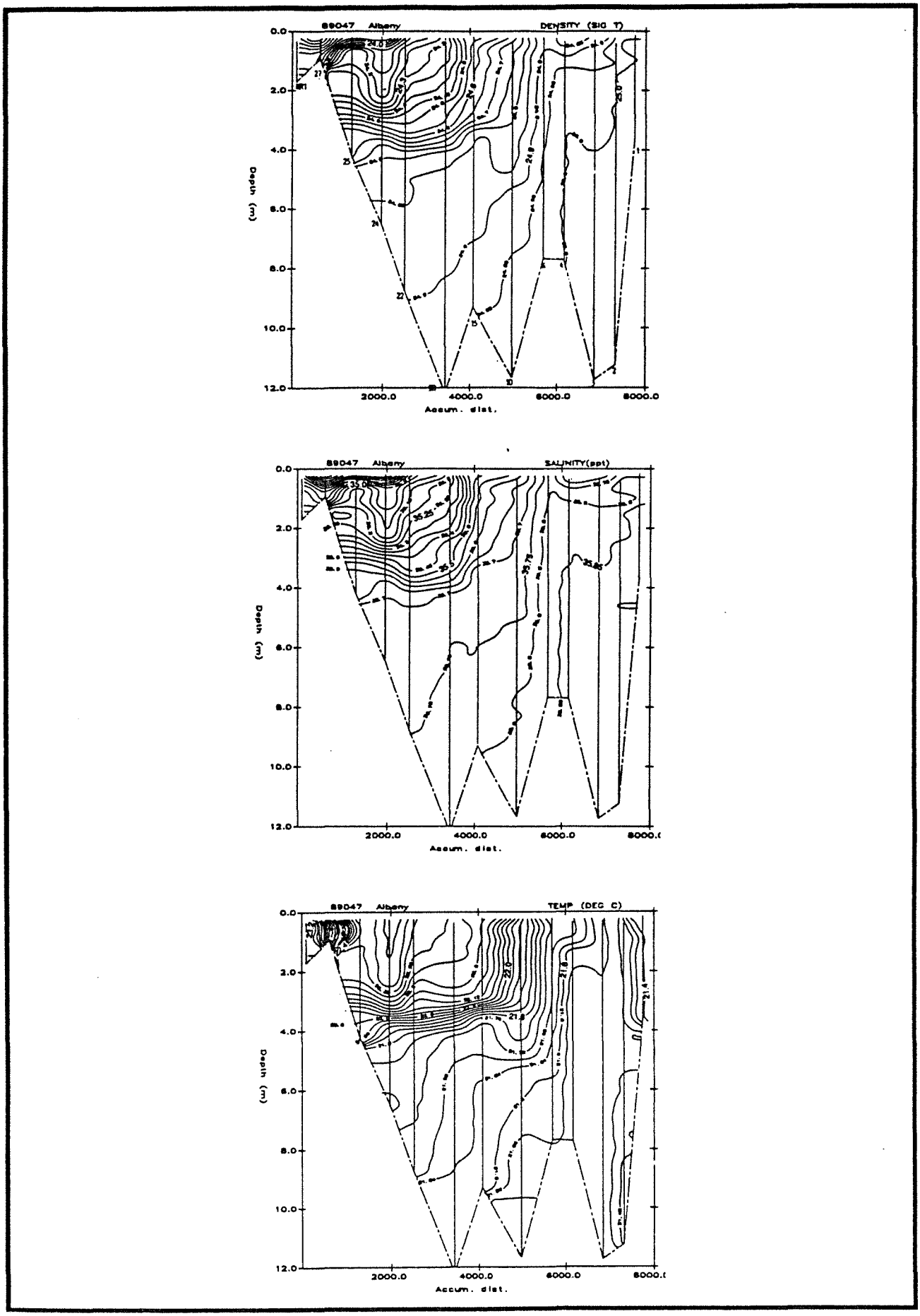

Figure 5.29 Density, salinity and temperature contour plot for transect T1. Data period: 1656 - 1740 16 February, 1989.

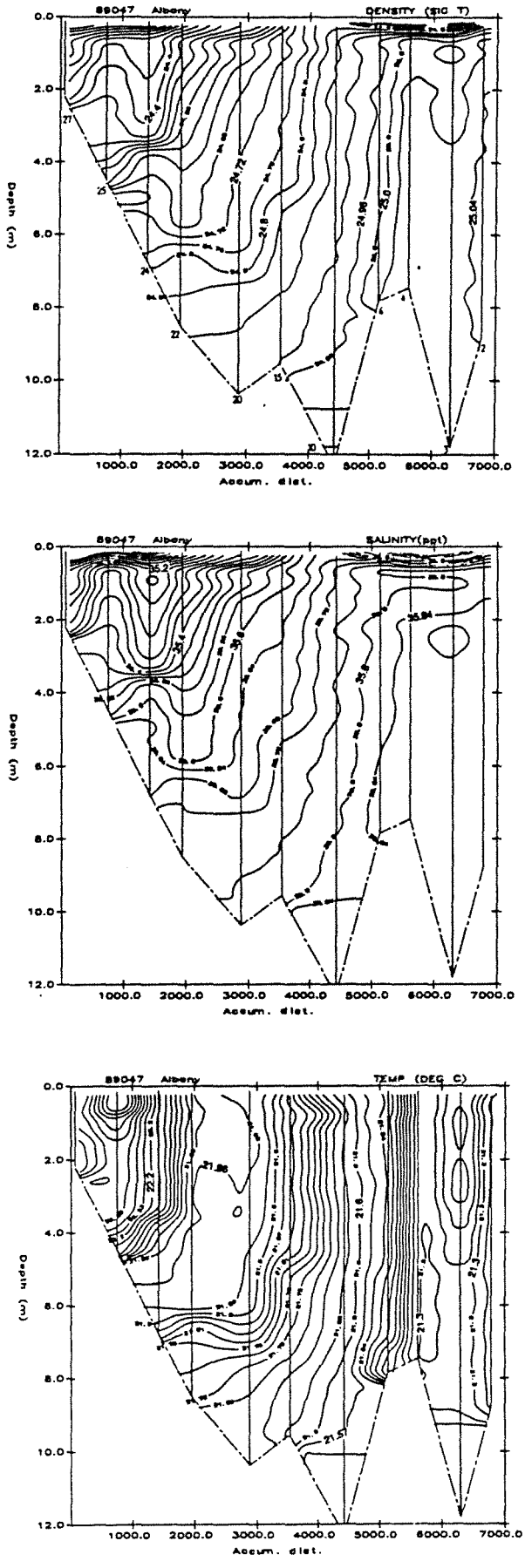

Figure 5.30 Density, salinity and temperature contour plots for transect T1. Data period: 2130 - 2242 16 February 1989.

This indicates the rapid re-adjustment of the density structure near the surface after the storm as a result of the baroclinic flow of buoyant surface water from the upper to the lower harbour regions. The baroclinic flow field also acted to tilt the bottom isopycnals towards the upper harbour as shown in Figure 5.30.

A final transect along T1 was performed between 2307 16 February and 0047 17 February and the resulting density, salinity and temperature structure is presented in the contour plots of Figure 31. By that time, 3 hours after the cessation of the storm, the baroclinically forced tilting of the density structure had almost completely eliminated any vertical homogeneity and a thin surface gravitational front of buoyant water capped the entire harbour and, as previously calculated, this front had a speed of the order of 30cm s^{-1}.

These data indicate that the density structure relaxes quickly after the cessation of a storm mixing event. The longitudinal structure tilts under a baroclinic forcing caused by the gradient of density between the lighter upper harbour waters and the denser lower harbour waters. This horizontal density gradient is greatest at the surface due to the direct input of relatively fresh water at the northern end via the rivers and consequently the relaxation of the density structure is most rapid in this region.

5.4 Differential heating and cooling

When winds are weak and hence Wedderburn numbers large, the role of wind drift in driving circulation is negligible. However, under such conditions the role of differential heating and cooling in setting up horizontal temperature, and hence pressure, gradients can assume a greater importance to mass transport in stratified embayments with variable bathymetry (Monismith and Imberger, 1988).

Figure 5.32a presents isothermal contours across transect T4 encompassing peripheral south-eastern shallows and deeper central waters, during the calm early morning of 17 February 1989 at approximately 0700, when solar radiation was still weak. As shown, the peripheral shallows were colder than the central waters and this was most likely the result of differential cooling by net long-wave, sensible and latent heat losses during the preceding night.

The harbour waters were warmed by the ensuing solar radiation (500 to 900 W m^{-2}) which followed during the morning and this is evident in Figure 5.32b, which presents the thermal structure across the same transect (T4) at approximately 1200. An interesting feature of these data is the differential heating between the peripheral shallows and adjacent deeper central harbour. The temperature rise of about 1 °C over the eastern shallows between 0700 and 1200 is consistent with predictive estimates utilising Beer's law for the exponential heating of a water column in conjunction with an allowance for additional absorption of heat due to bottom reflection of short-wave radiation (Patterson, 1987). In the central harbour regions the temperature rose by only about 0.2 °C. This differential heating could therefore set up density differences, between the expansive shallows and deeper central waters, of the order of 0.2kg m^{-3}.

The resulting surface gravity currents that could be driven by such gradients would have thickness of the order of 0.5m and speeds, according to equation 4.10, section 4.5.3, of the order of 2-3cm s^{-1}. Hence, under such conditions differential heating has the potential to set up a baroclinic circulation pattern that could drive peripheral waters out into the central harbour regions during warm periods at rates of the order of 1km per day.

This is an important result because it describes a mechanism that can flush waters slowly out of interior shallow embayments of water bodies such as Oyster Harbour. No velocity measurements to complement the CTD data are available and so a more quantitative analysis of this mechanism is not possible in this report. It is recommended however, that any future hydrodynamic studies in Oyster Harbour include an investigation of the role of differential heating in overall mass transport within the harbour.

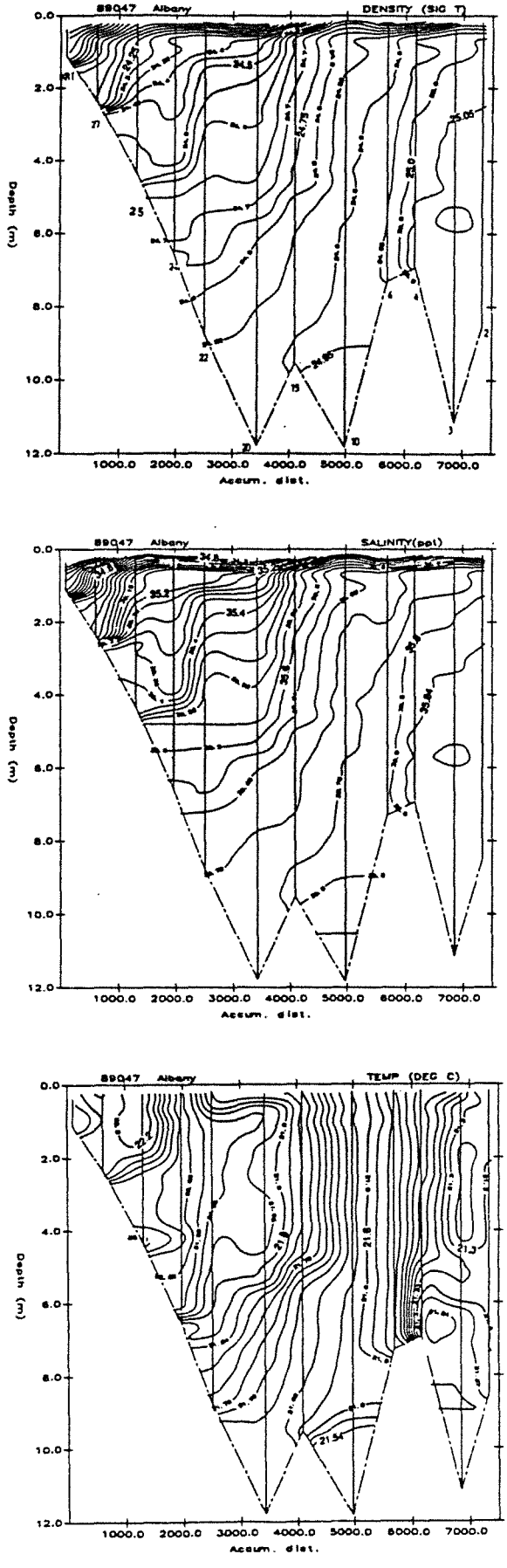

Figure 5.31 Density, salinity and temperature contour plots for transect T1. Data period: 2307 16 February - 0047 17 February 1989.

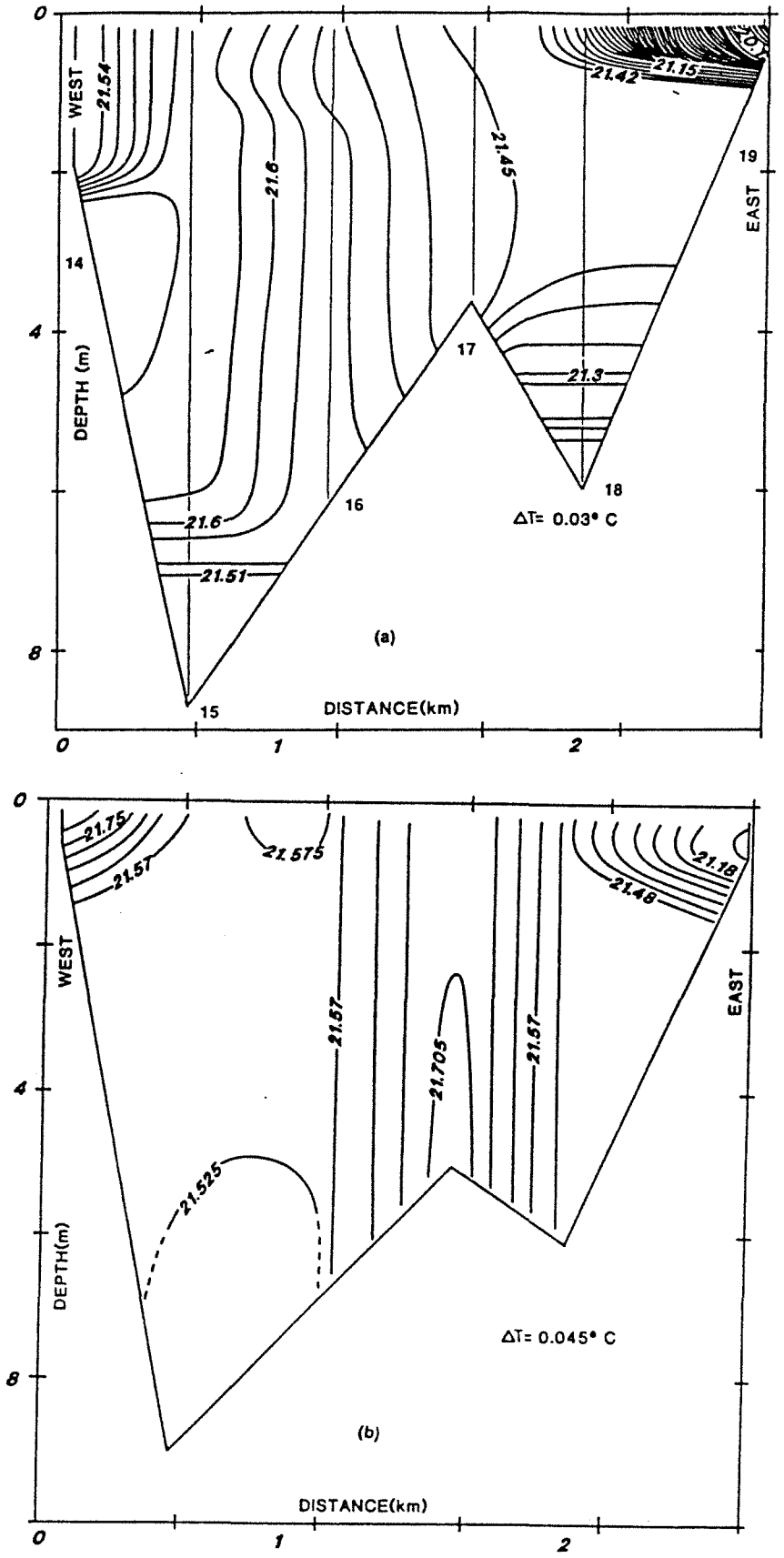

Figure 5.32 Temperature contour plots for transect T4. (a) Data period: 0707 - 0721 17 February, 1989; (b) Data period: 1224 - 1254 17 February, 1989.

5.5 Evaporation

In estuaries evaporation over shallow flats can lead to significant increases in the salinity of the water column. For example, in the Peel-Harvey estuarine system of Western Australia hypersaline water is formed during evaporation in summer with salinities exceeding 50 parts per thousand (Lukatelich, 1987).

McKenzie (1964) reports that during summer in Oyster Harbour salinities in the upper harbour can exceed those of the lower harbour, suggesting the occurrence of hypersaline water with salinities greater than that of the intruding marine wedge.

Average annual evaporation at Albany is approximately 1200mm. This is an average of about 3mm per day. This value is now taken as a first order estimate of evaporation during a warm summer day. As previously stated, the eastern margin of the harbour is extensively covered with shallow tidal flats having depths less than 1m. During a summer afternoon an evaporative loss of water of 3mm would raise the salinity of the water column by about 0.2 ppt in the shallows. Obviously, as the water depth increases the influence of evaporation would be reduced. For example, in a 10m deep water column such as in the central harbour, a 3mm evaporation could raise the salinity of the water column by no more than about 0.02 ppt. Hence, evaporative effects during a warm summer day could potentially lead to a spatially variable salinity field, with waters over the shallows being slightly more saline than waters in the deeper central regions.

The resulting salinity, and therefore density gradients, could drive density currents of the order of 2-3cm s^{-1} (see section 4.5.3). However, the increased temperature of the shallow waters subjected to heating and evaporation may counteract the effect of evaporation by lowering the density. Hence, a complicated horizontal pressure gradient field may be set up, but when temperatures between the adjacent regions of different salinity waters become similar, then the effect of the salinity gradients will be to set up a baroclinic exchange driven by density difference due to salinity difference. The CTD data collected in the south-eastern shallows during Wednesday 15 February 1989 returned salinities of up to 36.06 ppt. The salinity of intruding marine water at station 2 (entrance channel) prior to that day had maximum salinities of 35.9 ppt. This evidence suggests that hypersaline water may have been formed by evaporation during the preceding two days when the air temperatures reached about 22°C and sunshine was strong.

The present data set does not allow a more quantitative analyses of circulation caused by differential evaporation. Hence, it is recommended that any future hydrodynamic studies in Oyster Harbour investigate the potential of this mechanism in more detail.

5.6 Flushing characteristics

A useful starting point in an analysis of exchange between a semi-enclosed embayment and its adjoining ocean is to calculate a theoretical flushing time by the classical tidal prism approach, which assumes complete mixing between intruding ocean water and resident harbour water on each flood tide.

During a typical 14 day tidal cycle the diurnal change in water level ranges from about 1m during springs to about 0.3m during neaps. A flushing time of order 10 days is calculated using the tidal prism approach, given a typical spring-neap tidal variation. The inherent assumption in this calculation is however invalidated by the fact that the harbour was found to be typically stratified horizontally and vertically in summer during low wind conditions (less than about 5m s^{-1}), as shown above. The existence of stratification means that mixing within Oyster Harbour will be spatially and temporally variable, and hence flushing times for this system will vary as a function of both time and space. It was shown in the above analyses that the harbour approaches a fully-mixed state only during very strong and prolonged wind events. Also, with the tidal prism approach it is assumed that water that is advected out is not advected back in. This assumption is probably not strictly applicable for Oyster Harbour in view of the potential for outgoing ebb tidal pulses to be re-advected, in part, back into the harbour during following flood tides, as discussed in Section 5.2.4.

On each flood tide a marine wedge penetrates upstream via the entrance channel. This wedge forces resident buoyant harbour water to advect upstream and accumulate against the northern end of the harbour. The resulting stratification is characterised by vertical density differences of the order of 0.2 to 1.0kg m^{-3} (top to bottom) in the upper harbour, weaker vertical gradients in the lower harbour, a homogeneous water column in the entrance channel, and a longitudinal density gradient with the lower harbour greater in density than the upper harbour by up to 1kg m^{-3}.

During summer, buoyancy is introduced to the harbour water via solar radiation, riverine freshwater inputs in baseflows and groundwater. As a result of this continual buoyancy flux the surface waters in the harbour have a persistent downstream (southward) directed pressure gradient forcing a baroclinic flow towards the mouth as a relatively thin (less than 1m thick) surface density current. The measurements of stratification indicate that this feature maintains its vertical structure without significant mixing for winds less than about 5m s^{-1}. Hence, nutrients contained in these surface waters are not transported to the benthos under such conditions. During flood tides the surface waters are forced upstream by the barotropic tidal flow field. During ebbs the buoyant surface water propagates downstream as a thin layer under the combined barotropic and baroclinic forcings at rates that can flush water from the upper harbour out to the ocean in about 1-2 days or less.

In contrast to the horizontal density gradient field at the surface, the bottom water has a residual density gradient directed upstream (northward), due to the regular input of relatively dense marine water through the entrance channel. Hence, the wedge has a propensity to travel further upstream during floods than downstream during ebbs. In the absence of strong winds all other potential mixing agents (tide, atmospheric heating and cooling, and interfacial shear) do not mix bottom waters up to the surface. Hence, waters nearer the bottom reside in the harbour for longer times than surface waters. Some measurements of vertical structure during spring tides and low winds showed that there is the possibility that bottom pools of dense water can remain trapped in the deepest central harbour regions.

When winds climb above 5m s^{-1} vertical mixing appears to mix the harbour rapidly, with full-depth mixing during say 10m s^{-1} winds able to occur in about 6 hours. Basin-scale measurements of stratification during wind mixing events revealed that differential deepening occurs, with upper harbour waters maintaining some vertical structure due to the reduced fetch that most winds experience in that region. Wind mixing is most rapid in the central lower harbour region.

It is not possible to provide accurate quantitative estimates of flushing times for bottom water in Oyster Harbour, but they are likely to be significantly greater than surface waters, probably of the order of 3 to 10 days. Bottom water in the upper harbour is less frequently mixed by winds compared to bottom water in the lower harbour. In addition, ebb tides are not able to advect the bottom water of the upper harbour out to the ocean. Hence, this region of water will have the longest flushing times compared to surface water and water in the lower harbour. The wind mixing data indicate that typical strength sea-breezes are sufficiently strong to mix bottom waters in the lower harbour to the surface. Once this has occurred the upper half of the water column will gravitate towards the mouth in a lock-exchange manner leading to surface flushing times of the order of 1-2 days. Strong wind events occur with a frequency related to the passage of pressure systems and these have temporal scales of the order 3 to 10 days.

Peripheral harbour waters over the shallow areas, such as along the entire eastern margin, have much lower tidal current velocities than the deeper central waters. Transport in the shallows is therefore driven by a complicated interplay between wind forced currents, weak tidal currents, and density currents driven by differential wind deepening, differential atmospheric heating and cooling, or evaporation. All these mechanisms have the potential to drive surface water out from the periphery and in towards the central regions of the harbour in currents with speeds of the order 2 to 5cm s^{-1}. Hence, there is a slow, but persistent tendency for shallow peripheral waters to be flushed to the central harbour regions, where tidal flows and downstream surface gravitational fronts can drive them out to the ocean in times of the order of 1-2 days.

During ebb tides harbour water emanates out of the harbour as a barotropic jet. A significant proportion of this ejected water remains in the radial sink zone for the entry of ocean water back into the harbour on subsequent flood tides. It is estimated that up to 30 percent of ejected water could be re-advected back into the harbour during flood tides. Hence, the efficiency of hydrodynamic mechanisms that act to flush the harbour could be effectively reduced by up to about 30 percent, with the exact percentage depending on the phase of the tide and general circulation patterns within King George Sound.

6. Conclusions

6.1 Winter

During winter, river discharge traverses Oyster Harbour in times less than about 2 days as a fresh-to-brackish surface layer of less than 1m thickness, and typically undergoes little mixing. None of the mechanisms of tidal mixing, differential heating and cooling, penetrative convection, evaporation, or interfacial shear are able to mix the surface layer down to any great extent. Winds of less than about 5m s^{-1} do not significantly mix the surface layer vertically. However, when winds climb above this value to say 10m s^{-1} mixing to the bottom can occur in times of the order of 15 hours. Such winds do not generally occur during flood discharge events in winter. Hence, the surface front maintains its vertical structure.

The rotation of the earth probably deflects buoyant river discharge plumes towards the eastern bank. This is the likely explanation why there are extensive shallow areas along the eastern margin of Oyster Harbour heavily covered in sediments of alluvial origin.

Once through the harbour the river discharge ejects well out into King George Sound as a surface buoyant jet and this is an effective mechanism for nutrient export from the harbour.

Related environmental studies (Simpson and Masini, 1990) have shown that the majority of the annual phosphorus load into Oyster Harbour is carried by runoff associated with the break of the winter season, during the first 'flushes'. For example, about 40 percent of the total annual phosphorus load for 1988 entered the harbour during the first major discharge event.

It is therefore concluded that most of the nutrients that are carried into Oyster Harbour during initial winter flushes, when nutrient export is highest from the catchments, are effectively transported through the harbour in baroclinically driven surface gravitational overflows, and then ejected out the ocean in buoyant jets.

It is speculated, in the absence of sufficient data, that the weaker residual winter discharge that occurs between major flow events is more susceptible to mixing. This flow occurs continuously and leads to a weaker vertical stratification that can therefore be subjected to strong mixing by occasional winter storms.

6.2 Summer

In summer, the estuary is salt-wedge in nature and is generally vertically stratified in salinity, temperature and therefore density.

The tide drives a cyclic influx and efflux of marine water in the harbour as a bottom wedge through the mouth. This wedge can intrude up to 4km in from the mouth during the strongest spring flood tides. The efflux is generally less pronounced with some marine water remaining in the harbour during ebbs. Tidal currents are important to transport along the deepest alignment of the harbour. However, frictional damping appears to restrict the intensity of tidal currents over the extensive peripheral shallows of the harbour. Over these regions wind drift, and density driven surface currents assume a greater importance to overall circulation.

The rotation of the earth probably deflects tidal inflows to the western bank, and downstream directed buoyant gravitational fronts to the eastern bank.

Wind mixing is not able to appreciably mix the harbour vertically during low wind conditions when winds are less than approximately 5m s^{-1}. During low wind conditions a characteristic surface buoyant layer of water (slightly less saline than marine) was found to occur. This layer propagates downstream during ebbs with speeds reinforced by the density gradient between it and the adjacent ocean. Exit times for surface waters of the upper harbour by this baroclinic mechanism are calculated to be of the order 1-2 days.

However, during stronger winds, approaching 10m s^{-1} or more, vertical mixing is rapid in the central and lower harbour regions. A predictive methodology, utilising a Wedderburn number classification scheme, was applied to predict the potential of winds to mix the harbour as a function of time and wind velocity. The predictions and measured data both indicated that full-depth mixing can occur in times of the order of 6 hours during strong wind events. At the beginning of a strong wind mixing event, upwelling of bottom waters at the upwind end is initiated. As is common in enclosed or semi-enclosed stratified embayments, wind-mixing leads to differential deepening. In Oyster Harbour the upper harbour is vertically mixed more slowly by winds than the lower harbour due to sheltering and shorter fetch length for winds from most directions.

After a strong mixing event, the harbour is left relatively well-mixed vertically but longitudinally stratified, with the most saline water in the lower harbour. The density structure re-adjusts baroclinically after such an event with vertical stratification re-forming over the entire harbour in times of the order 3 hours or less.

Freshwater inputs from river baseflows and groundwater, along with solar heating, night cooling, patchy wind mixing and upwelling result in the setting up of horizontal density gradients at the surface within the inner harbour. On the basis of both field measurements and analytical predictions, it is postulated that such density gradients could drive surface exchange between the peripheral shallow regions of the harbour and the central deeper basins. It is estimated that baroclinic currents could flush peripheral waters out to the inner harbour in times of the order of one to two days.

During ebb tides harbour water emanates out of Oyster Harbour as a barotropic jet. A significant proportion of this ejected water remains in the radial sink zone for the entry of ocean water back into the harbour on subsequent flood tides. It is estimated that up to 30 percent of ejected water could be re-advected back into the harbour during flood tides.

An accurate quantification of flushing times for this harbour is difficult due to the complicated nature of stratification in summer and also due to the complicated inter-play between barotropic and baroclinic currents driven by the tide, wind, atmospheric heating and cooling, Coriolis force, and spatially patchy wind mixing. Flushing times for surface waters are probably of the order of 1-2 days. Flushing times for bottom waters are probably of the order of 1 to 10 days, depending on position in the harbour, the phase of the tide and on the strength of wind mixing, with flushing greatest in the lower harbour during strong wind mixing events, such as sea-breezes and storms. Bottom water in the upper harbour probably remains in the Oyster Harbour the longest before being flushed out to the ocean.

6.3 Water quality

In winter, during flood discharges of river water, vertical availability of nutrients to the benthos is low. It is more likely that during periods of lower flow, in between major discharge events, nutrients are made available to the benthic macroalgae by storm mixing.

In summer the stratification is relatively weak and regular sea-breezes and storm winds can readily mix the harbour vertically. Mixing is however, spatially variable with differential deepening being a common result of wind mixing.

Chronic loadings of pollutants such as phosphorus in river and groundwater flows are therefore readily mixed to the bottom by strong winds, which occur regularly in summer. Hence, reductions in these inputs, as well as in major inputs during winter, are required in order to address the problems of nutrient enrichment in Oyster Harbour.

The re-advection back into the harbour of significant portions of tidal ebb jets poses a problem for the long-term ecological health of waters of King George Sound in the vicinity of the Oyster Harbour mouth.

The identification of a significant loss of nutrients from the harbour to King George Sound, especially during winter flow events, suggests that an understanding of the ecological implications of long-term nutrient loadings to King George Sound should now assume importance. Relevant management Authorities should coordinate this task on the basis of an integrated catchment approach, with an understanding of the sources of nutrients from both the catchments and local inputs being an intrinsic component of any management strategies. Necessary to the task will be an adequate understanding of the hydrodynamics of King George Sound.

7. References

Appleyard, S.J. (1990). The flux of nitrogen and phosphorus from groundwater to the ocean in the Perth metropolitan region. Hydrogeology Report No. 1990/64. 1990. WA Geological Survey. (Prepared as a contribution to the Western Australian Environmental Protection Authority's Environmental Management Strategy for Cockburn Sound and Surrounding Waters)

Bureau of Meteorology. (1984). Western Australian Yearbook 1984. Vol. 22. Bureau of Statistics.

Chen, J.C. (1980). Studies on gravitational spreading currents. Ph. D. Thesis, California Institute of Technology, Report KH-R-40, Pasadena, California.

Csanady, G.T. (1985). Hydrodynamics of Large Lakes. Ann. Rev. of Fluid Mech., 7:357-386

D'Adamo, N. (1985). Mixing and transport in the Murray River estuary, Western Australia. M. Eng. Sc. Thesis, University of Western Australia, Nedlands, Western Australia, 6009.

Didden, N. and Maxworthy, T. (1982). The viscous spreading of plane and axisymetric gravity currents. J. Fluid Mech., 121:27-42

Fandry, C.B., Leslie, L.M. and Steedman, R.K. (1984). Kelvin-type coastal surges produced by tropical cyclones. J Phys. Oceanogr., 14:582-593

Fischer, H.B., List, E.J., Koh, R.C.Y., Imberger, J. and Brooks, N.B. (1979). Mixing in Inland and Coastal Waters. Academic Press, New York.

Fozdar, F.M. (1983). Mixed layer probe technical report. Environmental Dynamics Report No. ED-83-039. University of Western Australia.

Hearn, C.J., Hunter, J.R., Imberger, J. and van Senden, D. (1985). A tidally induced jet in Koombana Bay, Western Australia. Aust. J. Mar. Freshw. Res., 36:453-479.

Hebbert, R., Imberger, J., Loh, I. and Patterson, J. (1979). Collie River underflow in the Wellington Reservoir. J. Hydraul. Div. ASCE., 105:533-545.

Hillman, K., Lukatelich, R.J., Bastyan, G. and McComb, A.J. (1991 a). Water quality and seagrass biomass, productivity and epiphyte load in Princess Royal Harbour, Oyster Harbour and King George Sound. Technical Series No. 39. Environmental Protection Authority of Western Australia, Perth, Western Australia, 6000. 44 pp.

Hillman, K., Lukatelich, R.J., Bastyan, G. and McComb, A.J. (1991 b). Distribution and biomass of seagrasses and algae and induced pools in water, sediments and plants in Princess Royal Harbour and Oyster harbour. Technical Series No. 40. Environmental Protection Authority of Western Australia, Perth, Western Australia, 6000. 55 pp.

Hodgkin, E.P. and Di Lollo, V. (1958). The tides of south-Western Australia. J. Roy. Soc., 41:42-54.

Imberger J. and Patterson, J.C. (1981). A dynamic reservoir simulation model - DYRESM:5, pp. 310-361. In: H.B. Fischer (ed.), Transport Models for Inland and Coastal Waters. Academic Press, New York.

Imberger, J. (1985). The diurnal mixed layer. Limnol. Oceanogr., 30:737-770.

Imberger, J. and Hamblin, P.F. (1982). Dynamics of lakes, reservoirs and cooling ponds. Ann. Rev. Fluid Mech., 14:153-187.

Imberger, J. and Patterson, J.C.(1990). Physical Limnology. In: Advances in Applied Mechanics. T. Wu., Editor. Academic Press, Boston. Vol. 27, pp. 303-475.

Imberger, J., D'Adamo. and Oldham, C. (1990). Dynamics of the Venice Lagoon. A preliminary analysis of data collected between Monday 11 June - Saturday 16 June 1990. Centre for Water Research, University of Western Australia, Nedlands, Western Australia, 6009. Reference: WP 475 JI.

Imberger, J., Thompson, R. and Fandry, C. (1976). Selective withdrawal from a finite rectangular tank. J. Fluid Mech., 78:489-512

Ivey, G.N. and Patterson, J.C. (1984). A model of the vertical mixing in Lake Erie in summer. Limnol. Oceanogr., 29:553-563.

Kraus, E.B. and Turner, J.S. (1967). A one dimensional model of the seasonal thermocline: II. The general theory and its consequences. Tellus, 19:98-106

Luketina, D.A. (1987). Frontogenesis of Freshwater Overflows. Ph. D. Thesis, University of Western Australia, Report No. ED-87-227, Nedlands, Western Australia, 6009.

Luketina, D.A. and Imberger, J. (1987). Characteristics of a surface buoyant jet. J. Geophys. Res., 92:5435-5447.

Manins, P.C. (1976). Intrusion into a stratified fluid. J. Fluid. Mech., 74:547-560

McComb, A.J. and Lukatelich, R.J. (1986). Nutrients and plant biomass in Australian estuaries with particular reference to southwestern Australia. In: Limnology in Australia. (Ed. W.D. Williams and P. de Deckker). W. Junk publishers. Melbourne. pp433-455.

McKenzie, K.G. (1964). The ecological associations of an ostracode fauna from Oyster Harbour, a marginal marine environment near Albany, Western Australia. Pubbl. Staz. Zool. Napoli. 33:421-461.

Mills, D.A. and D'Adamo, N. (in preparation). Water Circulation and flushing characteristics of Princess Royal Harbour. Technical Series. Environmental Protection Authority of Western Australia, Perth, Western Australia, 6000.

Monismith, S.G. (1986). An experimental study of the upwelling response of stratified reservoirs to surface shear stress. J. Fluid Mech., 171:407-439.

Monismith, S.G. and Imberger, J. (1988). Horizontal convection in the sidearm of a small reservoir. Environmental Dynamics Rept. ED-86-161, Centre for Water Research, University of Western Australia.

Mortimer, C.H. (1974). Lake Hydrodynamics. Mitt. Int. Ver. Limnol., 20:124-197

Parker, G.J. and Imberger, J.(1986). Differential mixed-layer deepening in lakes and reservoirs. In: Limnology in Australia. (Ed: W.D. Williams and P de Deckker). W. Junk publishers. Melbourne. pp 63-92.

Patterson, J.C. (1987). A model for convective motions in reservoir sidearm. In: Topics in Lake and Reservoir Hydraulics (Ed: W.H. Graf and U Lemmin). Proceedings of Technical Session C1, XXII Congress, IAHR, 1987.

Pattiaratchi, C., van Senden, D.C. and Brown, S. (1991). Albany Wastewater Ocean Outfall Options: preliminary hydrodynamic investigations of effluent dispersion at the three proposed sites. Report No. WP 543 CP. Centre for Water Research, University of Western Australia. Nedlands, 6009, Australia.

Pollard, R.T., Rhines, P.B. and Thompson, R.O.R.Y. (1973). The deepening of the wind mixed layer. Geophys. Fluid Dyn., 3:381-404.

Prince, G.J. (1984). Contour plotting on the DJINNANG II. Report No. ED-84-082. Centre for Water Research, University of Western Australia. Nedlands, 6009, Australia.

Safaie, B. (1979). Mixing of buoyant surface jet over sloping bottom. J. Waterway, Port, Coastal and Ocean Div., ASCE, 105:357-373.

Sherman, F.S., Imberger, J. and Corcos, G.M. (1978). Turbulence and mixing in stratified waters. Ann. Rev. Fluid Mech., 10:267-288.

Simpson, C.J. and Masini, R.J. (1990). Albany Harbours Environmental Study 1988-1989. (Ed: C.J. Simpson and R.J. Masini). Bulletin 412, Environmental Protection Authority of Western Australia, Perth, Western Australia, 6000.

Simpson, J.E. (1982). Gravity currents in the laboratory, atmosphere and ocean. Ann. Rev. Fluid Mech., 14:213-234.

Spigel, R.H. and Imberger, J. (1980). The classification of mixed layer dynamics in lakes of small to medium size. J. Phys. Oceanogr., 10:1104-1121.

Thompson, R.O.R.Y. and Imberger, J. (1980). Response of a numerical model of a stratified lake to wind stress. In: Proc. 2nd IAHR Symp. on Stratified Flows, Trondheim. (Ed: T. Carstens and T McClimans). pp 562-570.

Thorpe, S.A. (1987). Transitional phenomena and the development of turbulence in stratified fluids: a review. J. Geophys. Res., 92:5231-5248.

Turner, J.S. (1973). Buoyancy effects in fluids. Cambridge University Press. Cambridge. pp. 368.

Wu, J. (1969). An estimation of wind effects on dispersion in wide channels. Water Resources Res., 5:1097-1104.